# SPE TRANSACTIONS

*devoted to plastics science and engineering*

VOL. 1, NO. 1 JANUARY 1961

BY THE SOCIETY OF PLASTICS ENGINEERS, INC.

# SPE TRANSACTIONS

*. . . is a new journal containing fundamental data in the field of plastics science and engineering. Each issue will contain a selection of polymer articles, both original and review type, including translations of significant articles from foreign publications. In addition to being readily available as a permanent reference source, SPE TRANSACTIONS will be regularly indexed in the permanent literature. Also, the table of contents of quarterly issues of TRANSACTIONS will be published in the preceding issue of the SPE Journal, also published by the Society.*


**Society of Plastics Engineers, Inc.**

*Executive and Business Offices*
**65 Prospect St.**
**Stamford, Conn.**



*1960 Officers of the Society—*

*President*— GEORGE W. MARTIN
*1st. Vice Pres.*— FRANK W. REYNOLDS
*2nd. Vice Pres.*— HAIMAN S. NATHAN
*Secretary*— JAMES R. LAMPMAN
*Treasurer*— JOSEPH B. SCHMITT
*Exec. Secretary*— THOMAS A. BISSELL

Neither the Society of Plastics Engineers, Inc., nor the SPE TRANSACTIONS is responsible for the views expressed by individual contributors either in articles published in SPE TRANSACTIONS or in technical papers presented at meetings of the Society.

*Editor*— MELVYN A. KOHUDIC
*Technical Editor*— MARK D. INSKEEP
*Layout, Production*— LEE COOPER
*Editorial Assistant*— ALICE L. NORVELL
*Circulation Manager*— LEWIS A. BERNHARD

*SPE Publications Committee*

MAURICE F. MALONE, *Adm.* — EUGENE C. QUEAR
DR. ALEX SACHER, *Chmn.* — DR. FRANK W. REINHART
DR. RAYMOND F. BOYER — IRVIN I. RUBIN
DR. JESSE H. DAY — DR. SIDNEY J. STEIN
DR. HERMAN F. MARK — PARKE WOODWORTH
FRANK A. MARTIN

*Editorial Advisory Board*

DR. FRANK W. REINHART, *Chmn.* — DR. HERMAN S. KAUFMAN
ROBERT W. BARBER — JOHN P. LOMBARDI
DR. LUTHER BOLSTAD — THOMAS F. McLAUGHLIN
EDWARD F. BORRO, SR. — ROBERT E. MONICA
BENJAMIN S. COLLINS — JULES PINSKY
WILLIAM CROLL — ROBERT D. SACKETT
EDWARD J. FITZPATRICK — EDWARD W. VAILL
RUSSELL M. HOUGHTON — FREDERICK WEHMER



• SPE TRANSACTIONS is Published at 215 Canal St., Manchester, N. H. Address changes, undeliverable copies and orders for subscriptions should be sent to 65 Prospect St., Stamford, Conn.

• *Permit for second-class matter at the Post Office at Manchester, New Hampshire, at special postal rate provided in paragraph (d-2), Sec. 34.40 P.L. and R., of 1918, applied for.*



• *Copyright by the Society of Plastics Engineers, Inc., 1961. Reproduction in whole or part without written permission is strictly prohibited.*



**— Subscription Rates —**

SPE Members
1 Yr.—$10 2 Yrs.—$18 3 Yrs.—$25

Non-Members
*(US and North America)*
1 Yr.—$15 2 Yrs.—$28 3 Yrs.—$40

Non-Members *(Overseas)*
1 Yr.—$25 2 Yrs.—$47 3 Yrs.—$67

# *Table of Contents*

VOLUME 1 • NO. 1

**ABSTRACTS** of Articles in this Issue ---------- 2

**A Study of the Polymerization of Thermosetting Polymers by Electrical Resistivity Techniques** ---------- 3

R. W. Warfield and M. C. Petree, *U. S. Naval Ordnance Laboratory, White Oak, Silver Spring, Maryland*

**Thermomechanical Studies of Amorphous and Crystalline Polymers** ------- 9

A. V. Sidorovich and E. V. Kuvshinskii, *Academy of Sciences, U.S.S.R. Moscow*

**Effect of Hydrostatic Pressure on Polyethylene Melt Rheology** ---------- 14

R. F. Westover, *Polymer Mechanics Section, Bell Telephone Co., Murray Hill, N. J.*

**Ultraviolet Degradation of Plastics and the Use of Protective Ultraviolet Absorbers** ---------- 21

R. C. Hirt, N. Z. Searle and R. G. Schmitt, *American Cyanamid Co., Central Research Division, Stamford, Conn.*

**Mechanisms of Ultraviolet Stabilization of Plastics** ---------- 26

J. H. Chaudet, G. C. Newland, H. W. Patton and J. W. Tamblyn, *Research Laboratories, Tennessee Eastman Co., Kingsport, Tenn.*

**A Study of Weathering of an Elastomeric Polyurethane** ---------- 31

C. S. Schollenberger and K. Dinbergs, *The B. F. Goodrich Company Research Center, Brecksville, Ohio*

**The Effect of Molecular Weight Distribution on the Flow Properties of Polyethylene** ---------- 40

D. R. Mills, G. E. Moore and D. W. Pugh, *Polymer Service Laboratories, U. S. Industrial Chemicals Co., Tuscola, Illinois*

**Hydroxy Alkyl Phosphate Esters as Curing Agents for Epoxy Resins** ------ 47

Marjorie St. Cyr, *Picatinny Arsenal, Dover, N. J.*

**EDITORIAL** Dr. Foster D. Snell, *President, Foster D. Snell, Inc., New York, N. Y.* ---------- 52

# abstracts of articles in this issue

## A STUDY OF THE POLYMERIZATION OF THERMOSETTING POLYMERS BY ELECTRICAL RESISTIVITY TECHNIQUES

R. W. Warfield and M. C. Petree

*U.S. Naval Ordnance Laboratory, White Oak, Silver Spring, Maryland*

Electrical volume resistivity measurements made isothermally during polymerization have been used to study the bulk polymerization of epoxide, polyester, and polyurethane polymers. The overall activation energy ($E_a$) for the polymerization of amine polymerized epoxide polymers has been found to be about 14 to 17 Kcal/mole.

## EFFECT OF HYDROSTATIC PRESSURE ON POLYETHYLENE MELT RHEOLOGY

R. F. Westover

*Polymer Mechanics Section, Bell Telephone Laboratories, Incorporated, Murray Hill, New Jersey*

A description is given of the procedure and equipment used for the purpose of studying the effect of hydrostatic pressure upon the capillary flow properties of polymer melts. Flow properties are reported for a low density polyethylene over a wide range of temperatures, die sizes, different pressures and hydrostatic pressures.

## MECHANISMS OF ULTRAVIOLET STABILIZATION OF PLASTICS

J. H. Chaudet, G. C. Newland, H. W. Patton, and J. W. Tamblyn

*Research Laboratories, Tennessee Eastman Co., Div. of Eastman Kodak Co., Kingsport, Tennessee*

The effectiveness of ultraviolet stabilizers of various types of polyolefin, cellulose ester, and poly (vinyl chloride) plastics was investigated. Most of these stabilizers were of the ultraviolet-absorbing type but two were of the nonabsorbing type. Exposures were made both outdoors and indoors in a Twin-Arc Weatherometer. The latter was modified by the addition of ten 20-watt fluorescent sun lamps to remedy the short-ultraviolet deficiency of the enclosed carbon arcs.

## THE EFFECT OF MOLECULAR WEIGHT DISTRIBUTION ON THE FLOW PROPERTIES OF POLYETHYLENE

D. R. Mills, G. E. Moore*, and D. W. Pugh

*U.S. Industrial Chemicals Co., Tuscola, Illinois*

The non-Newtonian flow behavior of polyethylene has been investigated with respect to the effects of molecular weight and molecular weight distribution. Effects of die geometry on melt fracture as well as preliminary extrudate orientation studies are discussed.

* Now with Keuffel & Esser Co.

## THERMOMECHANICAL STUDIES OF AMORPHOUS AND CRYSTALLINE POLYMERS

A. V. Sidorovich and E. V. Kuvshinskii

Translated from: *Vysokomolekuliarnye Soedineniia* 2, 778-84 (May 1960). A thermomechanical study was made of the softening of crystalline polymers during uniform, uniaxial stretch and also of the effect of the rate of heating upon the softening or amorphous polymers. The effect of the tensile force on the thermo-mechanical behavior of various polymers was measured over the range 20 to 100 kg/cm$^2$ and within wide temperature limits (—150° to 250°C). Ribbons 50 mm long, 2-4 mm wide and 0.05 to 0.5 mm thick served as specimens.

## ULTRAVIOLET DEGRADATION OF PLASTICS AND THE USE OF PROTECTIVE ULTRAVIOLET ABSORBERS

R. C. Hirt, N. D. Searle and R. G. Schmitt

*Central Research Division, American Cyanamid Co., Stamford, Conn*

The degradation of plastics by ultraviolet energy and the use of protective ultraviolet absorbers to improve stability necessitate studies along several lines. These include (a) the measurement of the ultraviolet spectral energy distribution of sunlight and of the indoor accelerated test sources, (b) the measurement of the extent of degradation as a function of the wavelength of the incident radiation, (c) an estimate of the absorbing effectiveness of the added protective agents, and (d) the stability of the protective ultraviolet absorbers themselves.

## A STUDY OF THE WEATHERING OF AN ELASTOMERIC POLYURETHANE

C. S. Schollenberger and K. Dinbergs

*B. F. Goodrich Co., Research Center, Brecksville, Ohio*

A study was designed to show the nature of weathering of an elastomer poly(ester-urethane), and to indicate methods of overcoming the deficiency. Unprotected polymer, when exposed to UV radiation in a Weatherometer, showed deterioration which is characterized by loss of tensile strength, some increase in modulus, and a decreased extensibility of surface skin.

## HYDROXY ALKYL PHOSPHATE ESTERS AS CURING AGENTS FOR EPOXY RESINS

Marjorie C. St. Cyr

*Picatinny Arsenal, Dover, New Jersey*

A new curing system which yields room temperature curing epoxy adhesives with high bond strength and softening point has been developed for service in contact with high explosives. Bisphenol A type resins cured with hydroxyl alkyl phosphate acid esters are used. Short pot life and relatively low alkali resistance are drawbacks of the system.

*clip these briefs for easy reference on 3" x 5" or other suitable filing cards*

# A Study of the Polymerization of Thermosetting Polymers by Electrical Resistivity Techniques

**R. W. Warfield and M. C. Petree**

*U.S. Naval Ordnance Laboratory*
*White Oak, Silver Spring, Maryland*

*This article describes a method for determining rates of polymerization and estimating extent of polymerization*

The increased use of thermosetting polymers has necessitated the development of new experimental techniques for studying the polymerization of these synthetic materials. Because of their polyfunctional nature, the existent methods for studying their rates of polymerization are for the most part empirical and limited in application. The only conventional technique which can be used to yield fundamental data is infrared absorption spectroscopy.

Recent papers (1, 2) have shown how electrical volume resistivity measurements made continuously under isothermal conditions may be used to quantitatively study the bulk polymerization of both amine and acid anhydride hardened epoxide thermosetting polymers. These techniques have now been applied to polyester, polyurethane and two additional amine hardened epoxide polymers. It is of interest to note that while this experimental technique was originally developed to study the polymerization of various thermosetting and thermoplastic polymers, more recently it has proven useful in studying the polymerization of propellant binders for solid propellants (21).

## Theoretical Considerations

Calculation of the overall activation energy for the polymerization process is critically dependent upon conducting the reactions under isothermal conditions. Under these conditions, the electrical volume resistivity of the material is monitored as the polymerization process proceeds. From the data so obtained, the maximum rate-of-change of the logarithm of the electrical resistivity is calculated and taken as an index of the rate of polymerization. An Arrhenius plot of these maximum slopes can then be made and yields a straight line having a slope corresponding to the overall activation energy of the polymerization process. This can be expressed analytically by considering the basic Arrhenius equation

$$k = A \exp\ (-E_a/RT) \qquad (1)$$

The value for k is taken to be $\left[\frac{d\ (\log \rho)}{dt}\right]$ max.

where $\rho$ is the resistivity, t is the time, T is the absolute temperature, A is a constant, and R is the gas constant, 1.987 cal/deg. mole.

It must be noted that, while this experimental technique does not separate the elementary steps of a complicated polymerization process, the calculation of the activation energy for the overall polymerization process represents the first step in the kinetic analysis of these reactions. It is of interest to note that Yamada (4) has used similar procedures to study the polymerization of other thermosetting polymers.

In addition to calculating the activation energy for the polymerization process, the activation energy for the electrical conduction process, $E_e$ can also be determined. $E_e$ is calculated from the slope of a semi-logarithmic plot of resistivity vs. the reciprocal of the absolute temperature.

At low electrical field strengths and at low temperatures conductivity in polymers is predominately ionic due to trace impurities (3). With increasing temperatures, the influence of additional ions arising from thermal dissociation becomes more significant (5). During poly-

merization the mobility of these ions is progressively restricted with a corresponding increase in the resistivity. After polymerization is complete, their mobility is extremely restricted; hence, the high resistivity of the polymers. It has been previously pointed out (1) that ionic mobility as evidenced by the resistivity of the system, does not necessarily decrease in proportion to the increase in the bulk viscosity of the polymer. This may be explained by considering that the viscosity as seen by the small ionized current carriers before gelation is that of the individual polymer chains and that only a small section of this chain need be displaced to allow the ion to diffuse under the influence of the applied electric field. Even after gelation, the initial space network is loose and relatively open in structure, and diffusion of the current carriers is still relatively easy. Only after the crosslinking density has considerably increased and the polymer has acquired a hard set does the rate of change of the resistivity exhibit an abrupt decrease.

## Experimental

### A. Apparatus and Experimental Technique

The continuous current monitoring device (CCMD), which is a simple application of Ohm's law, was used to determine the electrical resistivity of the various materials during and after polymerization. This device consists of a Keithley Model 210 electrometer, a Keithley Model 2008 decade shunt, and a sample cell. This instrumentation is required to monitor the large change in resistivity ($10^8$ to $10^{16}$ ohm-cm), which occurs during polymerization.

The sample cell in which polymerization is conducted consists of two small nickel plated concentric cylinders attached to a Teflon base plate. About 13 grams of the polymer are poured into the space between the cylinders. The sample cell is then placed in a small laboratory oven and isothermal conditions maintained within ±0.5°C during polymerization.

All values of the volume resistivity reported in this paper were made at a field strength of about 225 volts/cm. The temperature dependence of resistivity, before and after polymerization was determined by monitoring the resistivity of the material contained in the cylindrical electrodes as the sample was heated at the rate of about 15°C per hour. The sample cell and the experimental arrangement employed to record continuously the electrical resistivity have been previously described (6, 7, 8).

### B. Materials

The polymers used in this investigation can be defined in terms of starting materials, basic structural unit(s) and epoxide values. The epoxide polymer was Epon 828 (Shell Chemical Corp.) which is prepared from epichlorohydrin and bis(4-hydroxyphenyl) dimethylmethane (commonly known as bisphenol A) (16). The basic structural unit was given by Chapman and co-workers (11). Epon 828 has an epoxide value of 0.54 per 100 grams and a hydroxyl value of 0.08 per 100 grams. This polymer was polymerized by two different hardeners, tri(dimethylaminomethyl)phenol tri(2-ethyl hexoate), [DMP-30-EH] and diethylenetriamine, [DETA]. A polyurethane polymer (Thiokol Chemical Corp.) was also studied. This polymer is a reaction product of a polyester glycol and 2, 4-tolylene diisocyanate which is crosslinked with 40% of castor oil. The polyester polymer, Paraplex P-43 (Rohm and Haas Corp.) consists of 70% of an unsaturated polyester dissolved in 30% of monomeric styrene. The polyester component consists of a condensation polymer which is the reaction product of maleic and phthalic acids with propylene glycol. This linear polymer is crosslinked with styrene using 1% of methyl ethyl ketone peroxide as a catalyst and 2% of cobalt naphthenate as an accelerator. Based on infrared analysis, the basic structural unit is:

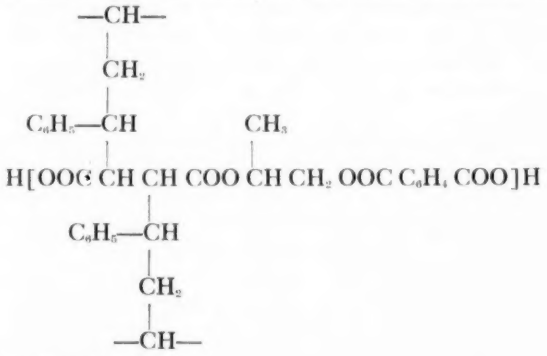


### C. Results

The results of this investigation are shown in *Figures 1 to 6*. *Figures 1 to 4* are semi-logarithmic plots of the electrical resistivity vs. time for a series of bulk isothermal polymerizations of the various systems studied. Whenever possible, each polymerization was conducted beyond the point where gelation occurred. The rate-of-change of the logarithm of the resistivity was temperature dependent, and the maximum slopes of the logarithm of the resistivity vs. time plots were used to prepare the Arrhenius plots shown in *Figure 5*.

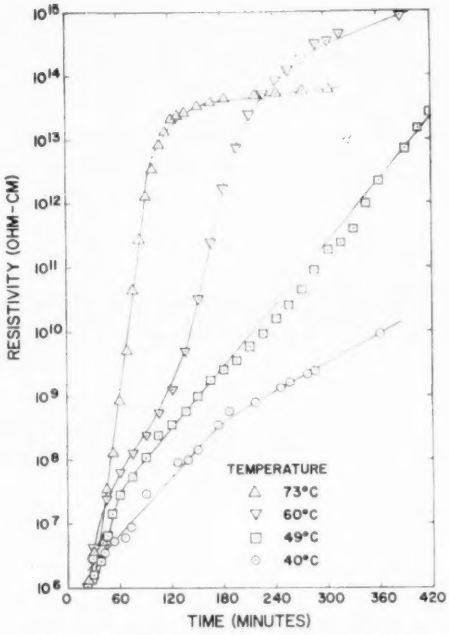


**Figure 1.** Isothermal polymerization of Epon 828 with 13% of tris (dimethylaminomethyl) Phenol tri (2-ethyl hexoate)

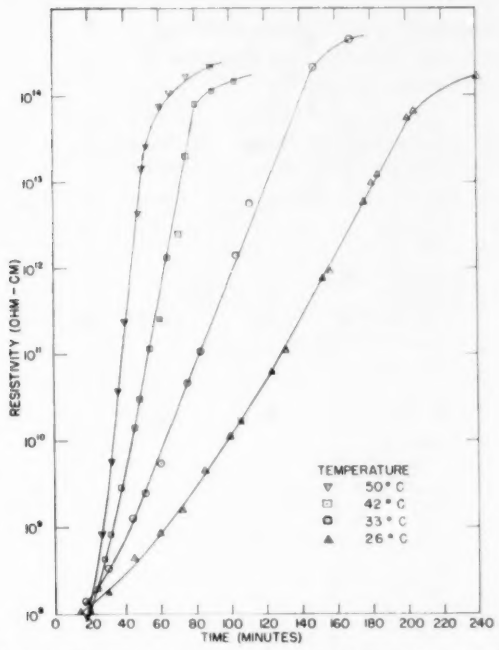


**Figure 2.** Isothermal polymerization of Epon 828 cured with 9.1% diethylenetriamine

The overall activation energies calculated from the slopes of the Arrhenius plots in *Figure 5* are given in *Table 1*, together with the time intervals considered. These values of $E_a$ for the epoxide polymers are in good agreement with published values. Previously $E_a$ was found to be between 11 and 17 Kcal/mole for the polymerization of an epoxide with an amine (2). Yoshida and co-workers (9) have found $E_a$ to be 13.9 Kcal/mole for the copolymerization of an epoxide with a polyester polymer. Belanger and Denham (10) have found $E_a$ to be 12.9 Kcal/mole for the polymerization of an epoxide with piperdine. Chapman, Isaacs and Parker (11) recently studied the reactions of epoxides, similar in structure with those used in polymerization reactions, with a series of amines. They determined Arrhenius parameters for these reactions and found that $E_a$ was between 13 and 14.5 Kcal/mole, except for the reactions of bulky epoxides with bulky amines, which gave values of 15.6 Kcal/mole.

No data are available with which to compare the value of $E_a$ calculated for the copolymerization of the Paraplex P-43. However, the value of 14 Kcal/mole appears very reasonable. The case of the castor oil base isocyanate is similar, in that no published values of $E_a$ are available for polymerizations of this type. The value of 11 Kcal/mole was calculated for the castor oil base isocyanate polymerization and appears reasonable. In comparison, McGinn and Spaunburgh (12) have found, for the reaction of various isocyanates with an adipic acid-diethylene glycol polyester having terminal hydroxyl groups, that $E_a$ will be of the order of 8 to 13 Kcal/mole.

*Figure 6* is an Arrhenius plot of the resistivity vs. the reciprocal of the absolute temperature for the four completely polymerized polymers, as well as for the uncatalyzed liquid Epon 828 and the Paraplex P-43. The activation energies for the electrical conduction process, $E_c$, were calculated from the slopes of these plots and are listed in *Table 1*. These values, ranging from 13 to 140 Kcal/mole, are in good agreement with previous work (2, 13).

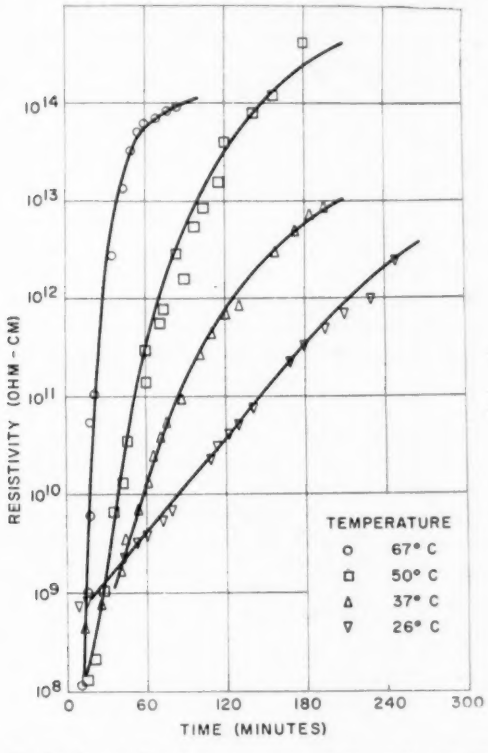


**Figure 3.** Isothermal polymerization of Paraplex P-43 polyester

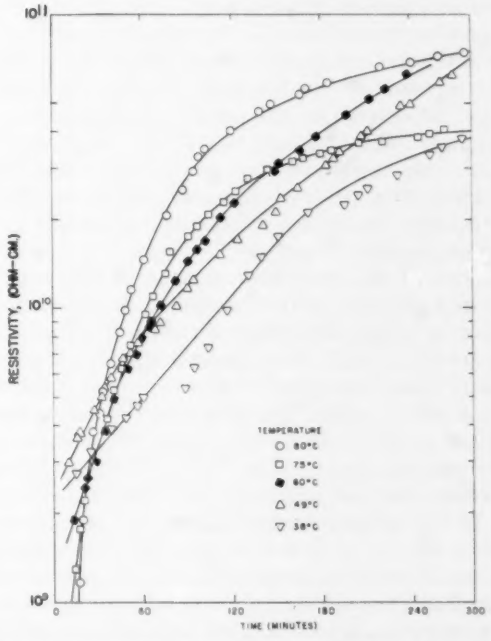


**Figure 4.** Isothermal polymerization of polyurethane polymer

**Table 1. Activation Energy for The Polymerization of Thermosetting Polymers $E_a$, Activation Energy for The Electrical Conduction Process $E_c$ and The Second Order Transition Temperature Tg**

| Polymer | Temperature °C | Time Interval | Maximum Slope ($min^{-1}$) | $E_a$ (Kcal/mole) | $E_c$ (Kcal/mole) | Tg, °C |
|---|---|---|---|---|---|---|
| Epon 828 + DMP-30-EH | 40° | 190-420 min. | $8.7\times10^{-3}$ | 17 | 30 | 67° |
| Epon 828 + DMP-30-EH | 49° | 120-480 min. | $1.67\times10^{-2}$ | | | |
| Epon 828 + DMP-30-EH | 60° | 140-190 min. | $6.00\times10^{-2}$ | | | |
| Epon 828 + DMP-30-EH | 73° | 52-89 min. | $9.26\times10^{-1}$ | | | |
| Epon 828 + DETA | 26° | 129-208 min. | $3.8\times10^{-2}$ | 14 | 140 | 92° |
| Epon 828 + DETA | 33° | 43-142 min. | $5.05\times10^{-2}$ | | | |
| Epon 828 + DETA | 42° | 44-72 min. | $1.07\times10^{-1}$ | | | |
| Epon 828 + DETA | 50° | 33-49 min. | $1.87\times10^{-1}$ | | | |
| Paraplex P-43 | 26° | 20-214 min. | $1.54\times10^{-2}$ | 14 | 46 | 128-130° |
| Paraplex P-43 | 37° | 34-83 min. | $4.08\times10^{-2}$ | | | |
| Paraplex P-43 | 50° | 38-74 min. | $1.00\times10^{-2}$ | | | |
| Paraplex P-43 | 67° | 14-21 min. | $2.86\times10^{-1}$ | | | |
| Polyurethane | 80° | 16-34 min. | $5.56\times10^{-2}$ | 11 | 16 | <30° |
| Polyurethane | 75° | 11-38 min. | $3.70\times10^{-2}$ | | | |
| Polyurethane | 60° | 60-120 min. | $1.52\times10^{-2}$ | | | |
| Polyurethane | 49° | 61-158 min. | $1.03\times10^{-2}$ | | | |
| Polyurethane | 38° | 112-283 min. | $5.84\times10^{-3}$ | | | |
| Liquid Epon 828 | — | — | — | — | 13 | — |
| Liquid Paraplex P-43 | — | — | — | — | 13 | — |

## Discussion of Reactions

The amine polymerized epoxide reactions rapidly proceed to completion at temperatures well below 100°C[2], and in general the slopes of the plots make the calculation of $E_a$ a simple matter. The polymerization of Epon 828 with 13% of tris (dimethylaminomethyl) phenol tri(2-ethyl hexoate), shown in *Figure 1*, is of particular interest because of the chemistry of the amine salt hardener and the polymerization process. Bondi and Parry (14) have studied the mechanism of the polymerization of epoxide polymers when reacted with amine salt hardeners and have concluded that the catalytic activity of this amine is determined by the rate at which the acidic component is esterified by the bulk epoxide monomer. Assuming that this is so, the reaction proceeds in a stepwise manner, the first and rate determining step being predominately an esterification reaction. The rate at which this esterification proceeds determines the rate at which the free amine becomes available for the second or crosslinking step of the reaction.

The end of the esterification stage of this reaction is shown in *Figure 1* by the changes in slope which occur in the early stages of the reaction. The changes of slope, which are temperature dependent, are particularly noticeable after about 60 minutes in the polymerization conducted at 60°C, after 70 minutes in the polymerization conducted at 49°C, and after about 180 minutes in the polymerization conducted at 40°C. Parry and Mackay (15) have observed similar slope changes in the early stages of this polymerization when using a dilatometric technique and the observed changes have been attributed to the mechanism outlined above. This polymerization reaction therefore represents a special case in which the initial step is one of esterification and not of crosslinking. The slopes of the resistivity vs. time plots used to calculate $E_a$ were those of the second or crosslinking step of the reaction. The constant value of the resistivity attained after about 240 minutes for the reaction conducted at 73°C indicates that polymerization was about complete.

The polymerization of Epon 828 with 9.1% of diethylene triamine is shown in *Figure 2*. This cold-setting hardener (16) is a highly reactive primary and secondary polyamine, and polymerizations conducted with it proceed rapidly to completion. This is shown in *Figure 2* where even the polymerization conducted at 26°C is

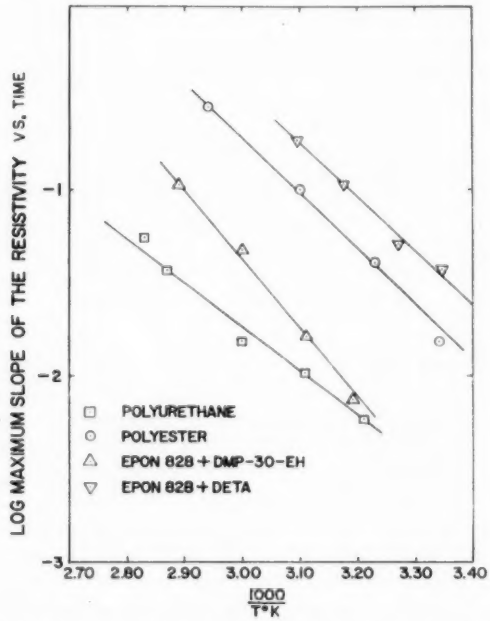


**Figure 5.** Arrhenius plots for the polymerization of thermosetting polymers

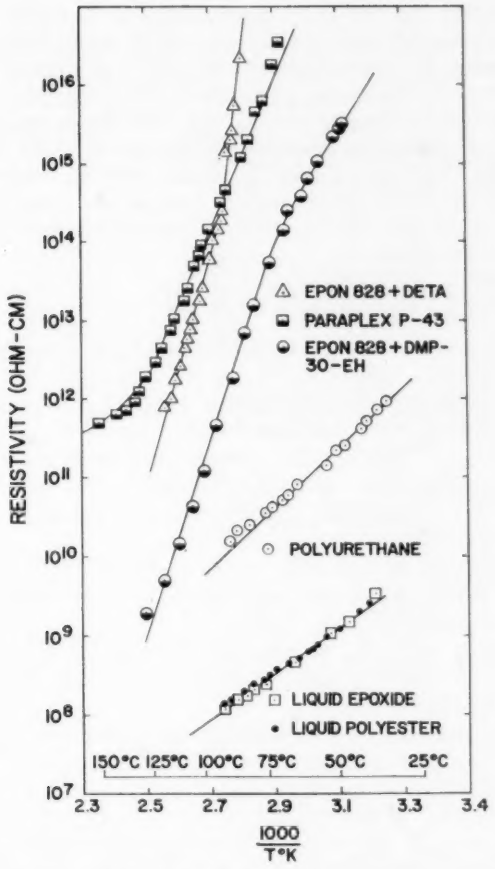


**Figure 6.** Temperature dependence of the electrical resistivity of thermosetting polymers

about complete after 240 minutes. It is believed that the optimum temperature at which to conduct polymerizations with this hardener would be somewhat below 26°C.

It has been observed, when using amines as hardeners for epoxides, that there is no evidence of any induction period. In the epoxide-hardener systems, considered in this and a previous paper (2), the polymerization, as is evidenced by the increase in the resistivity, begins as soon as the liquid polymer and the hardener are mixed. However, in many of the systems studied, a gradual increase to the maximum rate of polymerization was noted, particularly at lower temperatures.

The polymerization of Paraplex P-43 is shown in *Figure 3*. This polymerization proceeds rapidly to completion by means of a free radical mechanism. Source of the free radicals is the 1% methyl ethyl ketone peroxide.

*Figure 4* shows the polymerization of a castor oil base isocyanate polymer. It will be noted that the reactions conducted at 38°C and 49°C exhibit a greater scatter in the data points than is usually found with other polymers, but that the reactions conducted at higher temperatures do not exhibit this scatter. It has previously been observed, when polymerizing at low temperatures, that a scatter will be observed in the data points. This scatter will increase with decreasing temperature, which is believed to indicate that the polymerization is being conducted at too low a temperature.

Comparison of the data in *Figures 1, 2, and 3* indicates that the epoxide and polyester polymerization reactions considered here proceed rapidly to yield highly crosslinked polymers. Polymerization can be considered to be about complete when the resistivity becomes constant with time. The extent of conversion of the epoxide polymerizations is estimated to be of the order of 70 to 90%. A few infrared checks have been made, using the disappearance of the epoxide absorption band at a wave length of 10.92 microns as an index of the extent of conversion (7) and indications are that the conversion of Epon 828 with 13% of DMP-30-EH is of the order of 70 to 90% after about 3 hours at 73°C. Although the polymerization of the castor oil base isocyanate proceeds rapidly to yield a flexible polyurethane, the data in Figure 4 indicate that this polymerization appears to proceed in a more irregular manner than the other reactions considered in this paper.

The assumption has been made that the specific rate of polymerization is proportional to the maximum rate-of-change of the logarithm of the electrical resistivity. This assumption has been considered and discussed in a previous paper (2) and appears reasonable. The shape of a logarithm of resistivity vs. time plot is independent of the electrical field strength over the range 25 to 700 volts/cm.

The temperature dependence of the electrical resistivity of the polymers studied is shown in *Figure 6*. It has been shown (1) that during polymerization the temperature dependence of the resistivity increases with the extent of polymerization. For example, in *Figure 6*, the relatively small temperature dependence of unpolymerized liquid Epon 828 can be compared with the very high temperature dependence of Epon 828 when polymerized with diethylene triamine (DETA). Polymers not completely polymerized will exhibit resistivity vs. temperature plots having the same or slightly reduced slopes and displaced slightly toward lower temperatures. Thus, the temperature dependence of the resistivity and the displacement of the $E_c$ plot can be used as an index of the extent of polymerization.

The resistivity vs. temperature plot in *Figure 6* for Epon 828 polymerized with diethylene triamine (DETA) is of special interest. The activation energy for the electrical conduction process in this polymer was found to be about 140 Kcal/mole. Since this is a considerably higher $E_c$ value than has been found for any other polymer, an attempt to explain this high value must take into consideration not only the basic structure of these crosslinked polymers but also the relationship between the structure of the polymer and the nature of the electrical conduction process.

Recently Erath and Spurr (17) conducted a study of the structure of crosslinked epoxide polymers by means of electron microscopy and concluded that aggregates occur in the solid polymer. These aggregates, which are the active centers for polymerization, are termed "micelles" and are embedded in a matrix of less highly crosslinked polymer.

Polymerization of these polymers is a three-dimensional process which stops when lower molecular weight polymer becomes depleted in the immediate vicinity of the micelle (diffusion control). Since the micelles possess

a greater density than the less crosslinked matrix polymer, it would appear probable that electrical conduction would preferably occur in the matrix material rather than in the micelles. Electrical conduction in these polymers is an ionic diffusion process controlled by an activation energy (5, 13). It thus appears probable that polymers with a high micelle-to-matrix ratio would be expected to exhibit higher $E_e$ values.

The high rates of polymerization exhibited by the system, Epon 828 + DETA, may also be explained by the existence of micelles. Since micelles appear to be the center at which polymerization occurs, it would be expected that a high rate of polymerization would be indicative of the formation or occurrence of large numbers of micelles. Thus, in a rapidly polymerizing system, the large number of micelles present would necessarily result in a solid polymer characterized by a high micelle-to-matrix ratio, i.e., high extent of crosslinking and high $E_e$ values. It has previously been observed that the less highly crosslinked amorphous polymers will exhibit low $E_e$ values. Additional evidence which supports the micelle theory was noted by Erath and Spurr. Silicone polymers when studied by electron microscopy did not appear to contain micelles. Results obtained in this laboratory indicate that silicone polymers have low $E_e$ values. This would be expected of polymers with a low micelle-to-matrix ratio.

The significance of $E_e$ and its relationship to the extent of polymerization and to the structure of these polymers is currently under study. An interesting contribution to this study is a recent paper by Kallweit (18), who has noted, while determining the temperature dependence of the electrical resistance of plasticized polyvinyl chloride, that unexpected increases in the resistance occur in the vicinity of the second order transition temperature. This increase in the resistance has been attributed as due to dipole alignment. Such effects would not be expected in highly crosslinked epoxide and polyester polymers with their rigid molecular structure. However, it does appear that resistivity measurements can be employed to study plasticized crosslinked polymers. In a previous paper (2) the temperature dependence of the resistivity of a polyamide-epoxide polymer was studied, and the results indicated that this crosslinked polymer was internally plasticized.

It will be noted that the expected exponential temperature relationship is exhibited by the polymers shown in *Figure 6*. However, in many of the plots a change in the slope occurs over a relatively narrow temperature range. This change in slope is attributed to a second order transition occurring within the polymer (19). These transitions have been correlated with transitions determined by independent specific heat determinations (19, 20). The second order transition temperatures, Tg, obtained by this resistivity method are given in *Table 1*.

## Summary

The techniques presented in this article for studying the bulk polymerization of thermosetting polymers yield a relatively large amount of practical and theoretical information in a short time with a minimum of equipment. These techniques should prove to be particularly useful in determining rates of polymerization and in estimating the extent of polymerization. A further suggested use for these techniques would be in evaluating the reactivity of crosslinking catalysts. A number of other experimental techniques have been developed to follow the course of these reactions, but with the exception of infrared absorption spectroscopy none will yield fundamental data. It appears that the method employing electrical resistivity represents one of the most useful approaches in studying the bulk polymerization of thermosetting polymers.

## Literature References

1. Warfield, R. W., and Petree, M. C., *J. Polymer Sci.*, *37*, 305 (1959).
2. Warfield, R. W., and Petree, M. C., Paper presented at the 136th National Meeting, American Chemical Society, Atlantic City, New Jersey, September 1959.
3. Fineman, M., and Puddington, I. R., *Ing. Eng. Chem.*, *39*, 1288 (1947), *Can. J. Research*, *B25*, 101 (1947).
4. Yamada, S., *Bull. Chem. Soc.* Japan, *27*, 479 (1954). Yamada, S., and Hayashi, S., *Bull. Chem. Soc.* Japan, *31*, 503 (1958).
5. Kallweit, J. H., *Kunststoffe*, *47*, 651 (1957).
6. Aukward, J. A., and Warfield, R. W., *Rev. Sci. Inst.*, *27*, 413 (1956).
7. Aukward, J. A., Warfield, R. W., and Petree, M. C., *J. Polymer Sci.*, *27*, 199 (1958).
8. Warfield, R. W., *SPE Journal*, *14*, No. 11, 39 (1958).
9. Yoshida, Y., Nakatsuka, R., and Oshima, K., Kagaku to Kogya, *31*, 289 (1957), C. A., *52*, 2446 (1958).
10. Belanger, W. J., and Denham, J. H., Paper presented at 134th Meeting of the American Chemical Society, Chicago, Ill., September 1958.
11. Chapman, N. B., Isaacs, N. S., and Parker, R. E., *J. Chem. Soc.*, 1925 (1959).
12. McGinn, C. E., and Spaunburgh, R. G., Paper presented at 130th Meeting of the American Chemical Society, Atlantic City, N. J., September 1956.
13. Warfield, R. W., and Petree, M. C., *NavOrd Report 6246* (1958).
14. Bondi, A., and Parry, H. L., *J. Phy. Chem.*, *60*, 1406 (1956).
15. Parry, H. L., and MacKay, H. A., *SPE Journal*, *14*, No. 7, 22 (1958).
16. Allen, F. J., and Hunter, W. M., *J. Applied Chem.*, *7*, 86 (1957).
17. Erath, E. H., and Spurr, R. A., *J. Polymer Sci.*, *35*, 391 (1959).
18. Kallweit, J. H., *Naturwissen*, *45*, 384 (1958).
19. Warfield, R. W., *SPE Journal*, *15*, No. 8, 625 (1959).
20. Warfield, R. W., Petree, M. C., and Donovan, P., *SPE Journal*, *15*, 1055 (1959).
21. Warfield, R. W., J. Amer. Rocket Soc., *30*, 427 (1960).

## Acknowledgment

The authors would like to express their appreciation to Mr. Thomas J. Wade for valuable assistance in the experimental phase of this work.

# Thermomechanical Studies of Amorphous and Crystalline Polymers

A.V. Sidorovich and E.V. Kushinsky

*Institute for High-Molecular Compounds,*
*Academy of Sciences, USSR*

During derivation of a new high-molecular weight compound, there always arises the need to determine its state of aggregation and isomerization, as well as its temperature as a function of deformability. Based on these data, one may offer a hypothesis on the place which the newly synthesized material should take in relation to previously identified elastomers and plastics. The aim of our present work is to ascertain to what degree thermomechanical studies can help to solve this problem in the field of plastics.

## Description of Creep Tests

Under thermomechanical investigations of polymers we shall understand the drawing of creep curves (i.e., gradual increases of deformation), while maintaining conditions of constant load and increasing temperature at a fixed rate.[1]

We have previously described the apparatus for thermomechanical study of polymer coatings by a uniform, uniaxial stretch procedure (4). With heating accelerated to 60° per hour, we studied the influence of stress (in the range from 20 to 100 kg/cm²), preceded by elongation (orientation). It became evident what kinds of complications would be caused by structural regularity processes, which arose while heating the samples during the time of measurement.

In this paper, we present results of our research into crystalline polymers, as well as data on the influence of rate of heating on the thermomechanical curves of not only amorphous, but also crystalline polymers.

As before, thermomechanical studies were conducted during uniform, uniaxial stretching of samples under constant force.[2] In addition to the former test device (4), we also utilized improved apparatus (5).

As specimens, we used strips of coating 50 mm long, 2-4 mm wide, and 0.05 to 0.5 mm thick. Programming of the temperature regulating device assured linearity during the time of temperature increase in the −150° to +250° range at rates variable between limits from 0.4° per hour to 100° per hour (5).

## Amorphous Polymers

Thermomechanical curves of amorphous, linear, isotropic polymers (of the atactic polystyrene and the polymethylacrylate type) are characterized by the presence of an inflexion—of suddenly increasing deformation upon attainment of a pre-determined temperature—the softening point (*Figure 1, curve 1; Figure 3a, curve 1*). It can be simply shown that the increased deformation

[1] Sometimes this term is also applied to the measurement of temperature as a function of pliancy (deformation related to stress), or, conversely, its increase as a modulus of deformation—in a series of tests of discontinuous loading during periodic, stepwise increases of temperature (1). Such a set of experiments has been conducted by many investigators, who cannot be listed individually (2, 3). Having become aware of the specific functions of thermomechanical study and its significance as a unique, short-cut method, we propose the method outlined above.

[2] Stretch was determined like strain, relative to the original size of specimens.

*Translated especially for SPE TRANSACTIONS from "Vysomolekulyarnye Soedineniya" High Molecular Compounds, Vol. 2, No. 5, p. 778, 1960*

*by Harvey F. Fireside*
*Cyanamid International, New York, N. Y.*

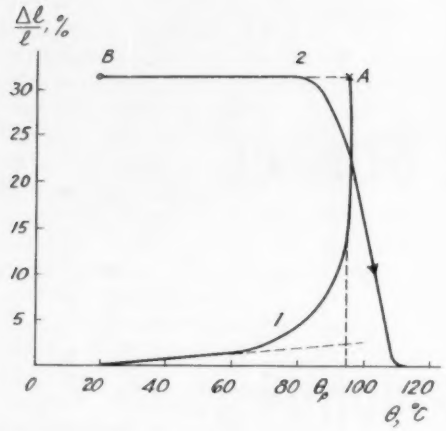


**Figure 1.** Polystyrene

KEY: Curve 1—Thermomechanical curve at stress of 50 kg/cm².
A—Point of initial cold-flow.
Curve 2—Repeated heating of specimen during extended stress.

has a creep of viscoelastic nature. Let us look for example, at the data in connection with polystyrene (*Figure 1*). Curve 1 = the initial thermomechanical curve of the specimen. At point "A" the experiment was discontinued. The sample was "frozen" (i.e., abruptly cooled). At point "Б" it was discharged. Curve 2 represents the change in length during post-heating of the discharging sample. The sample contracted to its original size upon reaching a temperature of approximately 112°C. It is apparent that, at temperatures greater than 80°, when molecular rearrangement begins to proceed with remarkable speed, the increased deformation "starts to freeze." Its disappearance in effect causes the contraction of the specimen. If a frozen sample is discharged, after that charged while its length is held constant, then one may observe the formation of tensile stress and its subsequent relaxation (4). All this means essentially: the growth of deformation creep in the softening region fundamentally reflects the establishment of viscoelastic deformation, accelerated at a fixed temperature.

As the experiment shows, the rate of establishing deformation rises quickly with stress. But it changes even more suddenly in accordance with temperature. Therefore, a change in the magnitude of tensile force, as well as a change in the rate of heating, shifts the thermomechanical curve somewhat along its temperature axis, without any appreciable alteration of its shape.

The position of the curve's inflexion can be fixed more accurately by calculating the point of intersection of extended linear sections of the curve. At this juncture, it is possible to determine the softening point "$\theta_p$", as shown in *Figure 1*. Then, by changing the temperature $\theta_p$, it is easy to specify the influence of various factors on the softening of amorphous polymers. From *Figure 2*, it is evident that in the case of polyethyleneterephthalate, for example, a rise in tensile force of 100 kg/cm² is accompanied by a 10° drop in temperature $\theta_p$, while slowing down heating to 37 at once lowers $\theta_p$ by 4°. The influence of the heating rate is still less in the case of styrene-butadiene (SKS-80) copolymer. Similar quantitative principles apply to the other amorphous polymers, (4).

In the case of amorphous linear polymers, the rate of increasing deformation varies with temperature very abruptly. Therefore, loss of the original shape of an article made of polymeric material is determined fundamentally by temperatures, regardless of any change in conditions of stress. An analogous rule applies to softening point. This explains why at different softening points, determined by standard methods, it is possible to predict how amorphous polymeric materials behave, in regard to the upper limit of their operating temperature.

## Crystalline Polymers

As far as crystalline polymers were concerned, we found the following to hold true: Isotactic polypropylene, polytetrafluoroethylene and polyethyleneterephthalate are distinguished by their vitrification temperature (corresponding to their softening point), as well as by their melting point. They were tested in the form of a commercially produced coating.

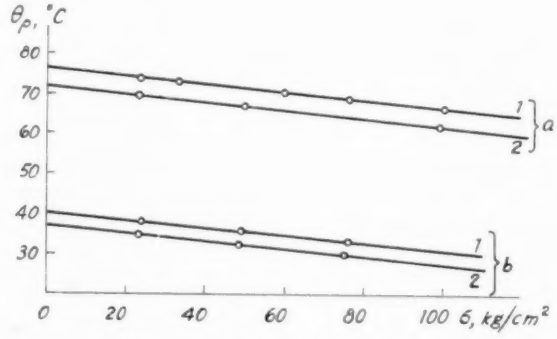


**Figure 2.** Relation of Softening Point to Stress at Different Warmup Rates

KEY: Curve 1 and 2—60° and 1.6° per hour
*a*—Amorphous polyethyleneterephthalate
*b*—Copolymer of butadiene-styrene SKS-80

A film of polyethyleneterephthalate was extruded amorphously. We accomplished its crystallization by heating to temperatures of 115° and 180°. By varying the warmup times, it was possible to obtain samples with differently constituted crystalline phases. By increasing the time of heating, we could observe the progressive cloudiness of samples.

Data for the thermomechanical curves in *Figure 3* were obtained for polyethyleneterephthalate exposed to different processing temperatures and stressed at 50 kg/cm².

Heating the sample to 115° in the course of 10 minutes has only a slight effect on the shape of the thermomechanical curve, displacing it to the side of greater temperatures. Increasing warmup time to 20 minutes causes a substantial change in the curve: its high-temperature segment becomes less steep.

It is known that quick growth of crystals precedes the induction period. Apparently at 115° this period is about 10 minutes, thereby explaining the steep nature of the curve for samples heated for 10 and 20 minutes. In the

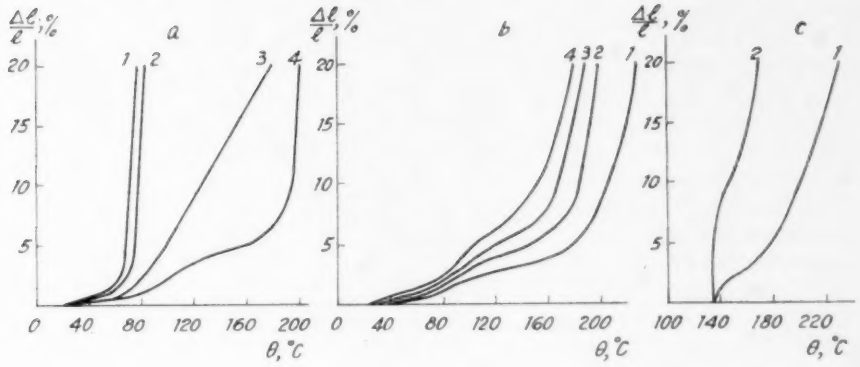


**Figure 3.** Polyethyleneterephthalate. Thermomechanical Curves of Specimens Exposed to Preliminary Heat Treatment:
KEY: *a*—stress of 50 kg/cm² strain
Curve 1—Amorphous specimen
Curves, 2, 3—Specimens preheated 10 or 20 minutes at 115°
Curve 4— Specimen preheated 1 hour at 180°
*b*—Specimens preheated 1 hour at 180°
Curves 1, 2, 3, 4—Stresses of 25, 50, 75, 100 kg/cm²
*c*—Specimens preheated 1 hour at 180°, with temperature at beginning of experiment at 135°
Curves 1, 2—Stresses of 25 and 100 kg/cm²

initial phase of the experiment, some polymers may develop additional crystallization. It proceeds with notable speed in polyethyleneterephthalate, for example, commencing at a temperature "$\theta$" of about 110°. Crystallization in the course of measurement ought to counteract the development of deformation and lessen the steepness of the thermomechanical curves. This phenomenon indeed takes place with polyethyleneterephthalate, as shown by *curve 3 of Figure 3a*.

The extent of the crystalline phase is undoubtedly considerable for specimens heated for 1 hour at 180° (curve 4). This is evidently reflected by origination of the thermomechanical curve in the intermediate temperature region, relative to its sloping section.

## High Temperature Behavior

From the data presented, it can be seen how markedly thermomechanical curves change in the high-temperature region under increasing degrees of crystallization of the polymer. At the same time, however, the curves do not change as much in the low-temperature regions (lower than $\theta_c$).

Part b of *Figure 3* presents a series of thermomechanical curves for polyethyleneterephthalate, crystallized at 180° by initial heating for 1 hour. Analogous curves were obtained for other crystalline polymers, including isotactic polystyrene. From these illustrations, it is evident that, ordinarily, thermomechanical curves of amorphous and crystalline polymers are distinguished by two temperature regions, corresponding to a sharp increase in their deformability.

The inflexion of the curves in the low-temperature region (at about 80° for polyethyleneterephthalate) is clearly due to softening of the amorphous component; i.e., by the transformation of the amorphous component of the polymer from a vitrified to a highly elastic state. The presence of the free, amorphous component of crystallizing polymers is undoubtedly the basic cause determining their cold flow—the relatively great deformability of crystalline polymers at temperatures higher than vitrification temperature.

Their high-temperature section—the sharp rise of curves at elevated temperatures ($\theta > 160 \div 180$ for polyethyleneterephthalate)—is apparently connected with the decreasing degree of crystallinity and with changes in plastic properties at an approach to the so-called temperature of complete melting of the crystalline component of the polymers.

It is apparent from *Figure 3a*, that (as was to be expected) to the extent that the crystallinity of polyethyleneterephthalate increases, its cold flow decreases and the breakdown of thermomechanical curves in the region of vitrification temperature grows weaker.

Apparently for polymers having a major portion in the crystalline phase the breakdown can practically disappear. For them, the low-temperature section of the thermomechanical curves may pass smoothly into the mid-temperature section. Actually, for polymers whose crystallization proceeds quickly and who have a high degree of crystallization potential—like polyethylene and isotactic polypropylene—thermomechanical curves are in the negative temperature region (where one should find their vitrification temperatures) at extremely sloping angles (*Figure 4a, and 5a*). With difficulty, one can

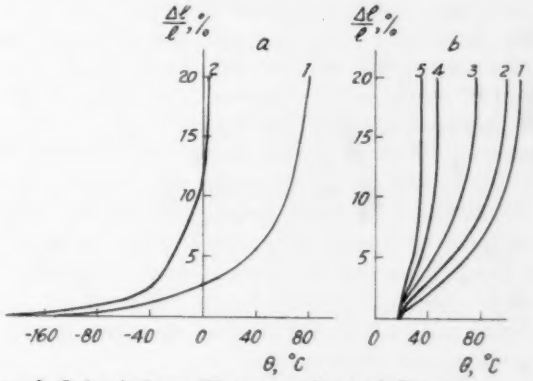


**Figure 4.** Polyethylene. Thermomechanical Curves
KEY: *a*—Temperature at beginning of experiment = 150°
Curve 1, 2—Stresses of 25 and 100 kg/cm²
*b*—Temperature at beginning of experiments = 20°
Curve 1, 2, 3, 4, 5—Stresses of 5, 10, 28, 50, 80 kg/cm²

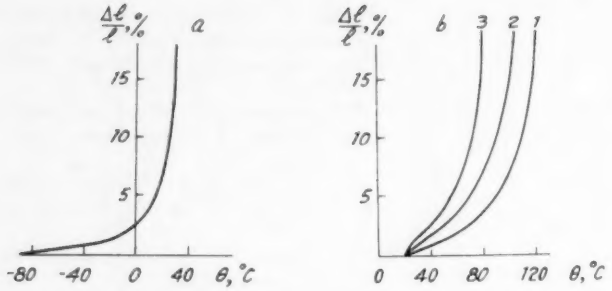


**Figure 5.** Isotactic Polypropylene. Thermomechanical Curves
KEY: *a*—Temperature at beginning of experiment = 80°, stress = 100 kg/cm²
*b*—Temperature at beginning of experiment = 20°
Curves 1, 2, 3—Stresses of 25, 35, 50 kg/cm²

make out a slight change in slope for polyethylene at $\theta = -95° \div -90°$, indicating that its amorphous component is softening. Dilatometric measurements of polyethylene show a slight inflexion in the curve for temperature coefficient as a function of volume expansion caused by heat, also located at $\theta = -80° \div 95°$ (6).

For a study of amorphous polymers whose softening point and hardening point were located in a narrow temperature range, the starting point for thermomechanical investigation had to be chosen below vitrification temperature ($\theta_c$). Crystalline polymers lose rigidity very gradually; therefore, the initial temperature could be chosen either lower or higher than $\theta_c$. The temperature of initial testing was clearly reflected by the shape of the thermomechanical curves. *Figure 3b* shows thermomechanical curves of crystalline polyethyleneterephthalate for experimentation, which was initiated at temperature $\theta = 135°$; i.e., located in the region between vitrification temperature and complete melting. Analogous functions are shown in *Figure 4a, 5b and 6*, for other crystalline polymers: Polyethylene, isotactic crystalline polypropylene, and polytetrafluoroethylene. Experiments with these polymers were initiated at a temperature $\theta = 20°$, located above their vitrification temperatures. From these illustrations, it is apparent that in all cases, thermomechanical curves consist solely of a single, steep, high-temperature branch.

The shape and location of thermomechanical curves for crystalline polymers indicates to a great degree the amount of tensile stress (*Figures 3, 4, 5, 6*). In experiments initiated at temperatures greater than vitrification temperature (*Figures 3c, 4b, 5b and 6*), at a pressure of $25 \div 100$ kg/cm² during the period the load was applied, the increase in deformation proceeds so quickly, that the curves begin as though from intermittently increased deformation. Subsequently, the increase of deformation proceeds much more slowly. In the following sections of the curve, a doubling of stress produces a tripling—even quadrupling—of deformation.

Data on the creep of crystalline polymers, obtained from tests of loading at constant temperature, show that the increase in deformation of protractedly loaded specimens proceeds with greater stress, but to a degree not exceeding stress (7, 8). Analogous findings can be de-

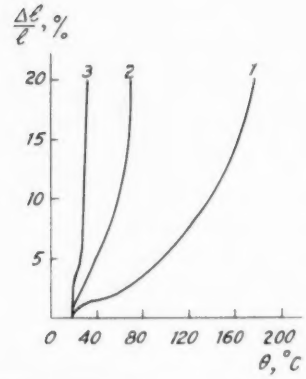


**Figure 6.** Polytetrafluoroethylene. Thermomechanical Curves. Temperature at Beginning of Experiments = 20°C.
KEY: Curves 1, 2, 3—Stresses of 25, 50, 75 kg/cm²

rived from thermomechanical curves obtained in tests initiated at lower than vitrification temperature.

Other observations were made for amorphous polymers during softening. For them, the relation of deformation to level of stress is unquestionably much closer. In addition, thermomechanical curves of these polymers undergoing increased stress are displaced only to a negligible degree by temperature. A change in the rate of heating likewise exerts little influence. These principles have this stipulation: that, for amorphous polymers in the softening range, the relation of rate of deformation to temperature is tremendous. (An increase of $1 \div 2°$ regularly causes a change in the rate.) Therefore, slight "shifts" in accordance with temperature may compensate for the influences of changing stress and changing rate of heating.

The behavior of crystalline polymers is completely different. From *Figure 7*, it is apparent that a twenty-fold increase in the heating rate (i.e., shortening by a factor of 20 the time a specimen remains under load in a given temperature range) may be compensated by a displacement of 6-10° in the direction of greater temperature. (In the case of amorphous polymers—see *Figure 2* and reference 4—for such an ample displacement at 1.5-2.5°.) Consequently, crystalline polymers in the cold-flow region, (i.e., at higher than vitrification temperature) evince

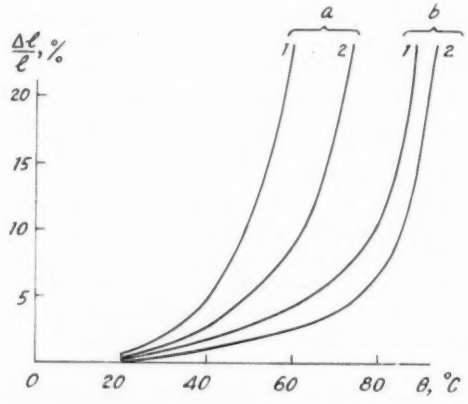


**Figure 7.** Polyethylene. Thermomechanical Curves at Warmup Rates of 1.5° per hour and 30° per hour = Curves 1, 2
KEY: Stresses *a* = 30, *b* = 10 kg/cm²

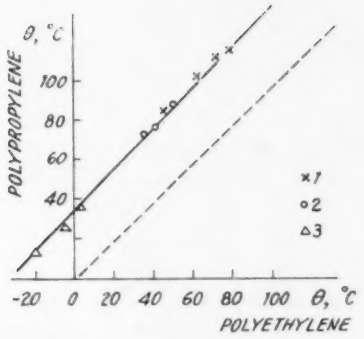


**Figure 8.** Polyethylene and Isotactic Polypropylene—Comparison of Relationship of Deformable Properties
KEY: 1 = 30, 2 = 50, 3 = 100 kg/cm²

a comparatively sloped temperature function plotted against rate of creep. (The increase in this rate is of a magnitude corresponding to a temperature rise of 10-15°.) Precisely for that reason, attainment of a given increase in deformation during reduced tensile stress requires warmup of polymers to much more highly elevated temperatures (see *Figure 6*).

For crystalline polymers, the level of stress-strain substantially changes the form of the thermomechanical curve. From the data of *Figure 4b*, it is apparent that thermomechanical curves begin to slope at a stress of 5-10 kg/cm², very markedly so at 80 kg/cm². Interaction of the influences of stress and temperature may determine the displacement in temperature, corresponding to the specimen's attaining a given elongation—for example, 20 per cent. Thus, for polyethylene, a change in stress from 5 to 80 kg/cm² causes displacement of its temperature from 105 to 30°—i.e., a 75° shift. It is even greater in the case of polytetrafluoroethylene (*Figure 6*): changing the stress from 25 to 75 kg/cm² causes a displacement of 154°.

## Polyethylene vs Polypropylene: Processing Temperature

The complexity of the thermomechanical behavior of crystalline polymers does not permit us to characterize it through an indication of only a single parameter—the softening point. However, based on thermomechanical curves, it is possible in this case to contrast the deformability properties of different polymers. For monotypic crystalline polymers, one can determine exactly to what extent the processing temperature of materials is affected by identical mechanical influences. In *Figure 8*, such a comparison is made for polyethylene and isotactic polypropylene. Along the axes are plotted temperatures corresponding to a given amount of deformation during identical stress of polyethylene on the abscissa—and isotactic polypropylene—on the ordinate. It is evident from these data that all the points lie on a straight line, displaced by 35° relative to the broken line which denotes a material identical to polyethylene in deformative properties. The shift of 35° indicates that the range of processing temperature for isotactic polypropylene is 35° higher than for polyethylene.

This is supported by results of previous investigations. Thermomechanical studies of amorphous polymer-plastics permit us to ascertain the softening point (as indicated by disappearance of the vitreous state, to detect previous elongation and the presence of structural processes [Lit. Ref. 4].

In order to determine reproducibly the softening point of amorphous polymers with about 1° error, it is necessary to maintain stress with ±5 kg/cm² precision, and warmup rates with ±50%.

For crystalline polymers, thermomechanical studies allow us to determine: a) the softening point of their amorphous segment, b) the temperature level of complete fusion (upper and lower limits) of the crystalline segment of polymers, c) the location of the cold-flow range, d) discrimination of the thermostability of monotypic materials (by the temperature displacement of their thermomechanical curves) (see *Figure 8*). Gathering more extensive data about polymers with various degrees of crystallinity undoubtedly will make it possible to utilize thermomechanical curves for an estimate of the degree of crystallinity of the polymers under investigation. For crystalline polymers, the conditions for reproducibility of thermomechanical curves are more difficult than for amorphous polymers. Nonetheless, their momentum under stress and their rate of warmup further indicate the feasibility of displacing discrete sections of thermomechanical curves within ±3 ÷ 5° limits.

## Conclusions

1. Studies were conducted on the softening of crystalline polymers by the thermomechanical methods, during uniform, uniaxial strain.

2. The thermomechanical behavior of crystalline polymers was found to differ significantly from that of amorphous polymers.

3. Basic characteristics of crystalline polymers were determined utilizing the thermomechanical method.

## Literature References

1. Kargin, V. I., Sogolova, T. I. Jour. Phys. Chem. Vol. 23, p. 530, 1949.
2. Kobeko, P. P., Kuvshinsky, E. V., Gurchevich, G. K., Reports of Acad. of Sci. USSR, Phys. Series, Vol. 3, p. 329, 1937.
3. Zhurkov, S. N., Lerman, R., Reports of Acad. of Sci. USSR, Vol. 47, p. 109, 1945.
4. Sidorovich, A. V., Vashchenko, V. S., Kuvshinsky, E. V., Jour. of Phys. Tech., Vol. 29, p. 514, 1949.
5. Sidorovich, A. V., Kuvshinsky, E. V., Lab. Bull., Vol. 26, p. 100, 1960.
6. Hunter, E., Oakes., W. G., Trans. Faraday Soc., Vol. 41, p. 49, 1945.
7. Polyethylene, London, Iliffe & Sons Ltd., 1957, p. 155.
8. Jean-Claude Millard, Industrie des Plastiques Modernes, Vol. 10, p. 31, 1958.

# Effect of Hydrostatic Pressure on Polyethylene Melt Rheology

R. F. Westover

*Polymer Mechanics Section*
*Bell Telephone Laboratories, Inc.*
*Murray Hill, New Jersey*

*Research on capillary flow behavior of polymers over a range of hydrostatic pressures up to 25,000 psi, over a wide range of temperatures, and with capillary diameters of 0.055, 0.090, and 0.125 inches*

The importance of the flow behavior of polymer melts over a wide range of temperatures, shear rates and die geometries has been well recognized and has stimulated numerous investigations. It has also been recognized, but not well documented, that pressure and time can have their effect upon the apparent viscosity and other flow properties of the polymer melt. A recent paper by Maxwell and Jung (1) has shown the effect of hydrostatic pressure upon the apparent viscosity of branched polyethylene and polystyrene at a constant shear stress and a single temperature for each material. Their results have shown that in the range of pressures found in present day processing equipment the effect of hydrostatic pressure should not be neglected.

Thermal energy is applied to a polymer to increase the distance between molecules and thereby reduce the inter- and intramolecular forces and their accompanying resistance to shear within the polymer melt. If pressure is applied to the melt there is a time dependent decrease in volume which has the effect of producing a higher viscosity in the melt than the temperature alone would warrant. If the melt temperature is low enough or if the pressure is high enough the melting point of the polymer can be raised to or above the polymer temperature by this application of pressure. Thus a time dependent crystallization can be induced in the polymer so that we would no longer have a true melt at a normal melt temperature.

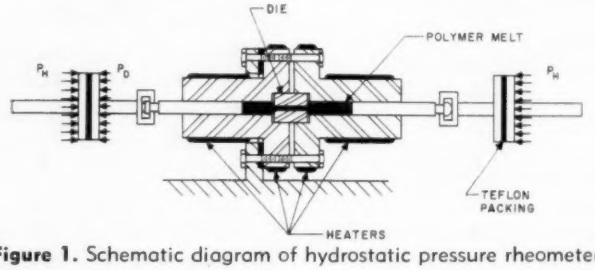


**Figure 1.** Schematic diagram of hydrostatic pressure rheometer

## Research Methods

For the purpose of this investigation a rheometer was designed and constructed to study the so-called capillary flow behavior of polymers over a range of hydrostatic pressures up to 25,000 psi, over the same range of differential pressures, over a wide range of temperatures and with inside die diameters of 0.055, 0.090, and 0.125 inch. Adding this new dimension of hydrostatic pressure to the already time consuming task made it essential that some degree of automation and labor saving be incorporated in the design.

A simplified schematic of the rheometer is shown in *Figure 1*. Twin split type heat chambers equipped with heaters and temperature controllers are bolted firmly together about an enclosed die. These chambers are aligned and secured to the main frame of the machine. A pair of specially constructed, low friction hydraulic cylinders are located at opposite ends of the rheometer in line with the heat chambers and die. One end of each of these hydraulic cylinder rods is coupled to one of the close fitting rams extending into the one inch bore of the heat chamber sections.

Discs of polymer punched from compression molded sheets are stacked tightly together to eliminate trapped air and are inserted under moderate pressure into the chamber on one side of the die. As the polymer starts

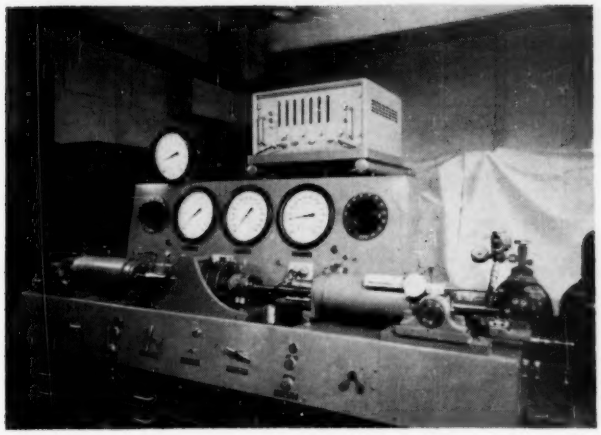

**Figure 2.** Photograph of rheometer in semiautomatic operation

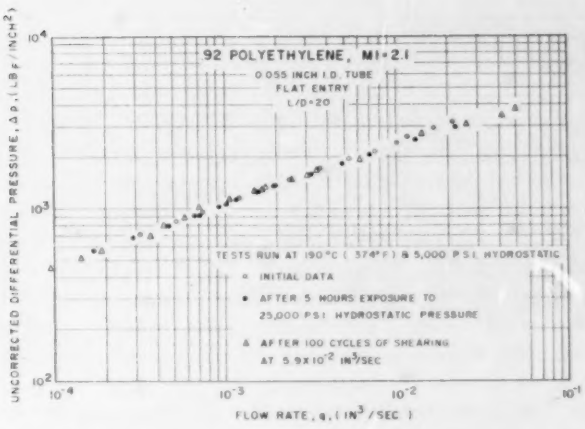
92 POLYETHYLENE, MI=2.1
0.055 INCH I.D. TUBE
FLAT ENTRY
L/D=20
TESTS RUN AT 190°C ( 374°F ) & 5,000 P.S.I. HYDROSTATIC
INITIAL DATA
AFTER 5 HOURS EXPOSURE TO 25,000 P.S.I. HYDROSTATIC PRESSURE
AFTER 100 CYCLES OF SHEARING AT 5.9X10⁻² IN³/SEC
UNCORRECTED DIFFERENTIAL PRESSURE, Δp, ( LB F / INCH² )
FLOW RATE, q, ( IN³ / SEC )

**Figure 3.** Effect of time, temperature and pressure history on melt flow properties

to melt, some of the melt passes through the die to come in contact with the other ram. After thermal equilibrium has been reached a hydrostatic pressure is exerted upon the melt by allowing oil at a pressure, $P_H$, controlled by pressure from a regulated nitrogen source, to enter the extreme ends of the hydraulic cylinders. Since the two rams and the two hydraulic pistons are respectively equal in area, the polymer melt experiences equal pressures on both sides of the die.

A differential pressure across the die is applied by allowing a lesser regulated nitrogen pressure, $P_D$, to act upon the inside face of either one of the hydraulic pistons *(Figure 1)*. This upsets the balance so that while the hydrostatic pressure remains constant at the entrance side of the die it is reduced at the exit side allowing flow to take place. Since the application of the differential pressure is independent of the system for applying the hydrostatic pressure, no reliability is sacrificed in the differential pressure vs flow rate data by testing at high hydrostatic pressures.

The photograph of the rheometer *(Figure 2)* shows the hydraulic cylinders to be trunnion mounted to allow for the occurrence of slight bending of the I-beam which serves as the backbone of the machine. The flow rate is determined by the volume swept out by the ram at the entrance side of the die. A digital timer is started and stopped by two specially built switches located 0.100 inch apart. These switches are opened by projections from the extreme ends of the hydraulic cylinder rods. The distance between switches is known to ½%. At the same time that the timer is stopped the differential pressure is automatically removed to conserve the charge of melt.

Preliminary tests made at high pressures and high temperatures revealed leakage of polymer along the rams. Three or four thin discs of Teflon punched to the same size as the bore of the heat chambers were added between the rams and the polymer to act as piston rings or wipers. The thermal expansion and the pressure on these discs eliminated the leakage for temperatures up to 250°C (482°F) with only a low friction force between the Teflon and the chamber wall.

A typical test run would be conducted as follows: After the heat chambers and die have come to thermal equilibrium, a charge of polymer discs followed by Teflon discs is loaded in one chamber under a pressure of a few hundred pounds per square inch. As some of the charge flows through the die the Teflon disc seals and the other ram are inserted and subjected to the same hydrostatic pressure until the sample has come to thermal equilibrium. This requires twenty-five or thirty minutes for polyethylene. Upon reaching the desired temperature the sample is then subjected to the desired test hydrostatic pressure. The bulk viscosity of the material does not permit an instantaneously complete volume change with pressure. A sufficient amount of time, usually five minutes, must be allowed until no motion of the ram on the charged side of the rheometer is observed on the dial type micrometer shown on the right in *Figure 2*. When the hydrostatic pressures are high enough to induce crystallization within the melt, then as much as 30 minutes may be required between tests run at different hydrostatic pressures.

The differential pressure is applied after the sample polymer has been temperature and pressure equilibrated. Flow rate measurements are not made until a sufficient amount of material has flowed through the die to allow a definite flow stream to be established at the entrance to the die. After observing the time required for the ram to advance the specified distance the differential pressure is increased and the same procedure is repeated. Ten to twenty flow rate determinations can be made before the major portion of the charge is pushed to the exit side of the die. The charge can then be pushed back through the die to return the rams to their original starting positions and the whole process of establishing flow lines and taking flow rate determinations at various differential pressures is continued. After completing the test at this one hydrostatic pressure the same procedure is repeated for other hydrostatic pressures. Before testing the poly-

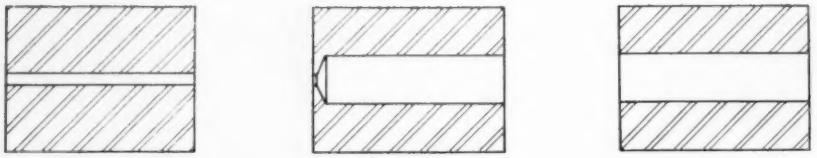
TUBE
PROVIDES BASIC UNCORRECTED PRESSURE-FLOW RATE DATA FOR WHICH CORRECTIONS SHOULD BE MADE TO PERMIT STUDIES OF FLOW WITHIN THE DIE
ORIFICE
CORRECTS DIFFERENTIAL PRESSURE FOR ENTRANCE LOSSES, RHEOMETER LOSSES, AND MELT RESERVOIR LOSSES
1" BORE
CORRECTS DIFFERENTIAL PRESSURE FOR RHEOMETER LOSSES AND MELT RESERVOIR LOSSES

**Figure 4.** Dies for the separation and study of pressure components or corrections

mer at another temperature the rheometer is cleaned and recharged with a new sample.

Questions may arise at this point in the reader's mind. Can leaving the polymer sample in the rheometer for two or three hours to conduct an extensive test be justified? Will ten passes through the die even at a low rate of flow degrade the sample? Does the polymer have any memory for its past pressure history in the melt stage?

The answers to these questions are shown graphically in *Figure 3*. Very little shear or thermal degradation is observed after 100 cycles of the most severe shearing, or after five hours of thermal and high pressure exposure. No permanent viscosity change due to the exposure to high pressure was observed. As an additional check on the effect of shear upon the sample, after the charge has been made ready for a new cycle through the die, repeat tests are made under the same conditions as those tests made just prior to the recycling.

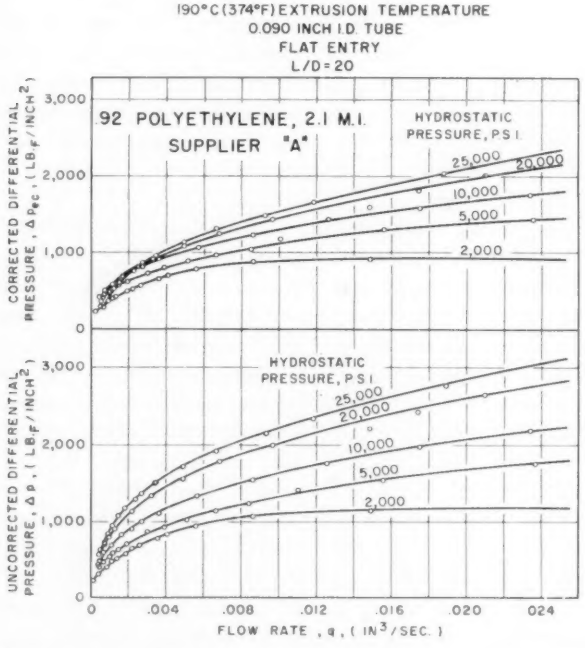


**Figure 5.** Comparison of entrance corrected and uncorrected flow data

## Calculating Entrance Loss

In an earlier paper by Westover and Maxwell (2) a method for correcting the differential pressure for entrance losses, rheometer losses and melt reservoir losses was described. This method was used and extended in this investigation. The method consists of subtracting from the observed differential pressure for the tube the pressure required to give the same flow rate through an orifice of the same diameter. This remainder is the differential pressure intended for use in the Poiseuille equation.

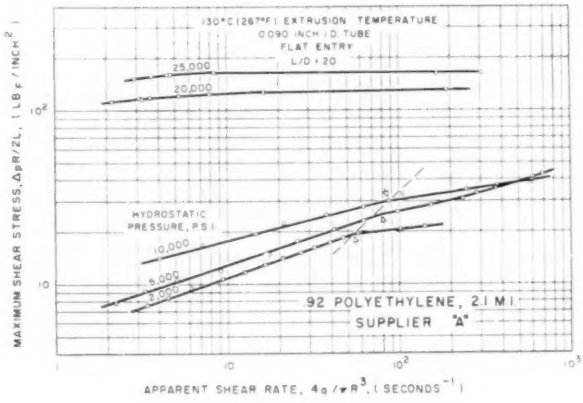


**Figure 6a.** Uncorrected

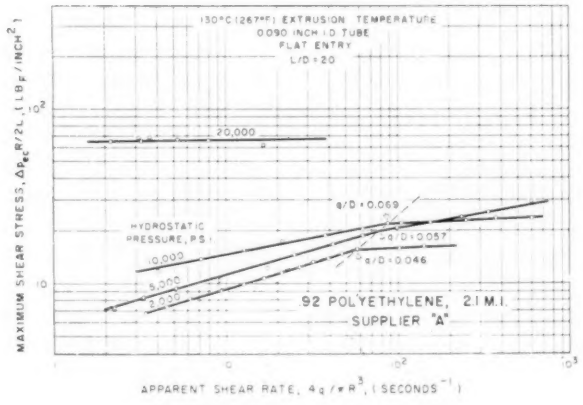


**Figure 6b.** Entrance corrected

**Figure 6.** Flow curves for polymer melt at 130°C showing effect of pressure induced crystallization

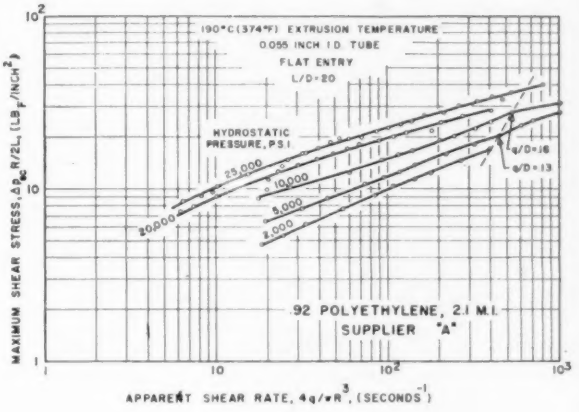


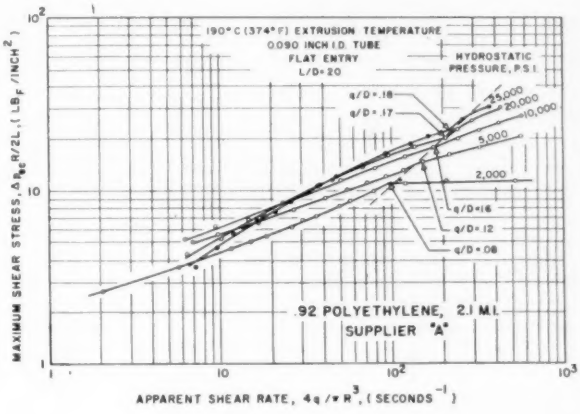


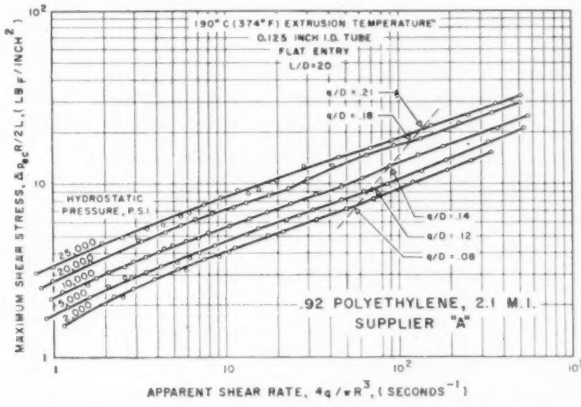


**Figure 7.** Shear rate vs shear stress curves for three different inside die diameters, showing q/D values at the change in slope

This separation of pressure components or losses can be carried a step further by subtracting from the differential pressure observed with the orifice the differential pressure required to give the same flow rate through a die having a one inch bore, *(Figure 4)*. This remainder is the entrance loss. For the dies used in this investigation having an L/D = 20, the entrance effect was 25% to 50% depending upon die sizes, polymer, temperature, flow rate, and hydrostatic pressure. If an L/D of 5, which is quite commonly used in rheological studies throughout the plastics industry, were used, then the entrance losses would have been from 75% to 80%.

*Figure 5* shows the same differential pressure vs flow rate data presented in the corrected and uncorrected form. The uncorrected data pertains to the presence of entrance correction in the data, but the rheometer and melt reservoir losses have been removed.

A major part of the work reported in this study was conducted upon a branched 0.92 density polyethylene with a 190°C melt index value of 2.1 grams/10 minutes. *Figure 6* shows both the entrance corrected differential pressure, $\Delta p_{ec}$, and the uncorrected differential pressure, $\Delta p$, employed in the maximum shear stress calculations and plotted separately against apparent shear rate. In addition to raising the shear stress vs shear rate curves with increased hydrostatic pressure there is an increase in the critical shear rate or flow rate at which the log-log plotted curves change slope abruptly. This critical point is usually associated with the appearance of a roughened extrudate. In Reference (2), Westover and Maxwell observed that this change in slope occurred at a critical q/D or flow rate to diameter ratio for different die diameters.

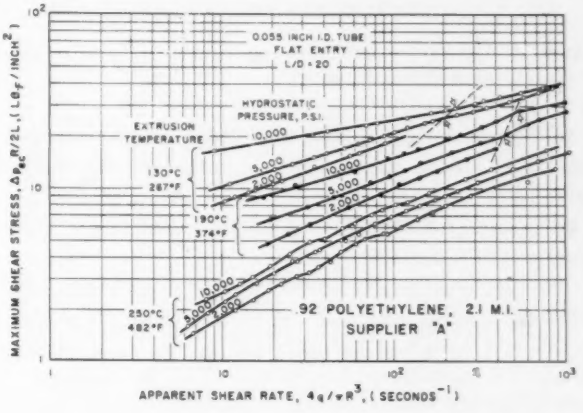


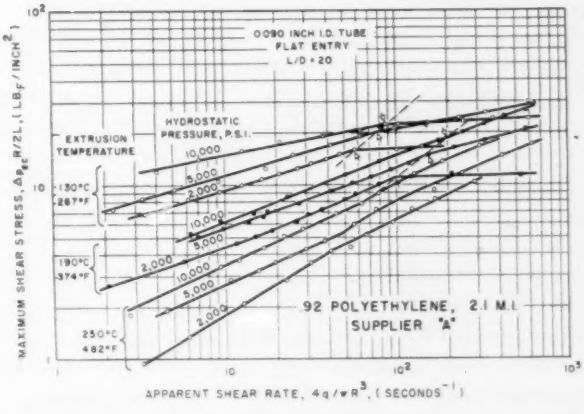


**Figure 8.** Shear rate vs shear stress curves as a function of temperature and hydrostatic pressure for two die sizes

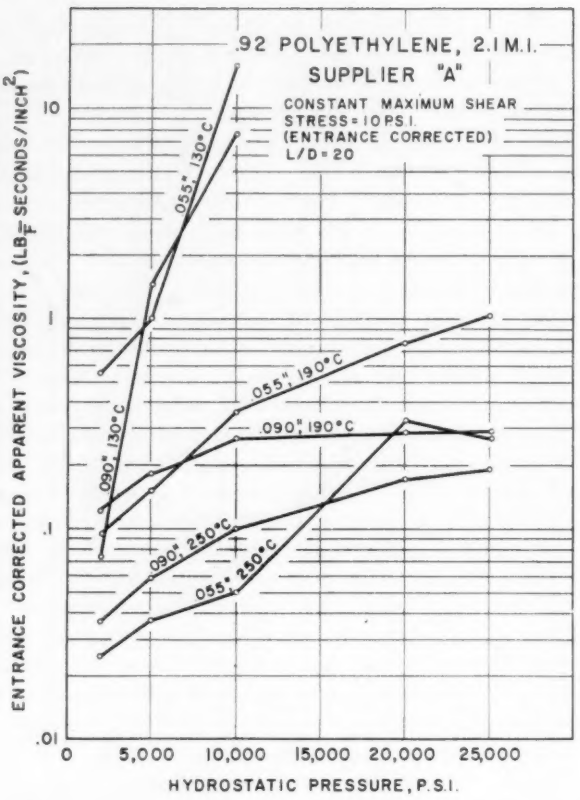


**Figure 9.** Apparent viscosity vs hydrostatic pressure at three temperatures and two die sizes

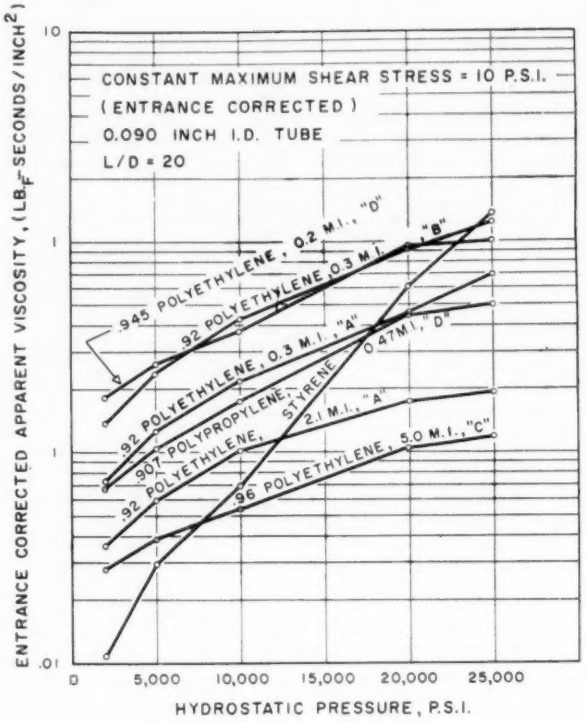


**Figure 10.** Effect of hydrostatic pressure on apparent viscosity for several polymer materials at 250°C and 10 psi maximum shear stress. Compare with Figure 11

In Figure 6 the polymer melt temperature is 130°C (267°F). This is sufficiently low to permit the inducement of crystals in the melt. Thus we have the large displacement between the 10,000 and 20,000 psi hydrostatic pressure curves.

Tests were made at 190°C (374°F) with three different die diameters, but with the same L/D of 20, to see if a critical q/D would be observed for the point of slope change for these three dies, *(Figure 7)*. There appears to be a close agreement between the q/D values for the critical points of the corresponding hydrostatic pressure curves. In addition it is noted that for any one tube diameter there is a straight line locus for these critical points on the curves corresponding to different hydrostatic pressures. No critical shear stress, serving as an indication of "melt fracture," (3) was observed in this study.

The 2,000, 5,000, and 10,000 psi hydrostatic pressure curves for three melt temperatures, 130°C, 190°C, and 250°C are all shown on the same graphs in *Figure 8* for the 0.055 and 0.090 inch diameter dies. The 20,000 and 25,000 psi curves would have overlapped the curves for another temperature, thus showing that an increase in hydrostatic pressure from 2,000 to 20,000 or 25,000 psi causes an apparent viscosity increase corresponding to a reduction of about 100°F or 50°C in the temperature of the melt.

The entrance corrected apparent viscosity for the three test temperatures and two die sizes are plotted against hydrostatic pressure in *Figure* 9. A constant entrance corrected maximum shear stress of 10 psi was maintained for the measuremer.t of viscosities. An increase in viscosity of a decade is observed over the complete pressure range for the higher temperatures and smaller die size. A hundred fold increase in viscosity for increasing pressure from 2,000 to 10,000 psi is observed for the 0.090 inch diameter die at 130°C (267°F) presumably because of the order that is pressure induced in the polymer at that temperature.

## Role of Crystallization

For purposes of comparison preliminary tests were performed on six other polymeric materials at 250°C (482°F) with the 0.090 inch diameter die. The seven graphs shown in *Figure 11* include data on three low density polyethylenes, two high density polyethylenes, polypropylene and polystyrene. From these graphs and the apparent viscosity vs hydrostatic pressure curves shown in *Figure 10* it is noted that the high density or more linear polyethylenes seem to be less pressure sensitive with regard to viscosity than are the low density or more branched polyethylenes. The higher molecular weight polyethylenes (low melt index) increase more in viscosity with pressure than do the lower molecular

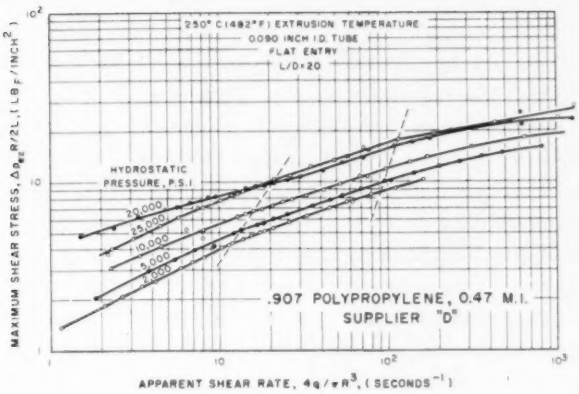


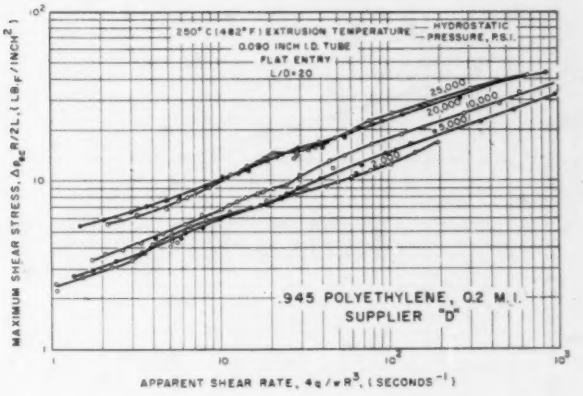


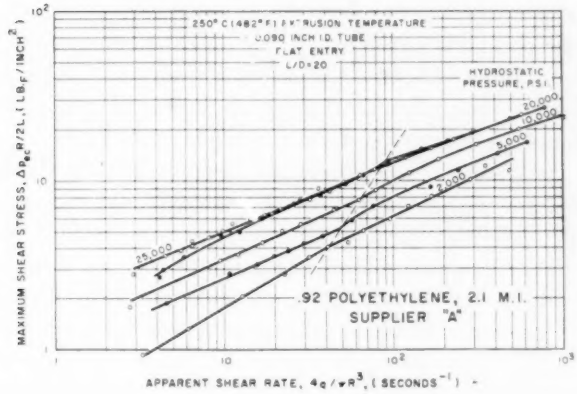


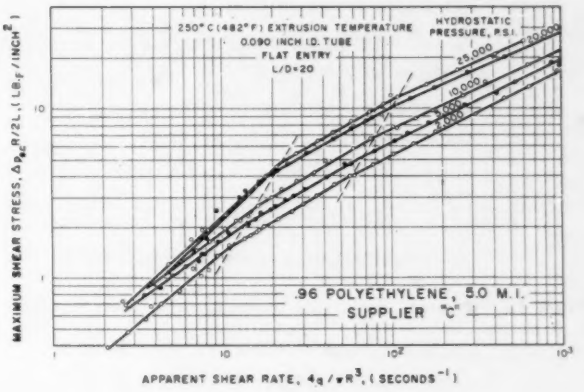


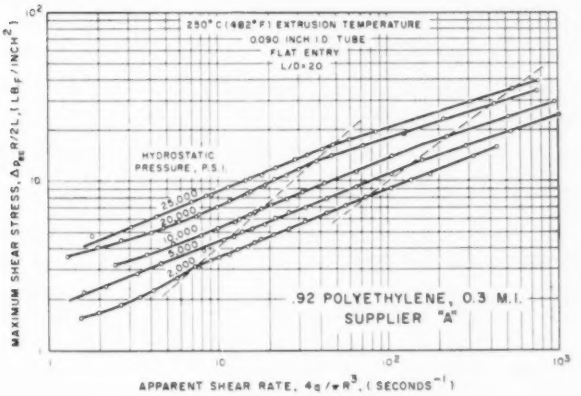


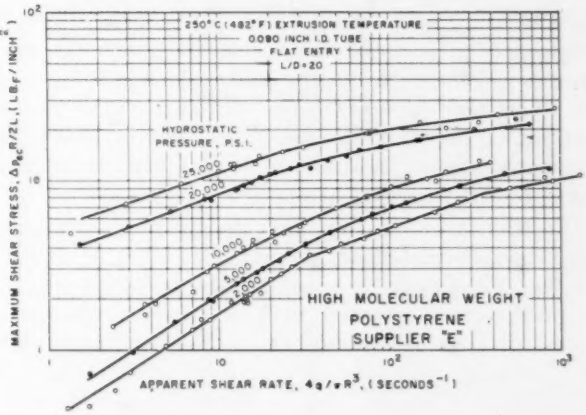


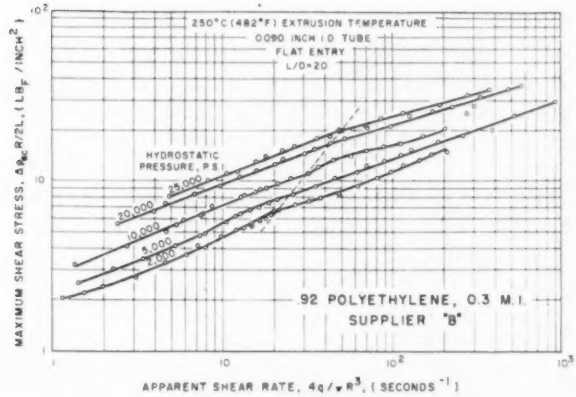


**Figure 11.** Flow curves for several polymeric materials at 250°C showing the reduced effect of pressure on viscosity for lower molecular weight (higher melt indices) and lower density polyolefins

### *Editor's Note*

*As this article goes to press, another analysis of the effect of static pressure on polymer melt viscosities, by James F. Carley, of the University of Arizona is being published in the 17th Annual Technical Conference Preprint Book. The work by Carley indicates that increasing static pressure at constant pressure drop reduce flow rates of plastic melts significantly, but the reduction is much smaller than the speed-up of flow brought about by an equal increase in pressure drop.*

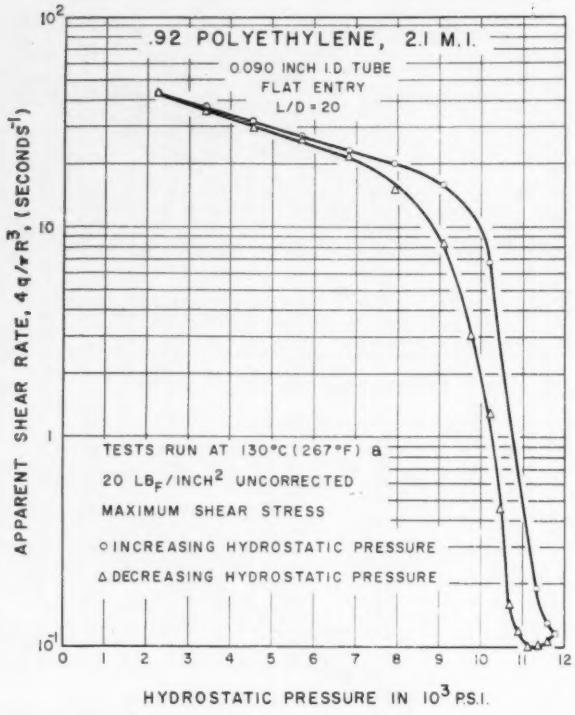


**Figure 12.** Apparent shear rate vs hydrostatic pressure at constant maximum shear stress showing pressure induced crystallization in polyethylene melt

weight polyethylenes (high melt index) of the same density or density range. The polypropylene sample responded to hydrostatic pressure in much the same way as did the high density polyethylene. The viscosity of polystyrene increased over one hundredfold as the hydrostatic pressure increased from 2,000 to 25,000 psi. Further studies of these and other materials are in progress.

In order to more exactly pin-point the hydrostatic pressure at which crystallization is induced at 130°C (267°F) in the .92 density, 2.1 melt index polyethylene, the rheometer was operated with a constant differential pressure and small increments of hydrostatic pressure. Five minutes time was allowed after each adjustment of hydrostatic pressure before the flow rate was measured. A hysteresis type curve of apparent shear rate vs hydrostatic pressure made from ascending and descending values of hydrostatic pressure is presented in *Figure 12*. In the curve for ascending hydrostatic pressure a straight line is observed on the semilog plot until between 8,000 and 9,000 psi where some crystallization or order within the melt causes a curvature. Rapid crystallization takes place above 10,000 psi. Increasing the time of exposure to the hydrostatic pressure increments before measuring the flow rate would reduce the area within the hysteresis loop which should approach a single equilibrium curve. This determination of melting pressure at 130°C (267°F) is in close agreement with values of about 10,000 psi reported for branched polyethylene by Park and Richards, (4) and by Matsuoka and Maxwell, (5). Using shear rate vs hydrostatic pressure data from the straight line or crystal-free portion of the curve in Figure 12, a calculation of the "elementary flow unit" of 27 carbon atoms was obtained. Kauzmann and Eyring (6) have reported 25 to 30 carbon atoms per "elementary flow unit" for n-paraffin chains of large molecular weight.

The significance to be given to the increase in apparent viscosity with pressure is as follows: An increase in the pressure at the entrance to an extruder die or a mold gate can result in a decrease in flow rate rather than the expected increase, because of a large increase in the apparent viscosity with increase in pressure. This can be easily visualized from the data presented for polystyrene.

Performance calculations for plastics processing equipment can be brought a step closer to reality by employing viscosity data taken at the appropriate hydrostatic pressure as well as at the appropriate temperature.

The final significant point to be made deals with the need for standardization of the conventional exit-to-air type rheometers with which no entrance corrections are normally made. If different length to diameter ratios are employed for dies of different laboratories, then the polymer extruded through the longer die will be exposed to a higher hydrostatic pressure at the die entrance. Therefore the data taken from dies of similar diameter, but dissimilar length to diameter ratios, should not be expected to yield comparable results since the conditions for the polymer are different for the various dies. Standardization with regard to temperature of the polymer melt without standardization of rheometer geometry does not really standardize the condition of the polymer melt.

## Literature References

1. Maxwell, B., and Jung, A., *Modern Plastics*, 35, No. 3, 174 (1957).
2. Westover, R. F., and Maxwell, B., *SPE Journal*, 13, No. 8, 27 (1957).
3. Tordella, J. P., Technical Paper, "Melt Fracture—Extrudate Roughness in Plastics Extrusion," Presented at Twelfth Annual National Technical Conference, SPE, Cleveland, Ohio, January 1956.
4. Park, W., and Richards, R. B., *Trans. Faraday Soc.*, 45, 203 (1949).
5. Matsuoka, S., and Maxwell, B. J., *Polymer Science*, 32, 131 (1958).
6. Kauzmann, W., and Eyring, H., *J. Amer. Chem. Soc.*, 62, 3113 (1940).

# Ultraviolet Degradation of Plastics and the Use of Protective Ultraviolet Absorbers

**R. C. Hirt, N. Z. Searle and R. G. Schmitt**

*Central Research Division, American Cyanamid Company*
*Stamford, Connecticut*

*The activation spectra of various plastics were obtained by detecting the formation of yellow species, carbonyl groups, and fluorescence, and by following the changes in the ultraviolet absorption. The "absorbing effectiveness" of the protective ultraviolet absorbers toward several sources was compared.*

Plastics exhibit various manifestations of degradation when exposed to ultraviolet light. By the use of protective ultraviolet absorbers to screen out the harmful radiation, the stability of the plastic can be considerably improved. Investigations of the degradation and protection are carried out under indoor weathering sources as well as under natural sunlight. For such studies it is necessary to consider at least four aspects. These include the measurement of the ultraviolet spectral energy distribution of sunlight and of the indoor accelerated test sources, and the measurement of the extent of degradation as a function of the wavelength of the incident radiation. Information on these two factors is useful in interpreting exposure test data obtained under varying illuminating conditions and also serves as an aid in choosing the absorber to be used for maximum effectiveness. The latter, the absorbing effectiveness of the protective agent, is the third aspect of the problem. The fourth aspect is the stability of the protective ultraviolet absorber itself. While these compounds are unique in that they are relatively unaffected by the ultraviolet light they absorb, they are not indefinitely stable.

## Light Exposure Sources

Studies on the ultraviolet spectral energy distributions of various indoor accelerated test sources and the compari-

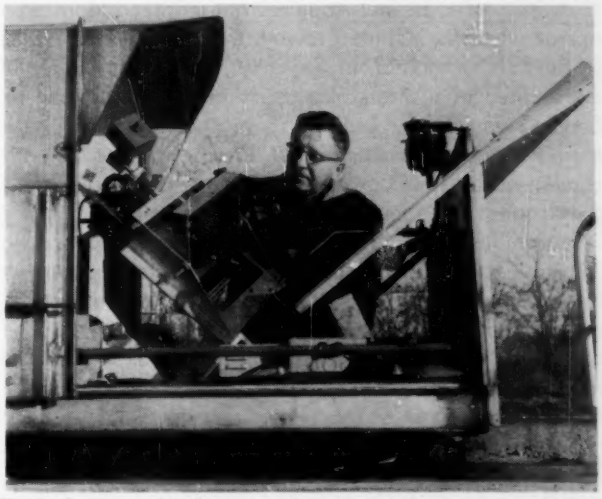

**Figure 1.** View of heliostat and protective housing.

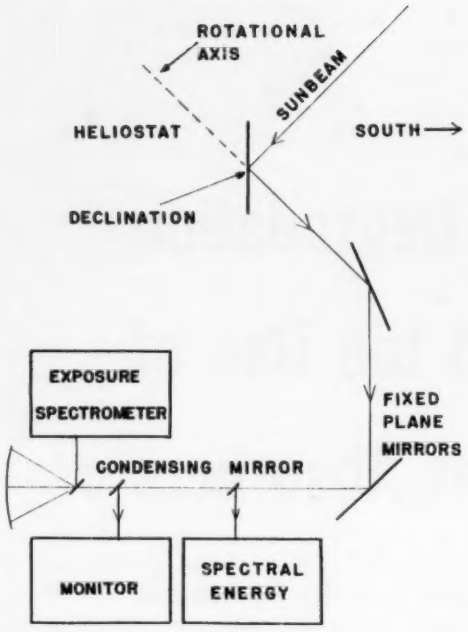


**Figure 2.** Schematic diagram of heliostat-spectrometer components.

son of these with natural sunlight have been described previously (1). The wavelength sensitivity, or the extent of degradation as a function of the wavelength of the incident radiation has been termed the "activation spectrum" of the plastic (2). Sunlight activation spectra have been obtained on various plastic materials by use of a heliostat-spectrometer. The construction and use of this equipment for polyesters has been reported (2).

Briefly, natural sunlight is directed by a heliostat (sun-following device) into a concave mirror and concentrated prior to being dispersed through a fast quartz spectrometer. The resulting beam is spread out across the plastic sample exactly as if the sample were a photographic plate in a conventional spectrograph. A view of the outdoor components of the apparatus is shown in *Figure 1*. It consists of a 12 inch square front surfaced aluminized mirror which is mounted to rotate about an axis parallel to the axis of rotation of the earth. The beam of light is intercepted by a similar stationary mirror and is reflected downwards into the building below. The optical system is shown diagrammatically in *Figure 2*. The beam is condensed by the concave mirror depicted at the left of the diagram, the focus of which is just beyond the smaller mirror mounted in front of the exposure spectrometer. The unit referred to as the "monitor" serves to integrate the energy during exposure. The energy received by the monitor covers the same wavelength range as that received by the sample and is correlated with the energy incident on the sample by means of a ferrioxalate actinometer solution. A third spectrometer was used for obtaining the UV spectral energy distribution of sunlight at various times of the day and seasons of the year. This was the same unit as was used for the comparison of the

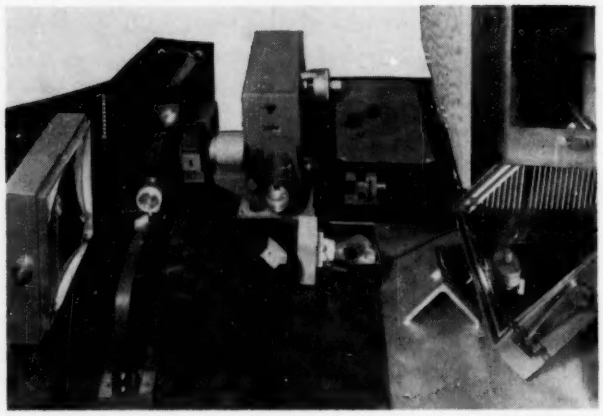

**Figure 3.** Indoor optical components, showing photochemical, spectral distribution, and monitoring spectrometers.

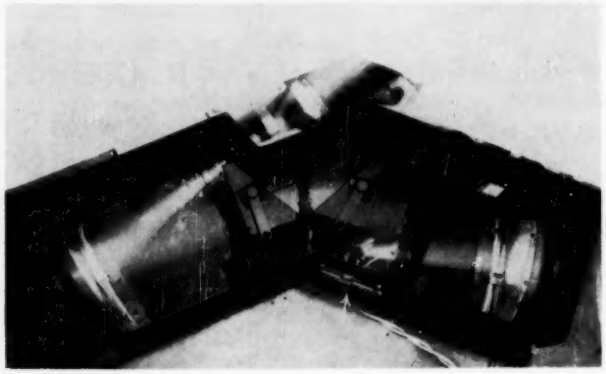

**Figure 4.** The photochemical spectrometer (top view, cover off).

spectral energy distributions of indoor test light sources. *Figure 3* is a photograph of the actual indoor optical components. In this picture the monitoring unit is to the right of the grating monochromator* used to obtain the spectral energy distributions.

* Bausch and Lomb.

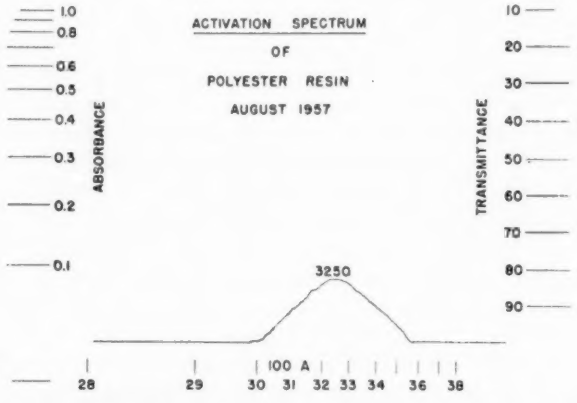


**Figure 5.** Microphotometer trace of activation spectrum of a phthalic-maleic polyester resin.

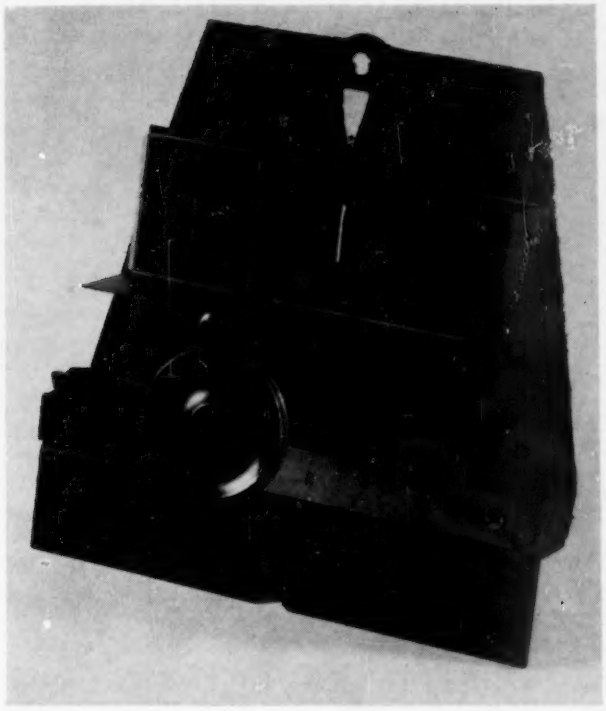

**Figure 6.** Vernier stage for microphotometry of irradiated plastic samples (with ultraviolet, infrared, or fluorescent light).

*Figure 4* is an inside view of the exposure monochromator. Two large quartz 30° prisms disperse the beam of light. The range between 2900 and 4000 Å is imaged on a 1 x 3" sample secured in the spectral plane at the exit window of the spectrometer. The actual area of the sample exposed to the beam is about 1 $cm^2$.

## Light Degradation Tests

Because the heliostat installation is dependent upon clear, sunny days, the apparatus was arranged so that a 1000-watt xenon arc can readily be substituted to illuminate the photochemical spectrometer on cloudy days, nights, and weekends. The ultraviolet energy distribution of the xenon arc has been shown to make an excellent approximation of noon sunlight (1). Almost identical activation spectra were obtained for both sunlight and xenon arc exposure.

The wavelength positioning on the sample is calibrated by means of a low pressure mercury arc serving as a line source. For such calibration, a photographic plate replaces the sample and is developed in the conventional manner after exposure. Samples for which the formation of yellow species was used as a criterion of degradation were scanned with a microdensitometer* using an AH3 mercury lamp and filters to isolate the 4358 Å line of mercury. The scale of the microdensitometer was calibrated by means of the photographic plate. A typical sunlight activation spectrum of a polyester is shown in *Figure 5*. Wavelengths near 3250 Å are most instrumental in producing yellowing. Below 3200 Å the decrease in sensitivity reflects the decrease in source intensity. Above 3500 Å the absorption of the plastic falls off sharply.

For polyesters and rigid polyvinylchloride, determination of extent of yellowing as a function of wavelength of irradiation is readily accomplished. These materials yellow in a matter of hours in the concentrated beam of the heliostat. For materials in which yellowing is slow to appear, other methods were employed for detecting the degradation and determining the activation spectra. These methods made use of the changes in ultraviolet and infrared absorbing characteristics or in fluorescence produced by irradiation. A vernier stage of a microscope was modified and adapted to various instruments replacing the microdensitometer. The converted stage, which is actually a moving slit arrangement, is shown in *Figure 6*. It is also calibrated by means of the photographic plate exposed behind the irradiation monochromator. For measuring the changes in ultraviolet absorbing characteristics, the stage was used in conjunction with the ultraviolet spectrophotometer*.

In the case of polyethylene and polypropylene, the most efficient way of detecting the effects of UV irradiation was by measuring the increase in infrared absorption in the carbonyl region, i.e., near 1720 $cm^{-1}$. The vernier stage was fitted to the beam of the IR-spectrophotometer†. It was found that the non-uniformity of the beam of this instrument was an advantage in these measurements. Only the intense portion of the beam had enough energy for the measurements. Integrated absorption intensities of the carbonyl band were determined as a function of distance along the sample, i.e., wavelength of incident radiation.

Opaque or optically-poor samples could not be handled by any of the three transmission techniques. Based on the appearance of a yellow-green fluorescence in poly-

* Knorr-Albers type.

* Cary 14.

† Beckman IR-4.

**Table 1. Measured activation spectra**

| Polymer Tested | Maximum of Activation Spectra | Means of Measurement |
|---|---|---|
| Polyesters (various formulations, see Ref. 2) | 3250 Ångstroms | blue light |
| Polystyrene | 3185 | blue light, fluorescence |
| Polyethylene | 3000 | infrared (carbonyl) |
| Polypropylene (non-heat-stabilized) | 3700 | infrared (carbonyl) |
| Polyvinyl chloride, homopolymer | 3100 | blue light, fluorescence |
| Polyvinyl chloride, copolymer with vinyl acetate | 3220 & 3640 | blue light, fluorescence |

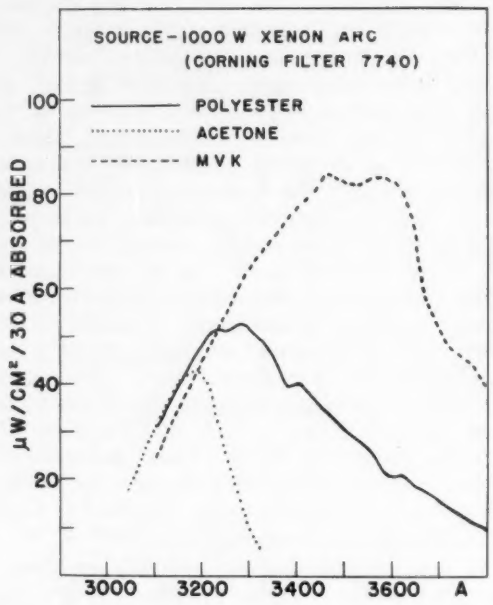


**Figure 7.** Calculated activation spectra for xenon arc and acetone, polyester resin, and methylvinyl ketone.

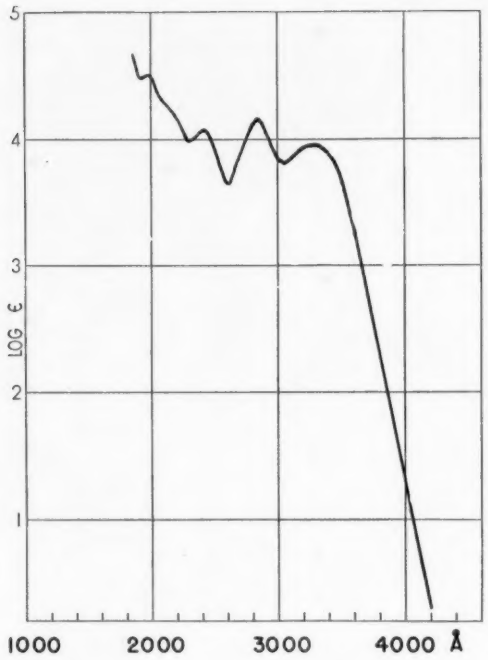


**Figure 8.** Absorption spectrum of 2-hydroxy-4-methoxybenzophenone.

esters and polystyrene, a fourth method for detecting degradation was developed. The vernier stage was combined with a fluorescent "blacklight" source and photomultiplier in such a manner that fluorescence could be measured from the same side of the sample as was illuminated. This technique was also useful for polystyrene in which yellowing is slow to appear, but which shows a brilliant fluorescence after short exposure to ultraviolet radiation. This has been described (3). The results for several polymers are listed in *Table 1*.

Presumably, activation spectra could be calculated by multiplying together at each wavelength band the intensity distribution of the source and the absorption spectrum of the material. This was tried for the polyethylene and polyesters. It was found that the calculated activation spectra corresponded with the measured only when an optically flat sample was used for absorption measurements. Otherwise, scattered light interfered with the absorption characteristics of the plastic. It was shown that multiplying the sunlight distribution by the absorption of acetone (the simplest ketone) also gave a good fit with the observed activation spectra. A similar calculation for monomeric methylvinyl ketone did not give as good a fit. The calculated curves for acetone, methylvinyl ketone and polyester are shown in *Figure 7*. This lends support to the theory that the photosensitive entities are isolated ketone groups scattered about in the polymer (2).

## Action of UV Absorbers

Outdoor and indoor exposure tests have demonstrated that protective ultraviolet absorbers do provide a considerable extension of the useful life of the plastic (4, 5, 6, 7). One of the most important aspects of activation spectra studies is that this information is useful in selecting the proper protective ultraviolet absorber for the plastic. Ideally, the absorber should display an absorption spectrum which matches that of the activation spectrum of the plastic obtained under the source to be used in actual practice. The sunlight activation spectrum of most materials peaks between 3100 and 3300 Å. An absorber which protects over a greater wavelength range, i.e., has the long wavelength maximum closer to the visible, has the undesirable effect of imparting a yellow color to the plastic. This is due to the long wavelength side of the absorption band extending into the visible region. The absorption curves of two typical protective absorbers are shown in *Figures 8 and 9*. CYASORB® UV 9, ultraviolet absorber, (2-Hydroxy-4-methoxybenzophenone) exhibits the long wavelength maximum at 3280Å in both a hydrocarbon or hydroxylic solvent. CYASORB® UV 24, ultraviolet absorber, (2, 2'-Dihydroxy-4-methoxybenzophenone) has its long wavelength maximum at 3540 Å in a hydrocarbon solvent only. In a polar medium, the peak is shifted to a position similar to that of (2-Hydroxy-4-methoxybenzophenone).

An estimate of the relative absorbing effectiveness of various compounds can be obtained by multiplying together at each wavelength interval the intensity of the source and the absorption of the protective absorber and summing the results. For this purpose, the spectral energy

® Trademark of American Cyanamid Company.

**Table 2. Absorbing Effectiveness of Ultraviolet Absorbers in "Watts per Gram"**

Energy of Source X Absorptivity of Compound
$\mu W/cm^2$ x liters/gm cm = $\mu W$ x 1000 $cm^3/gm\ cm^3$
= 1000 $\mu W/gm$

| Source | CYASORB* UV 9 | CYASORB* UV 24 |
|---|---|---|
| Sunlight (July 17, 1957) | 53.4 | 132.2 |
| Xenon Arc (1000 watt) | 67.2 | 128.4 |
| Fadeometer | 55.1 | 384.5 |
| S-1 Sunlamp | 15.9 | 24.4 |

* Trademark of American Cyanamid Company.

data of the various indoor sources and natural sunlight were punched into tapes for a digital computer† and the spectral data of various commercial and experimental protective absorbers were similarly punched onto tapes. Using the absorption in the form of specific absorptivities, with dimensions of liters per gram centimeter, and the spectral energy data in microwatts per square centimeter, the sums of the products have the dimensions of "watts per gram." *Table* 2 indicates the type of results obtained. These values are of interest in terms of comparison of various compounds for protection against any selected source. The absolute values have meaning only for the idealized condition of no self-protection. The "absorbing effectiveness" is independent of the characteristics of the plastic. Used in conjunction with the activation spectra, an estimate of the relative protecting effectiveness is obtained.

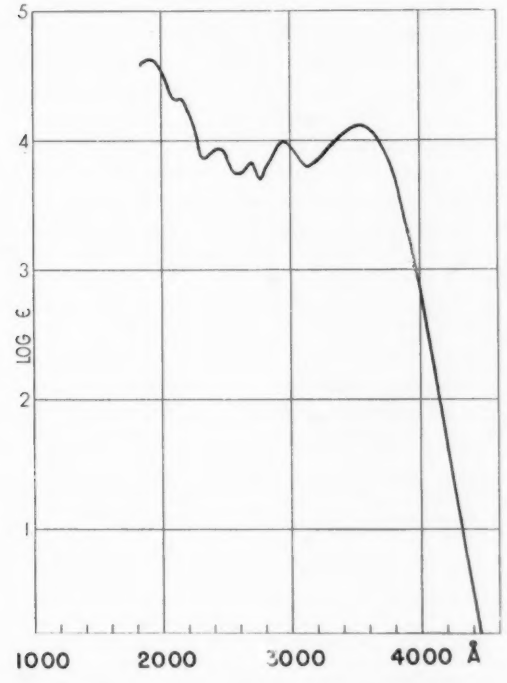


**Figure 9.** Absorption spectrum of 2,4-dihydroxy-4-methoxybenzophenone.

## Stability of UV Absorbers

The protective absorbers are not everlasting; they do photodecompose, but at a much slower rate than the materials which they are designed to protect. The photodecomposition was found to be dependent on a number of factors including the substrate in which the absorber is dispersed and the wavelength of irradiation. Information on the intermediates and final products of degradation should aid in understanding the mechanism of decomposition and the reason for the unique stability of these compounds. It has been found that irradiation of various substituted benzophenones in isooctane solution results in the formation of a conjugated acid as the main degradation product. It is interesting that the ring containing the ortho hydroxy group is the one which appears to break off from the carbonyl group. The remainder of the compound forms the acid. Further studies are being carried out, particularly on the o-dihydroxybenzophenones, which apparently do not form a conjugated system as a final product, but probably split off both rings from the C=O.

† Burroughs type E 101


## Acknowledgment

The authors wish to acknowledge the assistance of W. L. Dutton in designing the equipment used for determining activation spectra. We should also like to thank the statistics department for performing the computations necessary for the absorbing effectiveness values.


## Literature References


1. Hirt, R. C., Schmitt, R. G., Searle, N. Z., and Sullivan, A. P., paper No. SB45, presented before the Optical Society of America, Detroit, Michigan, Oct. 11, 1958; *J. Opt. Soc. Amer., 50,* 706 (1960).
2. Hirt, R. C., Schmitt, R. G., and Dutton W. L. *J. Solar Energy Science and Engineering,* 3, No. 2, 19-22, April 1959.
3. Hirt, R. C., Searle, N. Z., and Dutton, W. L., paper No. 164, presented before the Pittsburgh Conference on Analytical Chemistry and Applied Spectroscopy, March 4, 1960.
4. Coleman, R. A., and Weicksel, J. A., *Modern Plastics, 117,* (1959); N. L. Perry, *SPE Journal,* 550-5, July 1959.
5. Perry, N. L., *SPE Journal,* 550-5, July 1959.
6. Dean, R. T., and Manasia, J. P., *Modern Plastics,* 131-9, Feb. 1955.
7. Gantz, G. M., and Sumner, W. G., *Textile Research Journal, 27,* No. 3, March 1957.

# Mechanisms of Ultraviolet Stabilization of Plastics

*Nuclear magnetic resonance spectroscopy is a valuable tool for studying mechanisms of polymer stabilization*

J. H. Chaudet, G.C. Newland, H. W. Patton, and J.W. Tamblyn

*Research Laboratories*
*Tennessee Eastman Company*
*Division of Eastman Kodak Company,*
*Kingsport, Tennessee*

## ABSORBING STABILIZERS

The range of stabilization obtainable by the incorporation of ultraviolet stabilizers in plastics is illustrated by *Table 1* which gives data for cellulose acetate butyrate plastic. The basic formulation used was 100 parts of cellulose acetate butyrate (13% acetyl, 38% butryl), 12 parts of dibutyl sebacate, and 1 part of stabilizer. The ingredients were roll-compounded and compression-molded into 50-mil-thick sheets. Test specimens 2.5 × 0.5 in. were cut from these sheets. Weathering damage was followed by measurements of flexural strength [Tour-Marshall test for stiffness in flexure (2)] and embrittlement. The latter was defined to have developed when a break occurred at a bend angle of less than 90° in the Tour-Marshall test, the sample being bent with its weathered side on the outside of the bend. Usually this condition of brittleness was reached at about the same time that 25% of the initial flexural strength was lost.

Correlation between results obtained by weathering in the Weatherometer and outdoors seemed satisfactory, although some tendency for the Weather-Ometer to over-rate the stabilizers of intermediate effectiveness is apparent.

The first three stabilizers listed in *Table 1* are of the colorless, nondiscoloring type and, it may be of interest to note, are isomeric with each other. By utilization of colored stabilizers, greater degrees of stabilization may be obtained (3). The azo dye is soluble in the plastic. The last two stabilizers are dispersible pigments.

All of the stabilizers listed in *Table 1* (with the apparent exception of resorcinol monobenzoate, which will be discussed later) are of the type which act as primary absorbers of the incident ultraviolet radiation. That is, when incorporated in the plastic at concentrations of practical value, the stabilizer directly absorbs a very high percentage of the damaging ultraviolet radiation. Besides absorbing the ultraviolet radiation, the stabilizer also performs the much more important function of safe disposal of the absorbed energy (4). Stabilizers of this type may thus be described as inert filters, with emphasis on the term "inert".

A more quantitative description of the mode of action of such stabilizers may be expressed by defining a characteristic protective index (p), for any given damaging wavelength as follows:

$$p = \frac{\text{degradation of the unstabilized polymer}}{\text{degradation of the stabilized polymer}}$$

$$= \frac{\text{radiation absorbed by the unstabilized polymer}}{\text{radiation absorbed by the stabilized polymer}}$$

$$= \frac{\text{radiation absorbed by the unstabilized polymer}}{\text{radiation directly absorbed by the stabilized polymer + radiation indirectly absorbed by the stabilized polymer}}$$

Application of the Beer-Lambert law to this expression gives

$$p = \frac{I_o(1-e^{-k_u d})}{I_o(1-e^{-k_s d})(1-F_a) + I_o(1-e^{-k_s d})F_a(1-F_d)}$$

$$= \frac{1-e^{-k_u d}}{(1-e^{-k_s d})(1-F_a F_d)}, \qquad 1$$

where $I_o$ is the intensity of radiation, of the given wavelength, incident on the plastic, $F_a$ is the fraction of the total absorbed radiation which is absorbed by the ultraviolet stabilizer, $F_d$ is the fraction of $F_a$ which is harmlessly disposed of (that is, not transferred in a harmful manner to the polymer), $k_u$ is the absorption coefficient of the unstabilized plastic, $k_s$ is the absorption coefficient of the stabilized plastic, and $d$ is the thickness of the plastic sample.

In the derivation of Eq. 1 the following assumptions were made:

(a) the radiation is monochromatic, and
(b) the relation between degradation of the polymer and radiation absorbed by the polymer is independent of the presence of the stabilizer in the plastic system.

According to Eq. 1, the ideal stabilizer would have both $F_a$ and $F_d$ as close to unity as possible. For most of the common plastics it is no problem to find additives having sufficiently high $F_a$ by consulting tables of ultraviolet absorption spectra. It is much more difficult to maximize $F_d$. The successful stabilizer must be able to get rid of its absorbed energy by easy stages, at no time releasing to its surroundings a harmful amount of energy. It must also, of course, be able to survive the ordeal of absorbing an ultraviolet quantum without being irreversibly disrupted itself. Such a molecule probably needs to possess a considerable degree of internal lability, so that it may quickly distribute the original energy quantum from the spot at which it is first absorbed to a number of spots, each of which can safely handle the smaller packets of energy. Since all of the other quantities involved in Eq. 1 are directly measurable, $F_d$ may be evaluated for any given wavelength.

**Table 1. Stabilization of Cellulose Acetate Butyrate**

| Additive[a] | Stabilizing Effectiveness[b] | |
|---|---|---|
| | Hr. in Modified Weather-Ometer | Yr. Outdoors in Kingsport, Tenn. |
| None | 200 | 1 |
| Phenyl salicylate | 1,000 | 5 |
| Resorcinol monobenzoate | 1,800 | 7 |
| 2,4-Dihydroxybenzophenone | 2,400 | 8 |
| p-(p-Nitrophenylazo)phenol | >8,000 | — |
| 6,13-Dichloro-3,10-diphenyltriphenodioxazine | >22,000 | — |
| Carbon black (channel) | >30,000 | >10 |

[a] 1% concn.
[b] Exposure time required to cause 25% loss of flexural strength.

Equation 1 is believed to be a realistic representation of the protective index for a stabilizer in a polymer. This relation is based on the absorption of a single wavelength of incident radiation by the polymer. Hirt, Searle, and Schmitt recently showed that the degradation of several polymers is promoted to the greatest extent by ultraviolet radiation of a certain wavelength (5).

## Classification

Types of molecules likely to show high $F_d$, and therefore likely to be good ultraviolet stabilizers may next be considered. It is assumed that all eligible molecules have adequately high $F_a$.

**Those Which Fluoresce.** Fluorescence would seem to offer an ideal mechanism for chopping ultraviolet quanta into harmless pieces. Unfortunately, most efficient fluorescing molecules are not very stable themselves against ultraviolet radiation. Many of these compounds, such as phenylpyrazolines, benzoxazoles, and fluoranthenes, give good protection only until they are themselves destroyed by the ultraviolet radiation and cease to fluoresce. However, one light-stable fluorescent compound, 6, 13-dichloro-3, 10-diphenyltriphenodioxazine, was found to be an excellent ultraviolet stabilizer for cellulose ester plastics. This stabilizer gives a reddish brown plastic with a pinkish orange fluorescence. Its performance in cellulose acetate butyrate is illustrated in *Table 1*. This stabilizer is apparently in a class with carbon black for effectiveness.

**Those Which Can Rearrange.** A second type of molecular lability is represented by molecules capable of undergoing an energy-absorbing rearrangement following the absorption of an ultraviolet quantum (4). Preferably, this rearrangement should be reversible in the dark by a mechanism which does not release a harmful amount of energy to the surrounding polymer. An example of such a phototropic stabilizer is the azo dye, 4-(o-chlorophenylazo)-N, N-dimethylaniline. Other types of isomerizable compounds, such as arylamidines and arylimido ethers, have also shown activity as stabilizers for plastics. *Table 2* gives some examples of the effectiveness of such stabilizers in cellulose acetate butyrate plastic, tested under the same conditions as described for the compositions in *Table 1*. One such azo compound was included in *Table 1*.

**Chelates.** A third form of molecular lability is that possessed by the well-known salicylate (6) and 2-hydroxybenzophenone (7) stabilizers. As a common feature of their structures, these compounds contain a six-membered chelate ring involving a hydrogen bond:

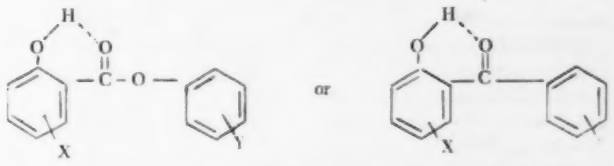


These configurations apparently offer a suitable path for rapid energy transfer and dissipation.

The NMR spectra of these stabilizers show hydroxy proton resonance absorptions at large negative field positions relative to the proton resonance of water. The

**Table 2. Isomerizable Stabilizers for Cellulose Acetate Butyrate**

| Additive[a] | Stabilizing Effectiveness[b]: Hr. in Modified Weather-Ometer |
|---|---|
| None | 200 |
| Phenyl N-phenylbenzimidate | 900 |
| N,N,N'-Triphenylacetamidine | 900 |
| N,N'-Diphenylacetamidine | 1000 |
| 2,4-Bis(phenylazo)resorcinol | 1200 |
| 2-Phenyl-4-phenylazophenol | >2000 |
| 4-Phenylazodiphenylamine | >2000 |
| 4-(o-Chlorophenylazo)-N,N-dimethylaniline | >2000 |
| 2,4-Bis(phenylazo)phenol | >3000 |
| 4-Phenylazoresorcinol | >6000 |
| 2-(p-Nitrophenylazo)-p-cresol | >8000 |

[a] 1% concn.
[b] Exposure time required for embrittlement.

NMR chemical shift value for the hydroxy group does not change with dilution, indicating that the hydrogen bonding in the chelate structure is predominantly an intramolecular effect. It was found that, the more effective these compounds were as ultraviolet stabilizers, the greater was the negative shift of the hydroxy proton resonance.

NMR shifts and stabilizing efficiencies for the 2-hydroxybenzophenone family of stabilizers, when tested at 1% concentration in cellulose acetate butyrate plastic, are shown in *Table 3*. Phenyl salicylate is included for comparison. The excellent correlation between the amount of NMR shift and the stabilizing efficiency is apparent.

The magnitude of the NMR shift is believed to be related to the hydrogen bond strength in the chelate ring: the greater the negative shift, the stronger the

**Table 3. Correlation Between NMR Shift and Stabilizing Effectiveness**

| Additive[a] | NMR Hydroxy Proton Shift, Cps. | Stabilizing Effectiveness,[b] Hr. in Modified Weather-Ometer |
|---|---|---|
| None | — | 200 |
| 2,6-Dihydroxybenzophenone | −160 | 600 |
| Phenyl salicylate | −220 | 1000 |
| 2,2'-Dihydroxybenzophenone | −220 | 1000 |
| 2,4-Dihydroxybenzophenone | −280 | 2400 |
| 2-Hydroxy-4,4'-dimethoxybenzophenone | −310 | >2600 |
| 3-Benzoyl-2,4-dihydroxybenzophenone | −340 | >4000 |

[a] 1% concn.
[b] Exposure time required to cause 25% loss of flexural strength.

**Table 4. Synergism Between Ultraviolet-Absorbing Pigments and Antioxidant in Low-Density Polyethylene**

| Additive | Concn., % | Stabilizing Effectiveness,[a] Mo. Outdoors in Kingsport, Tennessee |
|---|---|---|
| None | — | 12 |
| Lead chromate | 5 | 12 |
| Iron oxide | 5 | 12 |
| 2,2'-Methylenebis [6-tert-butyl-p-cresol] | 0.5 | 12 |
| lead chromate | 5 | >53 |
| 2,2'Methylenebis [6-tert-butyl-p-cresol] | 0.5 | |
| Iron oxide | 5 | >53 |
| 2,2'-Methylenebis [6-tert-butyl-p-cresol] | 0.5 | |

[a] Exposure time required to crack 5 out of 10 stressed samples.

hydrogen bonding in the chelate. Substituents *X* and *Y*, particularly *X*, determine the electronic density in the carbonyl and hydroxy groups, and, thus, the hydrogen bond strength. The desired substituents are those which increase the electronic density within the carbonyl group or decrease the electronic density within the hydroxy group, thereby increasing the strength of the hydrogen bond.

Variations in hydrogen bonding in these chelate structures do not cause large enough changes in the character of their ultraviolet absorption spectra to affect significantly the values of $F_s$ in Eq. 1. Therefore, it may be concluded that the hydrogen bonding is related to the ability of the stabilizer to dispose of its absorbed energy, that is, to the value of $F_d$ in Eq. 1. The stronger the hydrogen bonding in the chelate, the more effectively it can dispose of its absorbed energy and, consequently, the better it is as a stabilizer.

The NMR resonance shift of the chelate proton seems to be the first simple physical measurement which can give a prediction of the performance of a 2-hydroxybenzophenone light stabilizer. It is perhaps a measure of the $F_d$ factor for this type of stabilizer.

In polyethylene plastic, such a correlation is complicated by wide variations in compatibility from one stabilizer to another. Both 2-hydroxy-4-methoxybenzophenone and 4-dodecyloxy-2-hydroxybenzophenone, for example, show NMR shifts of about −300 cps., but the latter is much more compatible with polyethylene and a much better stabilizer for this plastic. Compression-molded plates of unstabilized low-density polyethylene, ⅛ in. thick, when weathered outdoors under stress, last about a year before cracking. The stress was applied by bending the specimens into a U-shape and holding them in this configuration during exposure. Similar samples containing 1% of 2-hydroxy-4-methoxybenzophenone showed exudation of the additive and cracked in 2 years. Test specimens containing 1% of 4-dodecyloxy-2-hydroxybenzophenone were nonexuding and are still un-

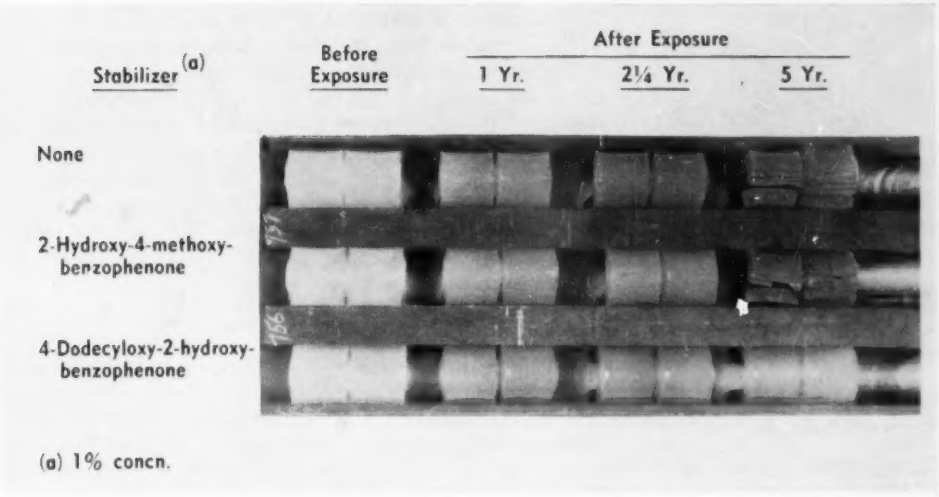


**Figure 1.** Weathering stability of stressed polyethylene

cracked at the end of 5 years. The appearance of these compositions after 5 years' outdoor exposure is shown in *Figure 1*. 4-Dodecyloxy-2-hydroxybenzophenone is an excellent weathering stabilizer for polyolefin plastics. It is essentially colorless and nondiscoloring during exposure.

### Fortification With Antioxidants

The improvement obtainable in the weatherability of plastic formulations by the addition of antioxidants to ultraviolet-absorbing stabilizers is well known. The light stabilizer may be of the soluble variety, like the salicylates or 2-hydroxybenzophenone derivatives (8, 9), or it may be a dispersed pigment (4). In the latter case synergism can be particularly pronounced, as shown in *Table 4* for some low-density polyethylene compositions weathered outdoors under stress, as described above, until 5 out of 10 samples developed cracks (10).

Apparently the weathering damage is by no means entirely caused by the initial photochemical processes, but is partly due to subsequent "dark" reactions. Such post-irradiation breakdown has been observed in most polymeric systems, for example, in cellulose esters (4) and in poly(vinyl chloride) (11). This thermal breakdown is caused by free-radical chain reactions which can be inhibited by the usual free-radical acceptors, such as antioxidants or the various types of stable free radicals. Many of these latter also possess favorable ultraviolet-absorbing characteristics and act efficiently as single light stabilizers, combining in one molecule inhibiting effects on both primary and secondary degradation reactions. Stable free radicals, such as certain hydrazyls, phenazyls, and nitroxides, were disclosed by McQueen to act as effective stabilizers for a variety of polymers (12). The fluorescent dioxazine stabilizer, described above, is another good example. This compound showed a high free-radical content when examined by electron paramagnetic resonance spectroscopy (13). Many carbon blacks probably represent the ultimate in this type of stabilizer. They are well known to contain stable free radicals (14). Their enormous effectiveness as light stabilizers for plastics is probably due to their ability to act efficiently in the double capacity of (a) inert, inner filters for the ultraviolet radiation to reduce the incidence of radiation damage, and (b) free-radical chain stoppers to reduce the propagation of the initial photochemical attack.

## NONABSORBING STABILIZERS

The ultraviolet stabilizers discussed so far have all been of the radiation-absorbing type described by Eq. 1. An apparent exception is resorcinol monobenzoate, listed in *Table 1*. Before exposure, this compound shows very little absorption of the sun's ultraviolet radiation, but develops such absorption quite rapidly during exposure in solution (15). This change is illustrated in *Figure 2* for 2-mil-thick films of cellulose acetate butyrate containing 0.15% of resorcinol monobenzoate, before and after various times of exposure under an RS-275 sun lamp (16). The absorption curve for a similar film containing the same amount of the isomer, 2, 4-dihydroxybenzophenone, is also shown for comparison. It may be seen that, upon irradiation, the absorption of the film

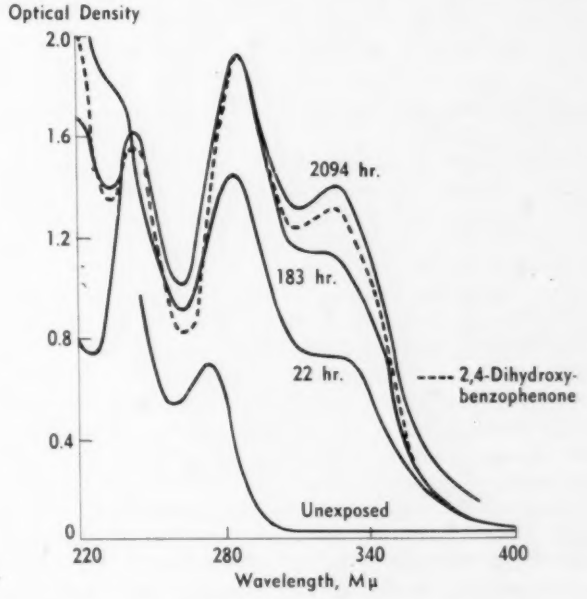


**Figure 2.** Photochemical conversion of resorcinol monobenzoate.

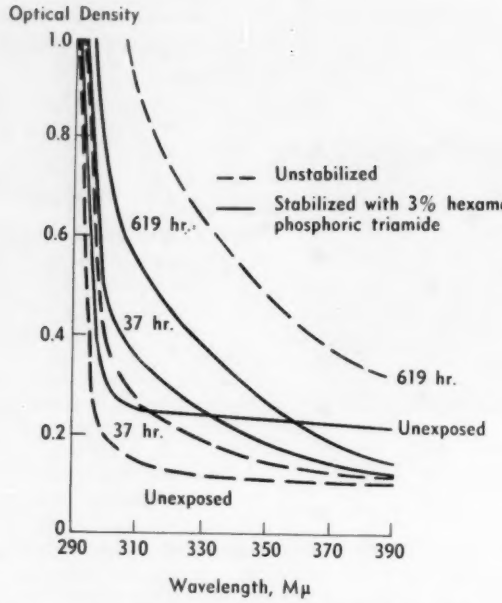


**Figure 3.** Effects of sunlamp exposure on ultraviolet absorption of poly(vinyl chloride) films.

containing the monobenzoate quickly approaches the absorption of the film containing the benzophenone isomer. The implication is strong that a photochemical conversion of the "nonabsorbing" resorcinol monobenzoate to the excellent ultraviolet stabilizer, 2, 4-dihydroxybenzophenone, occurs on irradiation of the former compound in the plastic, thus accounting, as follows, for the good stabilizing results obtained in practice with the monobenzoate:

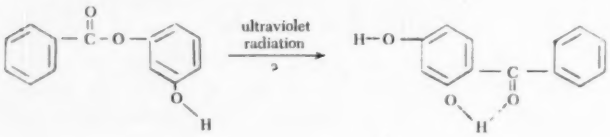


Resorcinol monobenzoate may be termed a pseudo nonabsorbing stabilizer.

An example of an apparently real nonabsorbing stabilizer, hexamethylphosphoric triamide (HPT), has recently been encountered in poly(vinyl chloride) plastic. The behavior of such a stabilizer would, of course, not be described by Eq. 1.

The ultraviolet absorption curves, before and after various exposures under an RS-275 sun lamp, of 4-mil-thick films of poly(vinyl chloride) containing 3% of HPT are shown in *Figure 3*. Corresponding curves for the unstabilized film are given for comparison. The HPT in the polymer shows no discrete, strong absorptions as does the conventional ultraviolet stabilizer. Only a general weak absorption below 360 mμ is observed. The exposure of the poly(vinyl chloride) plus HPT leads to some slight absorption increase; but this increase appears to be due mainly to the increase in the absorption by the polymer in this region. Note that the absorption by the polymer plus stabilizer is only approximately 60% of that of the polymer alone after the long exposure.

The mode of action of HPT is not fully understood (17). Nonabsorbing stabilizers have been reported as inhibitors of breakdown of plastics by high-energy radiations; for example, 10% of 3, 3'-dimethylthiocarbanilide increased the stability of poly(methyl methacrylate) by a factor of 3.7 against the degrading effects of $\gamma$- or pile irradiation (18). Some similarly efficient energy-transfer process may operate in the HPT-poly(vinyl chloride) system under ultraviolet irradiation. Such effects might be expected to be quite specific for given polymer-stabilizer pairs.

## Conclusion

Advances in the science of stabilization of plastics will result from a better understanding of the mechanisms by which stabilizers act. As an aid in the search for ultraviolet stabilizers whose effectiveness depends on the strength of an internal hydrogen bond, we recommend the use of nuclear magnetic resonance spectroscopy.

## Literature References


1. Tamblyn, J. W., and Armstrong, G. M., *Anal. Chem.*, 25, 460 (1953).
2. ASTM D747-58T, "ASTM Standards on Plastics," *American Society for Testing Materials*, Philadelphia 3, Pa., Sept. 1958, p. 309.
3. Burgess, A. R., "Polymer Degradation Mechanisms," *Nat. Bur. Stand. Circ. No. 525*, 155 (1953).
4. DeCroes, G. C., and Tamblyn, J. W., *Modern Plastics*, 29, 127 (1952).
5. Hirt, R. C., Searle, N. D., and Schmitt, R. G., Paper presented at the Regional Technical Conference of Plastics Engineers, Washington, D. C., Dec. 1, 1959.
6. Meyer, L. W. A., and Gearhart, W. M., *Ind. Eng. Chem.*, 37, 232 (1945).
7. Gantz, G. M., and Sumner, W. G., *Textile Research J.*, 27, 244 (1957).
8. Dow Chemical Co., Australian Patent 214,955 (1958).
9. Clark, G. A., and Havens, C. B., *Plastics Technol.*, 5 (No. 9), 41 (1959).
10. Tamblyn, J. W., Newland, G. C., and Watson, M. T., *Plastics Technol.*, 4 (No. 5), 427 (1958).
11. Birnthaler, W., and Falk, G., *Kunststoffe*, 49, 439 (1959).
12. McQueen, D. M., (to E. I. du Pont de Nemours and Co., Inc.), U. S. Patent 2,619,479 (1952).
13. Chaudet, J. H. unpublished results.
14. Castle, J. G., *Phys. Rev.*, 99, 341 (1955).
15. Meyer, L. W. A., and Gearhart, W. M., *Ind. Eng. Chem.*, 43, 1585 (1951).
16. Manufactured by General Electric Co.
17. Coover, H. W., Jr., McConnell, R. L., Newland, G. C., and Tamblyn, J. W., unpublished results.
18. Alexander, P., and Charlesby, A., *Nature*, 173, 578 (1954).


## Acknowledgment


We are indebted to many of our associates for helpful discussions of stabilization problems and for the synthesis of many of the stabilizers. In particular, we wish to acknowledge the assistance of Dr. G. M. Armstrong in the preparation and testing of the plastic compositions, and to thank Miss Evelyn McCurry and Mr. J. F. Elliott for help with the NMR measurements.

# A Study of the Weathering of an Elastomeric Polyurethane

C.S. Schollenberger and K. Dinbergs

*The B. F. Goodrich Company Research Center, Brecksville, Ohio*

This article describes detailed weather-resistance studies of a soluble, thermoplastic poly(ester-urethane) elastomer. The subject polymer, designated Estane 5740x1 by the B. F. Goodrich Chemical Company, was prepared as described in US Pat. No. 2,871,218 (*Figure 1*). It is a tough, strong, abrasion-, $\gamma$-radiation-, oil-, gasoline-, and ozone-resistant polymer which has good processing properties. The polymer has a Shore A hardness index of 85 and although not covalently crosslinked, it possesses the superficial properties of a rubbery vulcanizate (1).

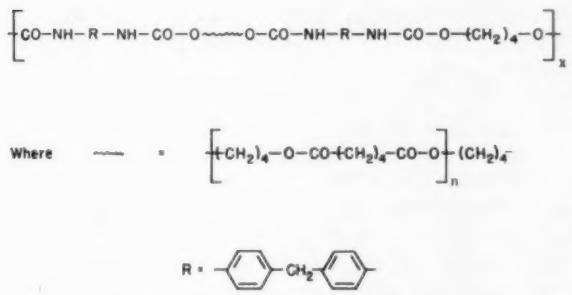


**Figure 1.** B. F. Goodrich's thermoplastic poly(ester-urethane) elastomer.

As with many useful polymers such as the nylons (2, 3), polyethylene (4), etc., polyurethanes undergo some degradation on exposure to natural and artificial weather conditions. With the unprotected subject elastomer, weathering is characterized by some loss in the tensile strength of exposed samples without appreciable changes in the modulus and ultimate elongation values. In spite of the loss in tensile strength, ⅛ inch dumbbells* of this unprotected poly(ester-urethane) elastomer retain 2000 to 3000 psi of tensile strength, about 500% ultimate elongation, and elasticity after twelve months outdoors. (*Figure 2*). But the weathering of the subject polymer was studied with the view of elucidating the nature of its weathering and then to provide compounds of superior weather resistance.

To begin the study, it was necessary to decide upon a convenient laboratory test which would accelerate the changes resulting from outdoor exposure and provide quick indications of the weather resistance of experimental compounds to guide day by day studies. A 154 hour Weatherometer exposure was selected for this purpose. The water spray portion of the Weatherometer cycle was omitted because it became obvious that the major factor in the degradation of such polyurethanes on outdoor exposure is sunlight, and as much synthetic sunlight as possible was desired in the accelerated test. Moreover, the Weatherometer necessarily runs hotter (85°-98°C) without, than with, the water spray, making the dry test still more severe. Hydrolysis is not a significant factor in the outdoor weathering of such polyurethanes and further, none of the protective agents added to the polymer was water soluble. It is recognized that the eroding effect of rainfall could change the picture if a migrating additive were under test as a protective agent in the polymer. In such a case rainfall could scour the bloom of protective agent from the surface of the sample, presenting a new and ultimately unprotected surface for attack.

*Table 1* compares the spectral distribution of the Atlas enclosed violet carbon arc used in the Weatherometer, with the solar spectrum (5).

The range 290 to 480 m$\mu$ in *Table 1* has proved to include the incident wavelength range which was found to sensitize the polyurethanes of this study to the degradation process. The Weatherometer supplies more intense radiation in this region than does incident solar radiation, considered to be adequate justification for the use of the Weatherometer as an accelerated weathering device.

* See test methods at end of article.

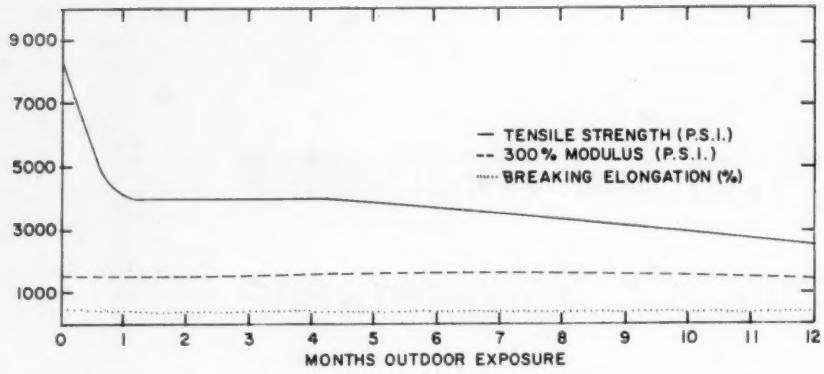


**Figure 2.** The effect of outdoor weathering on B. F. Goodrich's poly(ester-urethane) elastomer (0.075" thick, 1/8" dumbbells). Vertical axis numbers can be interpreted as psi of tensile strength, 300% modulus, or as percent elongation, by reference to legend.

The concurrent outdoor exposure of experimental compounds was practiced in this study as a check on Weatherometer predictions and as the ultimate measure of weather resistance. Samples were exposed at Brecksville, Ohio. They were mounted in an unshielded position at a 45 degree angle and facing south.

Weatherometer exposure was not used as a *quantitative* estimate of weather resistance in this work. For the most part it was found that 154 hours of Weatherometer exposure produced more degradation in *raw subject polyurethane* than that produced by a year of outdoor exposure. Generally, experimental stocks performing well in Weatherometer exposures also showed good performance outdoors.

When properly protected by effective age resisters it was found that the degradation produced in *compounded stock* by 154 hours of Weatherometer exposure roughly corresponds to the effect of a year of outdoor exposure.

In one case, the Weatherometer indicated stability considerably in excess of that actually realized on outdoor exposure.

That there should be such differences is not surprising, for if the *type* of conditions encountered in the weathering process is supplied by the Weatherometer, the *intensity* is different. This is by design—thus the accelerated nature of the test. One must expect a complex degradation process dependent on more than one agent to vary to some extent when the natural balance is modified in favor of particular agents, here intense ultraviolet radiation and heat. Tests show that subject elastomer samples extended 20% are not changed by exposure to 25 phm of ozone at 49°C for 150 hours,* ruling ozone (by itself) out of the picture as a significant weathering agent. Moreover, since the elastomer apparently has unlimited storage stability in contact with air, it is concluded that oxygen (by itself) is not responsible for the weathering. Although exposure in a quartz tube under a $10^{-6}$ mm. Hg vacuum to 154 hours of Weatherometer radiation insolubilized and toughened the polymer, it did not produce the surface embrittlement characteristic of a weathered sample. On the basis of the above findings it was tentatively concluded that the degradation of the subject polyurethane on weathering is due to an ultraviolet-promoted autoxidation.

* See test methods at end of article.

**Table 1. Comparison of the Spectral Distributions of Solar and Weatherometer Radiation**

| Spectral Range (mμ) | Percent of Total Radiation [to limit of fluorite transmission in the infrared (12,000mμ)] | |
|---|---|---|
| | arc enclosed in 9200-PX Globe[b] | noon June sunlight (Wash., D.C.)[a] |
| 279 to 290 | 0.05 | 0.00 |
| 290 to 320 | 4.6 | 2.0 |
| 320 to 360 | 6.2 | 2.8 |
| 360 to 480 | 15.0 | 12.6 |
| 480 to 600 | 8.3 | 21.9 |
| 600 to 1400 | 14.9 | 38.9 |
| 1400 to 4200 | 21.3 | 21.4 |
| 4200 to 12,000 | 29.65 | 0.4 |

[a] W. W. Coblentz, May 25, 1926.
[b] Pacini, March 31, 1932

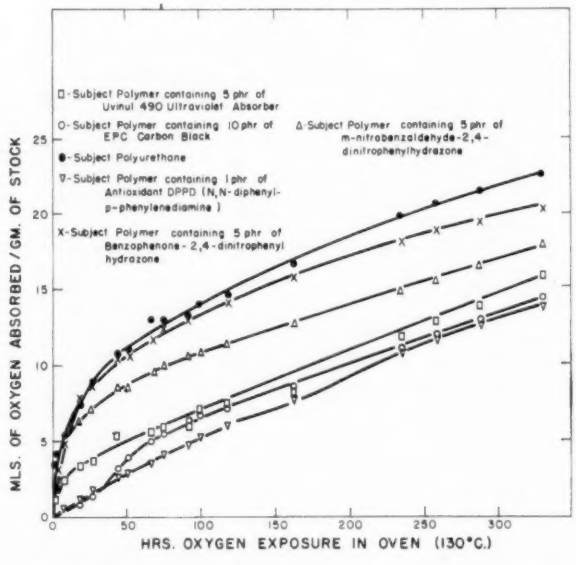


**Figure 3.** Oxygen absorption on thermal aging of subject elastomer and its compounds.

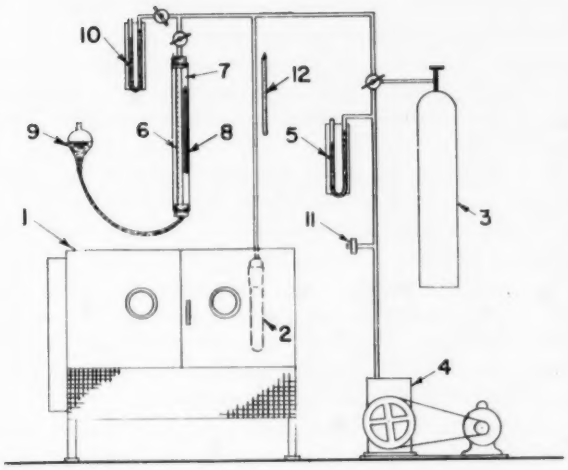


**Figure 4.** Apparatus for the study of ultraviolet-initiated autoxidation.

| | |
|---|---|
| 1 Weatherometer | 7 Water jacket |
| 2 Sample tube (quartz) | 8 Thermometer |
| 3 Oxygen cylinder | 9 Leveling bulb |
| 4 Vacuum pump | 10 Open manometer |
| 5 Vacuum manometer | 11 Outlet to the atmosphere |
| 6 Gas burette | 12 Thermometer |

The phenomenon might be explained in part as follows: incident solar energy initiates free radical chains in the polymer; the surface radicals in contact with air (oxygen) form hydroperoxides; the hydroperoxides decompose to produce an extensively crosslinked surface which is less extensible, insoluble, and by measurement five times less permeable to air than it was before exposure; the surface, still transparent to ultraviolet radiation, allows free radical formation under anaerobic conditions among the chains of the subsurface polymer; such free radical chains join by mutual interaction, producing a network which is looser than that of the surface, more flexible, and tougher.

It is believed that the initial loss in tensile strength of exposed samples is in part due to their embrittled surfaces. The failure of subsequent exposure to embrittle the sample more deeply and thereby further weaken it was considered to be due to the reduced air permeability of its continuous, tightly crosslinked surface.

Direct evidence of the ability of polyurethanes to autoxidize was obtained in the exposure of unprotected subject elastomer to 300 psi of oxygen at 80°C for 96 hours (oxygen bomb)*. This exposure halved the tensile strength of the sample (without affecting modulus or elongation) but did not insolubilize nor embrittle it.

On heating ASTM standard dumbbells of unprotected subject elastomer in an air oven at 100°C for 64 hours the polymer (elastomer) was essentially unaffected, however a seven day heating at 140°C resulted in losses of tensile strength (80%), 300% modulus (66%), and elongation (17%). The latter exposure did not embrittle the sample but thoroughly insolubilized it.

* See test methods at end of article.

Further evidence of the autoxidizability of this elastomer was obtained by determining quantitatively the uptake of oxygen by 25 mil thick microdumbbell* samples heated in a 130°C oven. *Figure* 3 shows the results of this experiment in which the unprotected polymer absorbed 22.5 ml of oxygen (STP) per gram of sample in 322 hours, ultimately melting.

## Chemical Composition Altered

The combined action of oxygen and ultraviolet radiation change the chemical composition of the subject elastomer detectably (*Table 2*). The 154 hour Weatherometer exposure of a 0.2 to 1.0 mil film of the raw polymer changed its composition as indicated in *Table 2*. A loss in carbon and hydrogen content and an increase in nitrogen and oxygen content are apparent in the exposed polymer.

The absorption of oxygen by 25 mil microdumbbells of raw elastomer in quartz on Weatherometer exposure was determined using the apparatus pictured in *Figure 4*. The quartz sample tube was charged with Drierite and Ascarite to absorb generated water and carbon dioxide, respectively. The results of this experiment are plotted in *Figure* 5. They show that the raw sample absorbed 32.7 ml of oxygen (STP) per gram of polymer during 242 hours of Weatherometer exposure. The sample retained only 10% of its original tensile strength after this exposure. By way of comparison, 25 mil thick microdumbbell samples of the subject elastomer in quartz, under high dynamic vacuum, were exposed to Weatherometer radiation for 147 hours. They retained 76% of their original tensile strength after this exposure and were insoluble. The slight surface embrittlement noted in the sample was attributed to the action of oxygen that was constantly drawn through leaks in the system during the exposure.

Additional studies of the chemical changes in the elastomer attending its weathering were made using infrared and ultraviolet absorption techniques and also the mass spectrometer.

The infrared absorption spectrum* of a 1.5 mil film of the subject elastomer supported securely on a sodium chloride crystal, was determined (A) before and (B) after 154 hours exposed in the Weatherometer. The two spectra are compared in *Figure 6*.

* See test methods at end of article.

**Table 2. Chemical Analysis of Raw B. F. Goodrich Poly(ester-urethane) Elastomer Before and After 154 hour Weatherometer Aging in Air**

| | % C | % H | % N | % O |
|---|---|---|---|---|
| Cal'd. | 63.03 | 7.13 | 3.56 | 26.28 |
| Found (Unaged) | 62.58 | 6.97 | 3.27 | 27.18* |
| Found (Aged) | 57.65 | 6.23 | 3.99 | 32.13* |

* By Difference

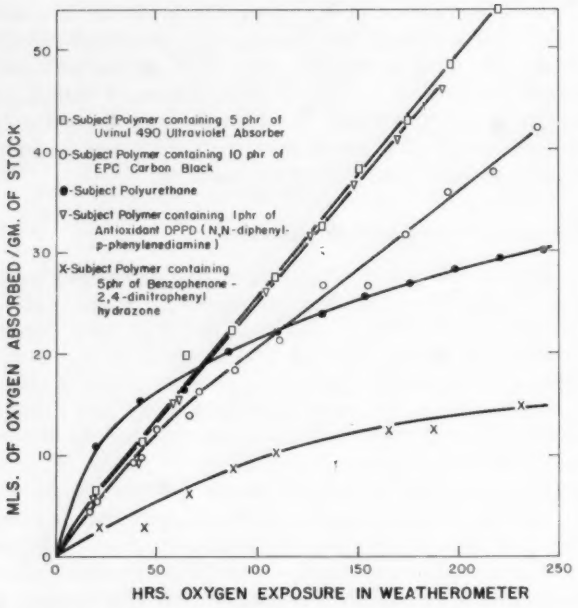
MLS. OF OXYGEN ABSORBED/GM. OF STOCK
HRS. OXYGEN EXPOSURE IN WEATHEROMETER
□-Subject Polymer containing 5 phr of Uvinul 490 Ultraviolet Absorber
O-Subject Polymer containing 10 phr of EPC Carbon Black
●-Subject Polyurethane
▽-Subject Polymer containing 1phr of Antioxidant DPPD (N,N-diphenyl-p-phenylenediamine)
X-Subject Polymer containing 5phr of Benzophenone - 2,4-dinitrophenyl hydrazone

**Figure 5.** Oxygen absorption on Weatherometer exposure of B. F. Goodrich's poly(ester-urethane) elastomer and its compounds.

A large decrease in the 6.25$\mu$ peak, disappearance of the 12.25$\mu$ peak, and slight decrease and smearing of the 13.0$\mu$ peak indicate *loss of aromatic structure;* a large decrease in the 6.5$\mu$ peak indicates the *loss of urethane structures* (amide II band); a decrease in the 3.45$\mu$ peak indicates *a loss of C-H structures;* the decrease of -NH- and the broadening of the 3.05$\mu$ peak (narrow and broad) suggest *hydroxyl formation;* a broadening and smearing of the 8.2$\mu$ peak which embraces ester and urethane "ether" oxygen indicates the formation of *a greater variety of "ether" oxygen atoms;* the broadening of the 5.8$\mu$ peak (ester and urethane carbonyl) indicates the *formation of more carbonyl groups.* (6).

*Figure 7* shows the infrared absorption spectrum changes of a thin but still somewhat heavier unsupported film of raw elastomer before and after 3 months of outdoor exposure.

A comparison of the spectra in *Figure 7* shows the changes on outdoor exposure to be much slower than the Weatherometer-induced changes but has been interpreted to indicate oxidative changes.

Pronounced changes in the ultraviolet absorption spectrum[c] of the elastomer are also apparent after Weatherometer exposure. *Figure 8* shows significant chemical changes to occur in an extremely thin film of the polymer after but one-half hour of such exposure.

The growth of an absorption peak at 270 to 310m$\mu$, believed to be due to the formation of a quinoid structure, and the simultaneous decline of the peak at 245m$\mu$, indicating a loss of aromatic structure, suggests the possibility of the autoxidation of the aromatic urethane groups in the polymer chains to the quinone-imide structure (*Figure 9*). Adams and Anderson (7) have studied diurethane oxidation in discrete molecules.

The tendency of quinone-imides to add active hydrogen substances (8) [here possibly the urethane groupings integral in adjacent chains] to themselves might account for the disappearance of the quinone absorption from the spectrum as well as contribute to the insolubilization of the polymer on extended weathering exposures.

Changes in its ultraviolet absorption spectrum similar to those resulting from Weatherometer exposure have also been produced in the subject elastomer by heating an extremely thin film of the polymer in air in the dark. At 140°C these changes are relatively slow.

[c] See test methods at end of article.

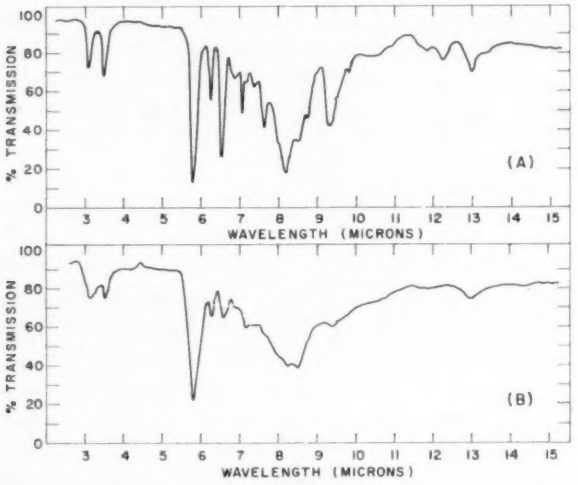


**Figure 6.** The infrared absorption spectrum of a 1.5 mil unsupported film of B. F. Goodrich's poly(ester-urethane) elastomer

(A) Unexposed
(B) After 154 hours in the Weatherometer

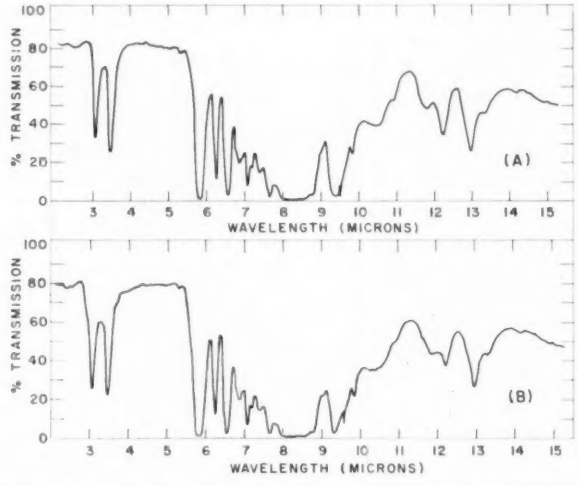


**Figure 7.** The infrared absorption spectrum of a thin unsupported film of B. F. Goodrich's poly(ester-urethane) elastomer

(A) Unexposed
(B) After 3 months of outdoor exposure.

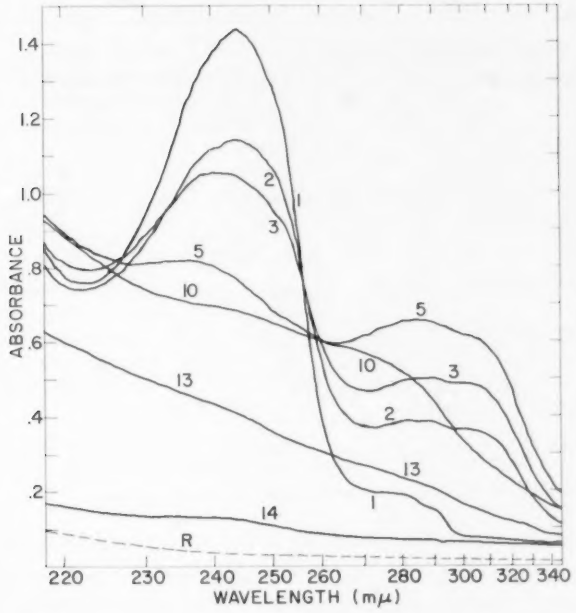


**Figure 8.** Changes in the ultraviolet absorption spectrum of an extremely thin film of B. F. Goodrich's poly(ester-urethane) elastomer on Weatherometer exposure

After (1) 0 hrs., (2) 0.5 hr., (3) 1 hr., (5) 2 hrs., (10) 12 hrs., (13) 42 hrs., (14) 196 hrs. exposure
R = Air to air reference

In an effort to shed more light on the processes involved in the photosentization of this elastomer a ten mil thick sheet of the raw polymer (elastomer) was placed in a quartz tube which was then sealed off under a vacuum of $10^{-6}$ mm of mercury and was exposed in the Weatherometer for 154 hours.* This treatment generated $6.92 \times 10^{-6}$ moles of gas per gram of polymer. By means of the mass spectrometer the composition of the gas mixture was found to be as indicated in *Table 3*.

The samples of this exposure were insolubilized by the treatment but were not discolored nor in any way embrittled. They appeared qualitatively to be as tough and strong after exposure as they were originally.

This experiment has suggested that the sequence of events shown in *Figure 10* may occur at the urethane bridge groupings of the polymer chains when it is irradiated with UV light in vacuo.

The ultraviolet absorption spectrum of the subject elastomer shows a fairly strong absorption in the 220-260mμ region and only minor absorption in the 290-345mμ region as was seen in *Figure 8*. Although no solar radiation of wavelength less than 290mμ reaches the earth, and only small amounts of Weatherometer radiation are of this wavelength range, Weatherometer radiation is entirely capable of obliterating the UV absorption spectrum of the polymer and of weathering it. Since the photo-excitation of a substance is generally conceded as probable only when the substance is exposed to radiant energy which is of appreciably absorbed wavelengths it was of considerable interest to discover that the elastomer undergoes degradation characteristic of weathering on extended Weatherometer exposure even when shielded by Corning optical filter No. 7380 which stops essentially all incident radiation of the type in question below 334mμ wavelength*. Such a filter does not stop the Weatherometer radiation causing the characteristic weathering of subject elastomer microdumbbells as is apparent in *Table 4*. These results suggest that the polymer must be undergoing photosensitization by radiation of wavelengths greater than 334mμ.

Although the absorption spectrum of the subject elastomer in the range 350 to 900mμ, determined in accord with our usual technique (i.e., extremely thin films), shows only the slightest absorption and no distinguish-

* See test methods at end of article.

* Transmits <0.5% below 334 mμ; transmits >60% above 365 mμ

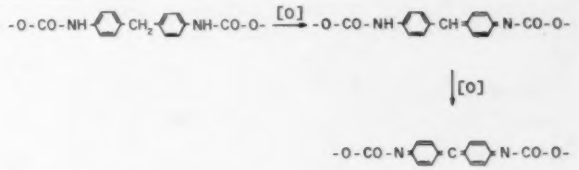


**Figure 9.** Possible course of urethane autoxidation.

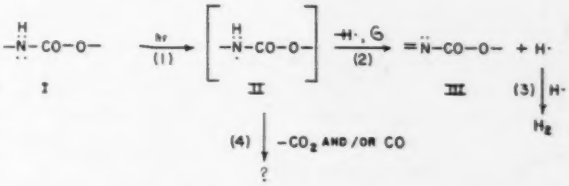


**Figure 10.** A possible reaction mechanism in the photosensitization of B. F. Goodrich's poly(ester-urethane) elastomer.

(1) An electron from the unshared pair on the nitrogen atom of the aromatic urethane bridges (I) in the elastomer chains is expelled on photoexcitation of the structure
(2) the transitory intermediate (II) expells a hydrogen atom and rearranges to the quinone-imide structure (Figure 9)
(3) hydrogen atoms combine to form molecular hydrogen
(4) the transitory intermediate (II) may lose carbon monoxide or carbon dioxide

**Table 3. Composition of Gases Evolved* From B. F. Goodrich Poly(ester-urethane) Elastomer in a High Vacuum during 154 hour Weatherometer Exposure**

| Evolved Gas | Mole % of Mixture |
|---|---|
| Hydrogen | 4.6 |
| Carbon Dioxide | 62.3 |
| Carbon Monoxide | 33.3 |

* Amount: $6.92 \times 10^{-6}$ moles/g. elastomer

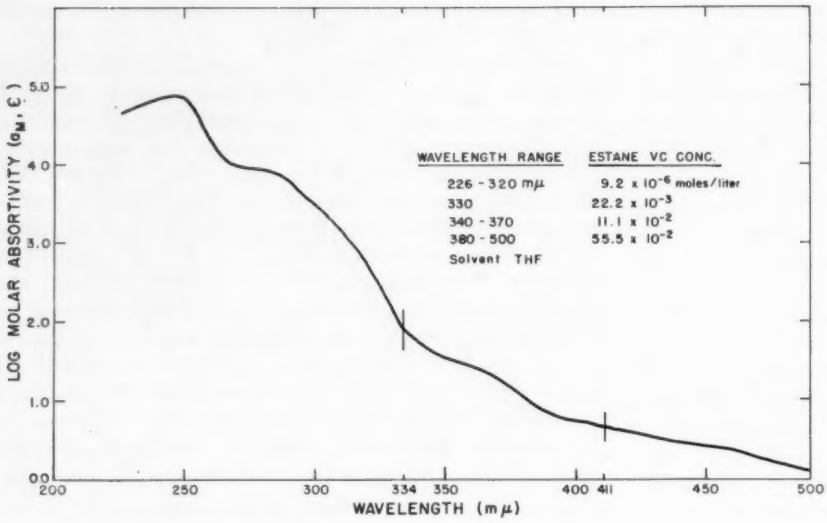


**Figure 11.** Ultraviolet absorption spectrum of B. F. Goodrich's poly(ester-urethane) elastomer in tetrahydrofurane solution.

able peaks, a determination of the molar absorptivity* of the polymer in tetrahydrofurane solution (which included measurements based on effective polymer concentrations and thus path lines considerably greater than were involved in the thin film technique) showed relatively slight, but none-the-less noticeable absorption in the range 334 to 500m$\mu$ (*Figure 11*). Closer consideration of this region of relatively minor absorption proved to be fruitful in the solution of our problem.

In following this lead, an optical filter (Corning No. 3387)** which stops essentially all incident radiation of the type being discussed below 411m$\mu$ wavelength, was employed to shield extremely thin films of the subject elastomer in a 42 hour Weatherometer exposure. Ultraviolet spectral stability determinations showed that this filter, in fact, stops the wavelengths responsible for the obliteration of the UV spectrum of the elastomer as is

* See test methods at end of article.

** Transmits <0.5% below 411 m$\mu$; cut, 436-466 m$\mu$; transmits 80% or more 541-750 m$\mu$.

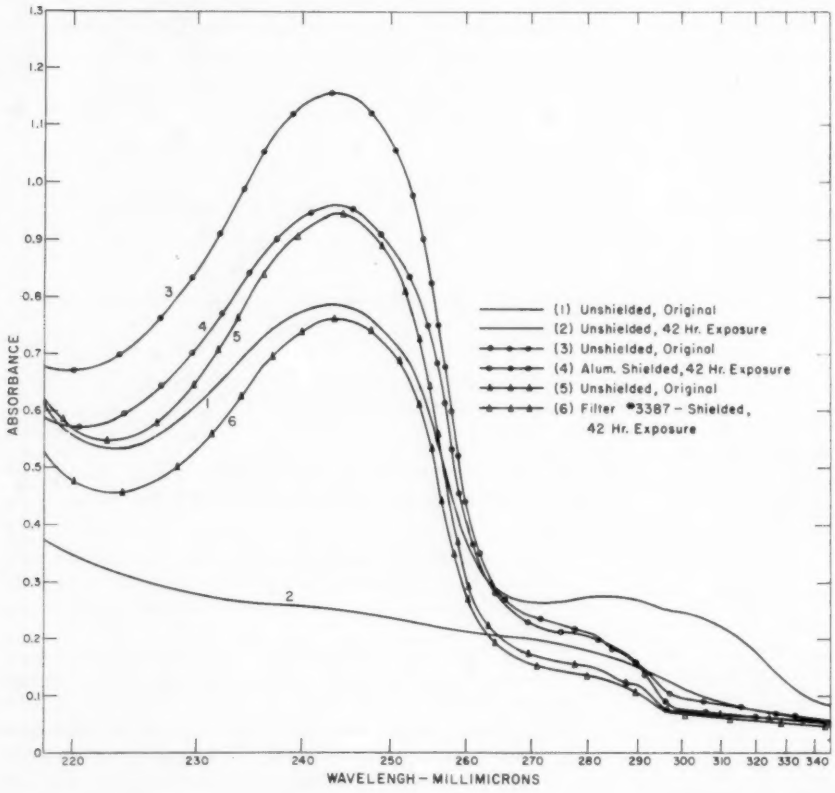
ABSORBANCE
WAVELENGH – MILLIMICRONS
(1) Unshielded, Original
(2) Unshielded, 42 Hr. Exposure
(3) Unshielded, Original
(4) Alum. Shielded, 42 Hr. Exposure
(5) Unshielded, Original
(6) Filter #3387 – Shielded, 42 Hr. Exposure

**Figure 12.** The effect of Weatherometer exposure on the ultraviolet absorption spectrum of B. F. Goodrich's poly(ester-urethane) elastomer: unshielded; shielded with aluminum foil; shielded with Corning Filter #3387.

**Table 4. The Effect of Corning Optical Filter #7380 on the Weatherometer Degradation of Subject Elastomer Microdumbbells**

| | Tensile Strength (psi) | Elongation (%) | Modulus (psi) |
|---|---|---|---|
| Unexposed Sample | 5980 | 612 | 1060 (300%) |
| Exposed* Sample (Unshielded) | 823 | 242 | 850 (242%) |
| Exposed* Sample (Shielded)** | 910 | 175 | — |

* Dry Weatherometer (154 Hours)
** Corning Optical Filter #7380.

apparent in *Figure 12*. The protective action of this filter was confirmed in stress-strain measurements of elastomer microdumbbells which were mounted behind it in a 154 hour Weatherometer exposure. This is seen in *Table 5*. This set of experiments demonstrates that the subject elastomer is photosensitized in weathering by the minor absorption of incident artificial or natural solar radiation of the wavelength range 334 to 411mμ.

## Custom Synthesis Program

Several ultraviolet absorbers have been tested as weather resisters in the subject urethane elastomer. Some prove to be fairly effective, others ineffective and still others incompatible. Having learned that the solar type radiation which photosensitizes the elastomer in weathering is in the range of about 334 to 411mμ commercial ultraviolet absorbers absorbing strongly in this range were sought. Highly effective materials of this type which are satisfactorily compatible with the elastomer are not readily found, so chemicals were "custom synthesized" to meet these requirements.

Crotonaldehyde-2,4-dinitrophenylhydrazone, of the many compounds prepared and examined, proved to have a fairly favorable combination of absorption characteristics, (max. log ε 4.3 at 360mμ, strong absorption at 340-410mμ), good compatibility with the subject elastomer, and good stability.

**Table 5. The Effect of Corning Optical Filter #3387 on the Weatherometer Degradation of Subject Elastomer Microdumbbells**

| | Tensile Strength (psi) | Elongation (%) | 300% Modulus (psi) |
|---|---|---|---|
| Unexposed Sample | 5980 | 612 | 1060 |
| Exposed* Sample (Unshielded) | 1000 | 250 | — |
| Exposed* Sample (Shielded)** | 5935 | 645 | 1527 |

* Dry Weatherometer (154 Hours).
** Corning Optical Filter #3387.

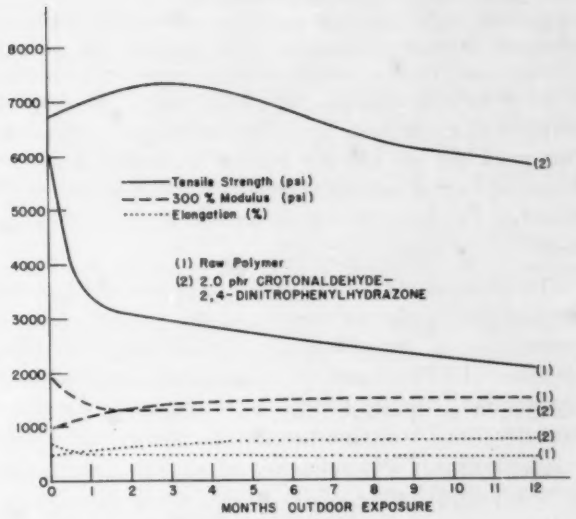


**Figure 13.** Changes in the stress-strain properties of B. F. Goodrich's poly(ester-urethane) elastomer and its compound with 2.0 phr of crotonaldehyde-2,4-dinitrophenylhydrazone on outdoor exposure.

After 12 months of outdoor exposure the excellent effectiveness of this compound at 2.0 phr as a subject elastomer weather resister is seen in *Figure 13*. Microdumbbell samples were involved in this exposure.

The above concentration of this ultraviolet absorber prevented surface embrittlement of the stock during the exposure. The additive imparts a red-orange color to the stock.

Of the commercial ultraviolet absorbers examined to date, U. V. Absorber 24* (1) 2, 2'-dihydroxy-4-methoxy

* American Cyanamid Co.

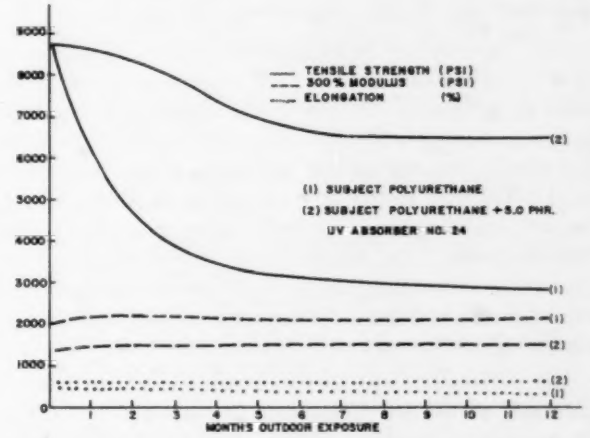


**Figure 14.** Changes in the stress-strain properties of B. F. Goodrich's poly(ester-urethane) elastomer and its compound with 5.0 phr of UV Absorber No. 24 (Am.Cyan.Co.) on outdoor exposure (25 mil microdumbbells).

benzophenone (1) is of most interest. It is soluble in and compatible with subject urethane elastomer. Although relatively high concentrations (5.0 phr) of this material are required, twelve month outdoor exposure tests show it to provide a transparent amber stock showing the retention of stress-strain properties indicated in *Figure 14*. This stock did not develop surface brittleness during exposure and there was no evidence of absorber bloom. UV Absorber 24 shows strong absorption in the wavelength range, 300-370m$\mu$.

The effect of several conventional amine and phenolic antioxidants on the weathering of the subject elastomer proved to be beneficial. N, N'-diphenyl-p-phenylenediamine (DPPD) and N, N'-di($\beta$-naphthyl)-p-phenylenediamine (Agerite White) were the most effective of those examined in twelve month outdoor exposure studies.

*Figure 15* shows the changes in stress-strain properties of 75 mil thick ASTM dumbbell samples of the elastomer and its compounds with the most effective amine-type antioxidant tested (DPPD), and with 1.0 phr of the most effective phenolic-type antioxidant tested, methylene-bis(2-hydroxy-3-tertiary butyl-5-methyl benzene (Antioxidant 2246). None of the antioxidants examined proved capable of preventing the surface embrittlement of exposed stocks.

Carbon black proves to be a most effective weather resister for subject urethane elastomer. EPC, HAF, SRF, MT, ISAF, FF, FEF and MPC blacks have been tested and all improve the weather resistance of the polymer. An easy processing channel black, Wyex, was rated the most effective of those examined, and a medium thermal black, Thermax, the least effective.

*Figure 16* shows the change in stress-strain properties of 25 mil microdumbbells of unprotected subject elastomer and its compounds with 1.0 and 10.0 phr of EPC black on 12 months of outdoor exposure. The lower black concentration allowed some surface embrittlement of the sample during the exposure whereas 10.0 parts completely prevented surface embrittlement.

The stability of black-loaded subject elastomer to weathering must be due, in part, to the opacity of carbon black to incident radiant energy. It may also be explained in Szwarc's suggestion (9) that such high energy radiation yields free radicals in polymers which proceed to bond covalently to the free edge "active centers" or to the aromatic rings of contained carbon particles. Rather than degrading, the black-loaded stocks knit together. *Figure 16* shows increases in both tensile and modulus values on the outdoor exposure of the subject elastomer containing 10.0 phr of carbon black.

The performance of carbon black as well as a fairly effective ultraviolet absorber, Uvinul 490*, (Antara Chemicals) as weather resisters is difficult to reconcile

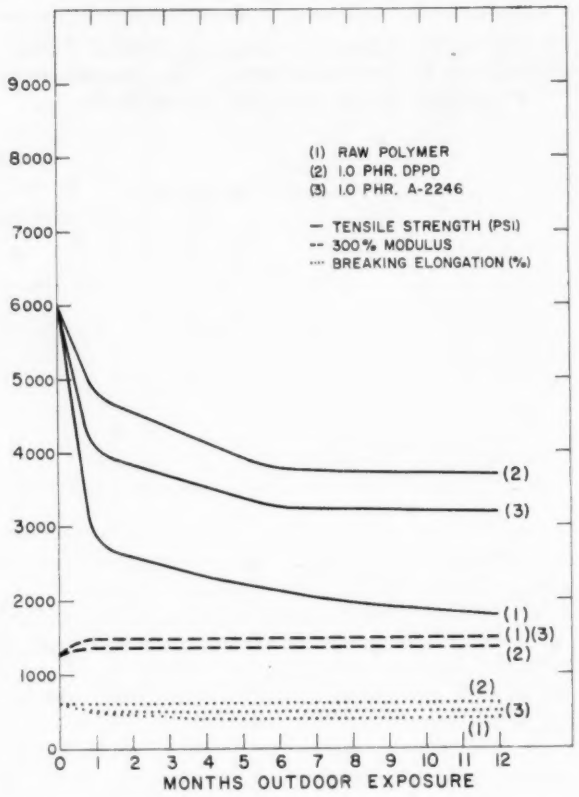


**Figure 15.** Changes in the stress-strain properties of B. F. Goodrich's poly(ester-urethane) elastomer and its DPPD and A-2246 compounds on outdoor exposure.

with the tendency of their compounds to absorb oxygen on Weatherometer exposure as is apparent in a reconsideration of *Figure 5*.

On the other hand, a reexamination of *Figure 3* clearly shows the stabilizing action on the subject elastomer of carbon black, DPPD, and Uvinul 490 in oxygen absorption determinations at 130°C.

In summary, the work discussed in this article demonstrates, among other things, the following important points:

(1) the weathering of the subject elastomeric polyurethane is a photosensitized autoxidation process.

(2) radiant energy capable of photosensitizing the subject urethane polymer in the weathering process is of the wavelength range 334 to 411m$\mu$.

(3) although not immune to the weathering process, unprotected elastomer still retains a high degree of mechanical strength and flexibility after extended outdoor exposure.

(4) carbon black, certain ultraviolet absorbing chemicals, and certain antioxidants, when added to

* 2,2'-Dihydroxy-4-4'-Dimethoxy-Benzophenone, and a mixture of other tetra-substituted benzophenones.

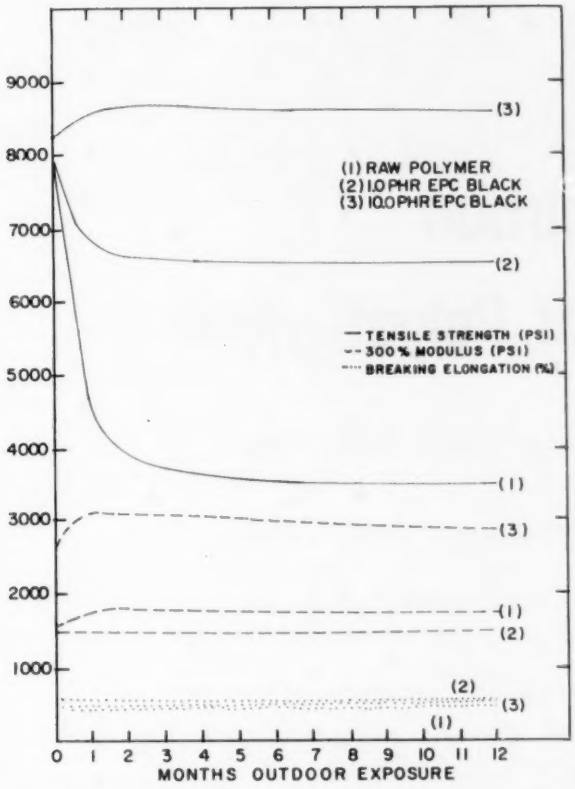


**Figure 16.** Changes in the stress-strain properties of B. F. Goodrich's poly(ester-urethane) elastomer and its EPC black compounds on outdoor exposure.

the subject elastomer type, provide useful compounds of superior weather resistance.

The authors wish to express their appreciation to the United States Army Signal Research and Development Laboratory, Materials Branch, Electronic Parts and Materials Division, Fort Monmouth, New Jersey, who sponsored this research and to the following B. F. Goodrich Company personnel: Mr. S. Caprette, Mr. A. Hawthorne and Miss M. J. Ferguson for their help in determining and interpreting absorption spectra, and to Messrs. D. Diller and E. H. Rowe for the mass spectrometric analyses.

## Test Methods Used in Experimental Work Described in this Article

*Stress-strain measurements* were made on the Scott L6 tensile tester, (Scott Testers, Inc., Providence, Rhode Island), 20"/minute jaw separation rate. Three dumbbell sizes were involved in the testing of this study:

(a) Die C, ASTM D412-51T, sample 0.075" thick

(b) Die D, ASTM D412-51T, sample 0.075" thick. Referred to as "*¼" dumbbell*" in text.

(c) Special die identical with Die D(ASTM D412-51T) but 0.25" shorter in neck. Sample 0.025" thick. Referred to as "microdumbbell" in text.

*Weatherometer exposures* were performed in the Twin Lamp Type HVDL-X Weatherometer 220 volts, 60 cycle (Atlas Electric Devices Corp., Chicago, Illinois).

*Ozone exposure* was performed according to ASTM test method D1149-55T.

*Oxygen (bomb) exposure* was performed according to ASTM test method D572-53 (excepting temperature which was 10°C higher).

*Infrared absorption spectra* were determined on pressed films of the polymer using the Perkin-Elmer, Model 231, Infrared Spectrophotometer.

*Ultraviolet absorption spectral* changes on Weatherometer exposure were determined on very thin films of the polymer (made by brushing 1% tetrahydrofuran solutions on quartz slides) using the DK-2 Beckman Ratio Recording Spectrophotometer.

*Molar absorptivity* of the polymer was determined on solutions of the polymer in tetrahydrofuran using the DK-2 Beckman Ratio Recording Spectrophotometer. In determining molar absorptivity the repeating unit of the polymer was used as is customary, as the molecular weight value in calculating concentrations. The general method described by M. G. Mellon on page 194 of "Analytical Absorption Spectroscopy", John Wiley & Sons, Inc., New York, New York, 1950 was used. See also page 5 of "Ultraviolet Spectra of Aromatic Compounds" by R. A. Friedel and Milton Orchin, John Wiley & Sons, New York, New York, 1951.

## Literature References

1. Schollenberger, C. S., Scott, H., Moore, G. R., *Rubber World*, Jan., 1958, 549-555.
2. Hamilton, C. W., Leininger, R. I., Sommerman, G. M. L., *Wire and Wire Products, 31*, 187 and 233, (1956).
3. Achhammer, B. G., Reinhart, F. W., Kline, G. M., *J. Applied Chemistry, 1*, 301 (1951).
4. Biggs, B. S., Hawkins, W. L., *Modern Plastics, 31*, 1 121 and 203 (1953).
5. *Bulletin WO-246-T*, Atlas Electric Devices Co., Chicago 10, Illinois.
6. Bellamy, L. J., "*The Infrared Spectra of Complex Molecules*", London: Methuen & Co., Ltd., New York: John Wiley & Sons, Inc., 2nd Ed, 1958.
7. Adams, R., Anderson, J. L., *J. Amer. Chem. Soc.*, 72, 5154, (1950).
8. Adams, R., Acken, D. S., *J. Amer. Chem. Soc.*, 74, 3657-9, (1952).
9. Szwarc, M., *J. Polymer Sci., 19*, (93), 589, (1956).

# The Effect of Molecular Weight Distribution on the Flow Properties of Polyethylene

D.R. Mills,* G.E. Moore** and D.W. Pugh

*U.S. Industrial Chemicals Company, Tuscola, Illinois*
** Now with Foster-Grant*
***Now with Keuffel & Esser Co., Hoboken, N. J.*

*The fact that two polymers may have the same melt index does not necessarily mean that the flow behaviors will be the same. Molecular weight distribution provides one key to the answer. Increase in molecular weight distribution increases sensitivity to pressure*

The non-Newtonian flow behavior of polyethylene has been investigated with respect to the effects of molecular weight and molecular weight distribution. Effects of die geometry on melt fracture as well as preliminary extrudate orientation studies are discussed. Differences in processability between polyethylenes of similar melt indices and densities can be explained from information related to molecular weight distribution. Maximum "recoverable orientation" (elastic limit) of the extrudate is observed to occur at the critical shear rate. The "type" of melt fracture observed appears to be related to the nature of the polyethylene sample.

## Rheology

The flow properties were determined in a gas activated, capillary viscometer*. The capacity of the barrel is about 20-25 grams permitting extensive study over a wide range of shear stresses. Temperature control was maintained with a thermistor unit. Temperatures up to 225°C are possible with this particular instrument. Flow curves obtained with this instrument can be reproduced with little or no variation. Dies used in studying entrance effects on flow and melt fracture are described in *Table 1*.

**Fractionation.** The procedure for fractionation (1) was essentially as follows: polyethylene was dissolved in a solvent at a temperature above the crystalline melt point. Suitable quantity of non-solvent was added until the cloud point was reached. Subsequent heating caused return to solution. From this point on, small temperature decreases were made removing successively lower molecular weight material until the final low molecular weight fraction was removed as residue. Subsequent washing and drying resulted in a white, powdery fraction. In this manner, rather large fractions were obtained (2-5 grams) thus permitting extensive characterizations.

**Extrudate Annealing.** Extrudates were annealed for the orientation study by placing a specimen of known dimensions in a polyethylene glycol medium at a temperature above the crystal melt point. After a 60 second annealing period, these were dried and cooled and the amount of retraction or shrinkage measured.

**Calculations.** Flow property calculations were based on assumptions used in previous work (5). The shear stresses were calculated at the walls. Shear rates were not corrected for die end effects.

$$\alpha = \frac{PR}{2L}; \quad \gamma = \frac{4Q}{\pi R^3}$$

P = Pressure drop  L = Orifice length
Q = Volume flow rate  R = Orifice radius

**Table 1. Geometry of Dies Used**

| Die | Included Entry Angle (degrees) | Capillary, Inches Length | Diameter |
|---|---|---|---|
| #10 | 180 | 0.176 | 0.0193 |
| #11 | 140 | 0.176 | 0.0193 |
| #15 | 90 | 0.176 | 0.0193 |
| #28 | 40 | 0.176 | 0.0193 |

* Manufactured from design of C.I.L. by Pressure Products Inc., Hatboro, Pennsylvania.

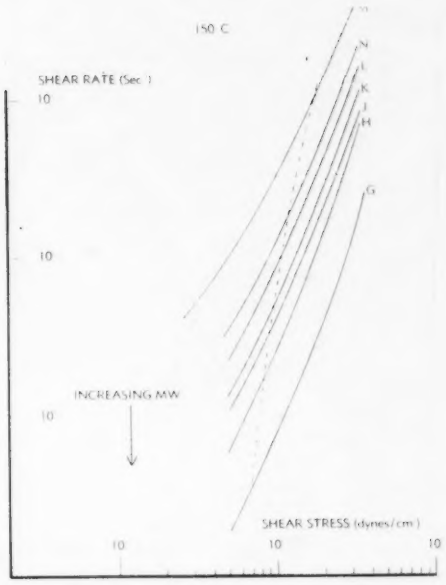


**Figure 1.** Effect of molecular weight on melt flow properties. See page 43 for key to resins.

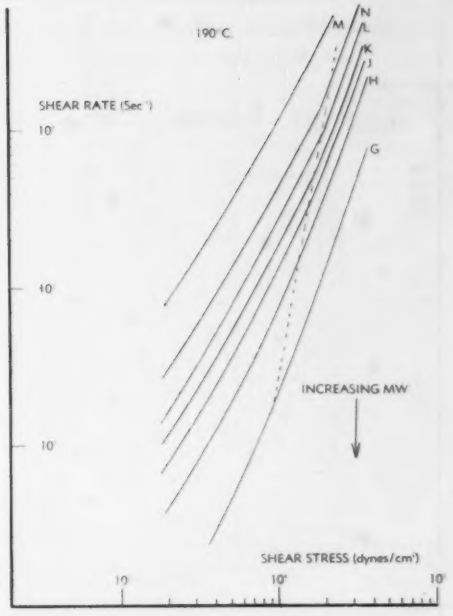


**Figure 2.** Effect of molecular weight on melt flow properties at 190°C. See page 43 for key to resins.

**Polyethylenes.** A general description of the polyethylenes used in this study is found in *Table 2*. The molecular weight distributions are qualitatively indicated as wide or narrow depending on synthesis. The type of polyethylene is noted as linear (L) or branched (B).

## Melt Flow Properties

**Molecular Weight.** The effect of molecular weight on melt flow properties is shown in *Figure 1*. As the molecular weight decreases (MI increases), the shear rate at a given shear stress becomes greater. A noticeable decrease in the slope of the log shear rate—log shear stress plot is observed as the molecular weight decreases. Hence, the differences in flow rates at very high shear stresses decreases within a given series of polyethylenes. In *Figure 2*, the same series at 190°C. is shown. This same effect is even more pronounced at this higher temperature. It is observed that the slope for a given curve decreases as the temperature increases.

In the case of linear polyethylenes, this same effect is observed. Corresponding plots of a linear series at 150°C. and again at 190°C. are shown in *Figures 3 and 4* respectively. A very significant difference between the linear and branched plots is noted. The linear polymers show a very sharp "break" in the flow curve as depicted in these figures. This "break" is reproducible and no noticeable "hysteresis" has been observed. After this sharp increase in shear rate at the critical shear stress (function of temperature), the flow curve returns to a more gradual increase in slope. It is observed that the melt fracture point for linear polymers coincides with this "critical" shear stress where the sharp break occurs. At 190°C., this "break" point is the same for all the linear polyethylenes in this series (*Figure 4*).

Thus, an increase in molecular weight results in a decrease in the absolute shear rate but in an increase in the rate of change of the shear rate (greater slope).

**Molecular Weight Distribution.** In comparing polyethylenes of different series or from different producers, the importance of molecular weight distribution cannot be overemphasized. The fact that two polyethylenes have the same melt index cannot always be used to describe quantitatively their flow behavior under different conditions unless they come from a known series.

*Figure 5* vividly illustrates this fact. Three polymers, each with a melt index of approximately 6, are compared. The wide molecular weight distribution charac-

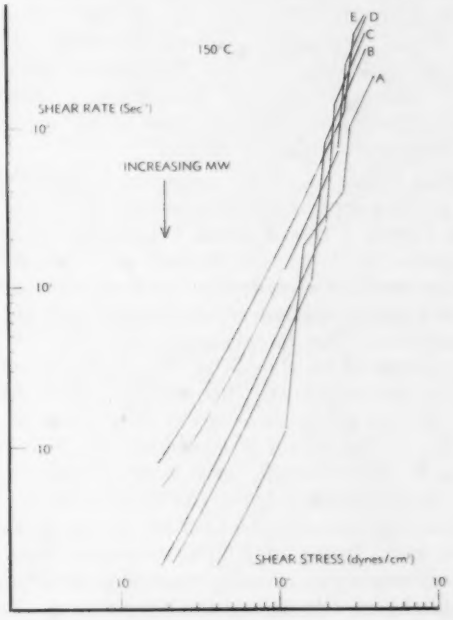


**Figure 3.** Linear polyethylene, at 150°C. The linear polymers show a sharp break in the flow curve.

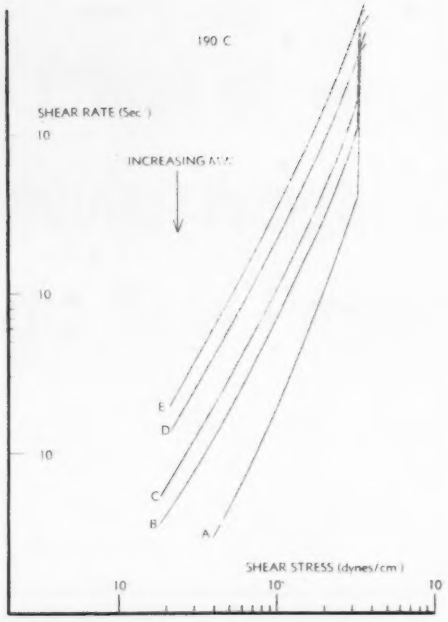


**Figure 4.** Linear polyethylene, at 190°C. "Break point" is the same for all linear polyethylenes.

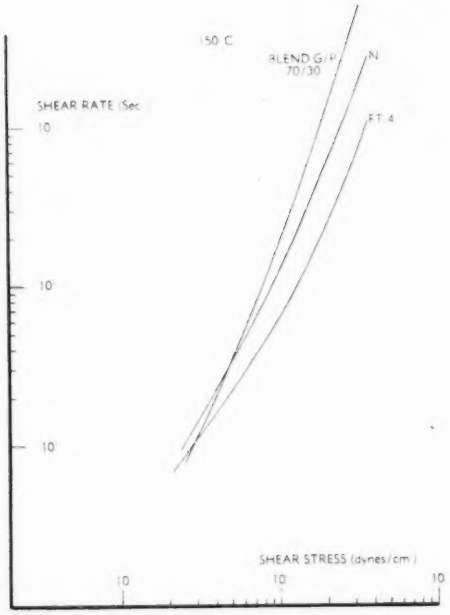


**Figure 5.** Effect of molecular weight distribution on flow properties.

terized by the blend shows extreme pressure sensitivity with a corresponding high slope. The fraction of the experimental polyethylene exhibits relatively low slope characteristic of a narrow molecular weight distribution. The whole polyethylene, *N* depicts intermediate flow behavior representative of its synthesized molecular weight distribution. As a further illustration, *Figure 6* compares the blend of melt index 6 with a whole polyethylene of melt index 22 and relatively narrow distribution. While in the region of melt index shear stress, a definite difference exists (MI 22 and 6), we note that this difference is reduced as the shear stress increases until at about 2 x $10^6$ dynes/cm$^2$ the shear rates are the same. From these examples, we conclude that an increase in molecular weight distribution for a given average molecular weight increases its sensitivity to pressure. This means that the slope of the log shear rate —log shear stress curve is greater.

Another factor of primary interest in nearly all processing is the temperature dependence of flow of a material. In *Figure 7* a wax blend (wide MW distribution) is compared with a polyethylene of relatively narrow molecular weight distribution and approximately the same melt index. Curves at 150°C. and 190°C. for both are compared. The temperature sensitivity of the two can be compared by examining the displacement of each curve on increasing the temperature from 150°C. to 190°C. At any given shear stress, it is observed that the shear rate of the blend is increased less than the polyethylene *N*. For example, at 6 x $10^5$ dynes/cm$^2$, the increase in temperature from 150°C. to 190°C. doubled the shear rate for the blend but increased the whole polymer by a factor of 3. This example illustrates the decreased sensitivity of wide molecular weight distribution polyethylenes to changes in temperature.

This apparent dependence of the activation energy of viscous flow (temperature sensitivity) on number average molecular weight has been advanced by Fox and Flory (6) based on their observations with plasticized polystyrene. As the distribution increases, the number average molecular weight decreases and so does the activation energy of viscous flow (temperature sensitivity).

**Linear–Branched Blends.** A series of six blends of linear polyethylene and branched polyethylene of nearly the same melt indexes have been investigated. The changes in the shape of the linear flow curve were investigated in relation to the concentration of branched

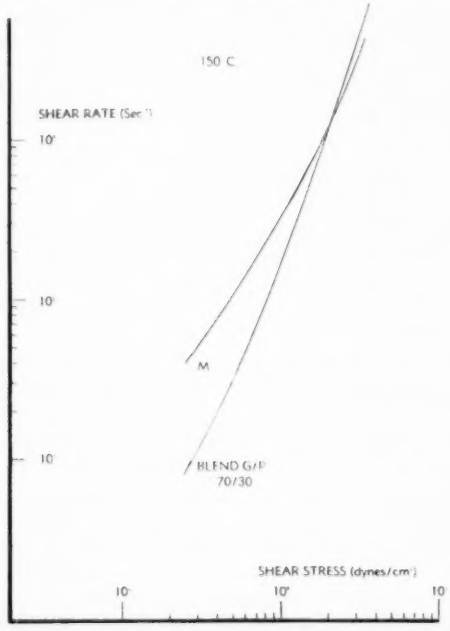


**Figure 6.** Molecular weight distribution—effect of blending with low MW PE wax.

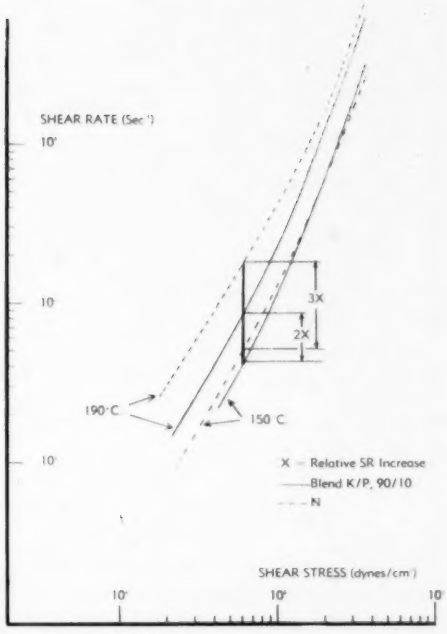


**Figure 7.** Effect of MW distribution on temperature sensitivity.

polymer. The changes in flow up to even 20% concentration of branched polymer are small. In *Figure 8*, the curves have been displaced along the abscissa to show the effect of the branched material on the *shape* of the curve. The small arrow designates melt fracture onset. The 80% linear blend shows a smooth, but increasing slope. At 90% linear, the characteristic "break" in the curve returns. Some properties of these blends are included in *Table 3*.

## Extrudate Properties

Previous investigators (2, 3, 4, and 5) have studied melt fracture and the conditions related to the onset of melt fracture. In most cases, (2, 4 and 5) the studies were related to the conditions at which melt fracture was observed with a particular defined polymer. In our work, as well as that of Spencer and Dillon (3), it became apparent that not only were the conditions important but that these conditions might bear an interesting relationship to the polymer properties.

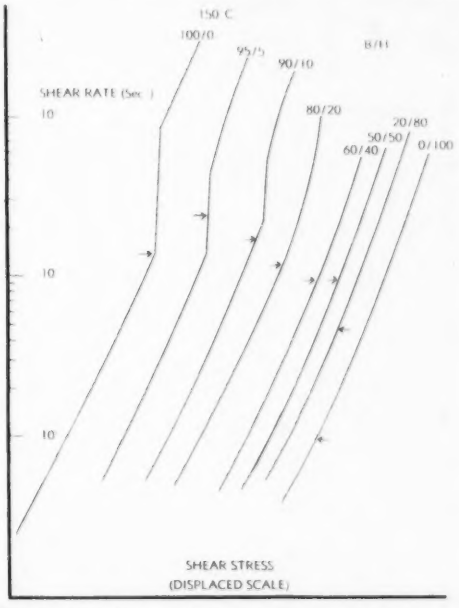


**Figure 8.** Blends, shape of flow curves. Curves have been displaced along the abscissa to show effect of branched material on the shape of the curve.

**Table 2. Polymers Studied**

| Designation | Polymer | Melt Index | Density | Molecular Weight Distribution | Type |
|---|---|---|---|---|---|
| A | Marlex T-2* | .2 | 0.965 | W | L |
| B | Marlex T-9* | .9 | 0.965 | W | L |
| C | Marlex T-15* | 1.5 | 0.965 | W | L |
| D | Marlex T-35* | 3.5 | 0.965 | W | L |
| E | Marlex T-50* | 5.0 | 0.965 | W | L |
| G | P-300** | .3 | 0.915 | N | B |
| H | P-301** | 1.0 | 0.915 | N | B |
| J | P-100** | 2.0 | 0.918 | N | B |
| K | P-200** | 2.9 | 0.918 | N | B |
| L | P-201** | 5.1 | 0.918 | N | B |
| M | P-202** | 21.6 | 0.918 | N | B |
| N | P-203** | 7.8 | 0.918 | N | B |
| P | AC-6 (PE Wax)*** | — | — | — | B |
| R | P-239** | 4.9 | 0.928 | W | B |
| S | DND-2450 | 1.0 | 0.917 | W | B |
| T | Exp. Polymer | 1.0 | 0.925 | N | B |
| W | P-208** | 22.9 | 0.922 | N | B |
| Y | P-206** | 4.9 | 0.923 | N | B |

* Trade name, Phillips Pet. Co.
** "Petrothene", USI Polyethylene Resins
*** Tradename, Allied Chemical, Low MW PE Wax
**Note:** The notation F- preceding any polymer designation in this report refers to a narrow molecular weight distribution fraction of that polymer.

**Die Entrance Angle.** Recent references (4, 5 and 7) to the phenomena of melt fracture indicate that die entry angle is an important factor. Bagley (7) indicates that with a 60° included angle, the critical shearing stress may be many times that observed using a flat entry die (180° included angle). Several postulations have been advanced (3, 4 and 7) as to why the entry angle is so vital in determining the critical shear stress. *Evidence that the fundamental properties of the polyethylene considered is a vital factor in melt fracture has been obtained.* Several polyethylenes have been examined, using the four dies described previously in *Table 1*.

In the tabular presentation (*Table 4*) two polyethylenes are compared with respect to melt fracture onset and entry angle. As the shear stress increases, the tabulated sequence of melt fracture in relation to the die geometry is observed.

**Table 3. Properties: Branched/Linear Blends**

| B/H | Melt Index, g/10 min. | Density, g/cc | $\eta$ | Crystalline MP °C. |
|---|---|---|---|---|
| 100/0 | 0.6 | 0.965 | 2.60 | 135 |
| 95/5 | 0.8 | 0.960 | 2.03 | 135 |
| 90/10 | 0.7 | 0.959 | 1.98 | 135 |
| 80/20 | 0.7 | 0.955 | 1.88 | 134 |
| 60/40 | 0.7 | 0.944 | 1.75 | 133 |
| 50/50 | 0.7 | 0.940 | 1.67 | 133 |
| 20/80 | 0.8 | 0.925 | 1.43 | 132 |
| 0/100 | 0.9 | 0.916 | 1.14 | 109 |

**Table 4. Sequence of Melt Fracture (Included Angle)**

| Increasing Shear Stress | Wide MW Distribution (R) | Relatively Narrow MW Distribution (Y) |
|---|---|---|
| ↓ | 90° | 90°-180° |
| | 140° | 140° |
| | 180° | 40° |
| | 40°* | |

* (No M.F. observed within S.S. range)

Significantly, it is observed from *Table 4* that in the case of the wider molecular weight distribution polyethylene of the same melt index, that the 180° included angle die was not the first to give melt fracture as the shear stress increased.

*Figures 9 and 10* compare two polyethylenes of melt index 0.9. Polymer H (*Figure 9*) is a high molecular weight, low density, branched polyethylene; whereas Polymer B is a high density, linear polyethylene. H exhibits melt fracture with all four dies in a very narrow shear stress range, $1 \times 10^6 - 1.3 \times 10^6$ dynes/cm$^2$. The sequence in this narrow range is similar to the narrow distribution polymer in *Table 4*. A change in the location of the "break" point in the linear flow curve is observed as the die geometry is changed. The sequence of fracture is similar to that observed for Y and H. The wide molecular weight distribution branched polyethylene is the only one of these four where the fracture sequence appears different. Further evidence is required to determine whether this phenomena is definitely related to molecular weight distribution.

The dependence of the critical shear stress on molecular weight has been proposed by Spencer and Dillon (3) where (for polystyrene) the critical shear stress was found to vary inversely with the molecular weight. *Figure 11* depicts the critical shear stress versus the melt index obtained on the low density, branched series and the high density, linear series. If we compare each series within itself, we can compare the critical shear stress with molecular weight, at least qualitatively, by using the melt index as an inverse indication of molecular weight. The branched polyethylenes show a trend as found by Spencer and Dillon, the critical shear stress decreasing with increasing molecular weight. Little difference exists in the slope of the 150°C. and 190°C. plots, although the critical shear stresses are higher at 190°C.

The linear polyethylenes show a similar dependence of critical shear stress on molecular weight at 150°C. However, at 190°C., the critical shear stress appears to be independent of molecular weight. A further examination of the critical shear rate in relation to molecular weight is indicated for the future. As indicated by the plot of critical shear rate versus melt index (*Figure 12*), the critical shear rate varies inversely to the molecular weight also. Both series at both temperatures show a definite dependence on the molecular weight.

In addition to these qualitative observations, it has been observed that the molecular weight distribution is another factor in the critical shear rate determination. As

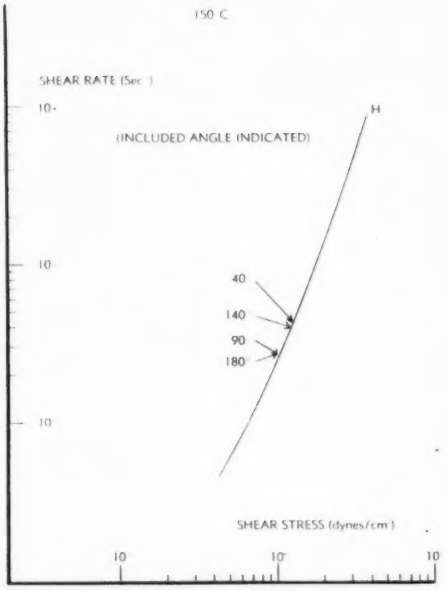


**Figure 9.** Effect of entrance angle on melt fracture onset branched polyethylene.

molecular weight distribution increases the onset of melt fracture occurs at higher shear stresses. It is significant, however, that the melt fracture observed is different from that obtained on narrow molecular weight distribution polyethylenes. The type of melt fracture obtained apparently depends on the same variables as melt fracture itself. Three general classes have been observed in the case of polyethylenes, that for branched PE, that for linear, and that for very narrow molecular weight fractions.

## Processing Factors

The observed swelling of the extrudates has interesting applications in extrusion and injection molding.

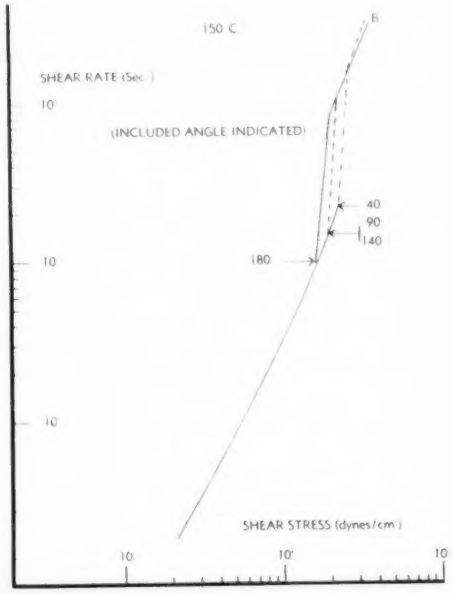


**Figure 10.** Effect of entrance angle on melt fracture onset linear polyethylene.

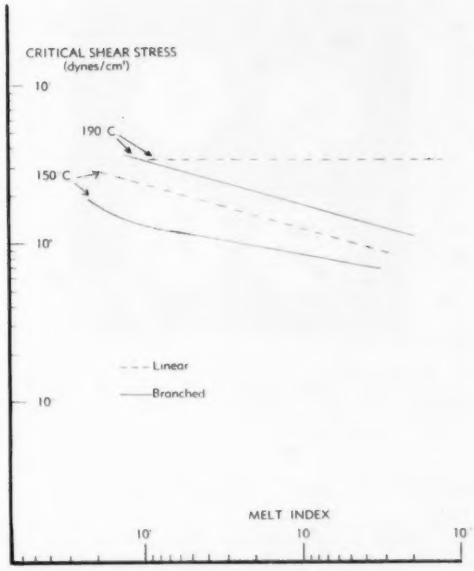


**Figure 11.** Effect of MW on critical shear stress.

Draw-down rates, blow ratios, film shrinkage and optical properties are some of the factors influenced by the extrudate recovery or swelling. No attempt has been made to relate the observations here to these properties. Branched polyethylene shows an increase in extrudate cross section as molecular weight decreases. As the shear rate increases, this difference becomes more pronounced. Conversely, the linear polyethylenes show a slight increase in cross section with molecular weight. It is observed that the cross section decreases rapidly after the critical shear rate for both linear and branched polyethylene.

As the temperature of extrusion increases, this decrease in extrudate cross section after melt fracture becomes less evident, (*Figure 13*). As observed before, the critical shear rate increases with temperature. The cross section also increases in the higher shear rate region. At low shear rates, the change introduced by changing

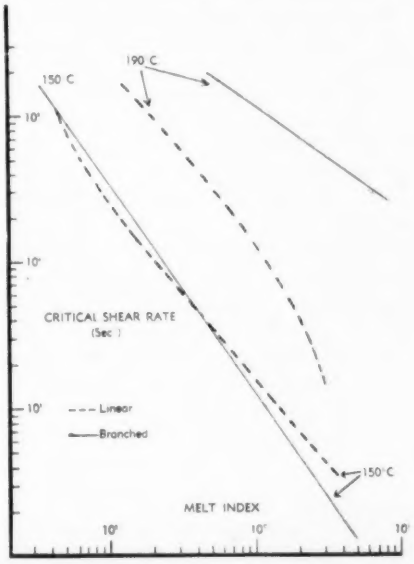


**Figure 12.** Effect of MW on critical shear rate.

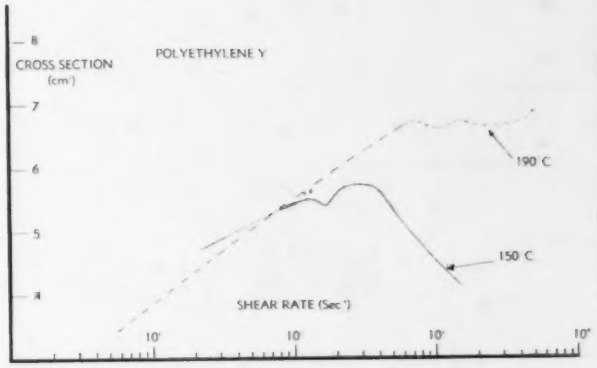


**Figure 13.** Effect of temperature on extrudate swelling.

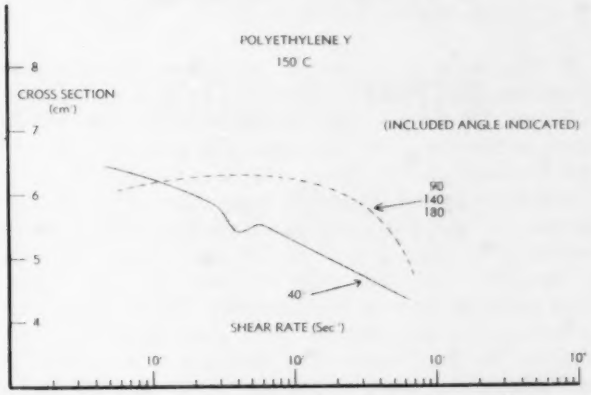


**Figure 14.** Effect of entrance angle on extrudate swelling.

temperature from 150°C to 190°C is small. Beyond melt fracture, the extrudate cross section measurements become less reliable thus resulting in somewhat undefined results in some cases.

Increased molecular weight distribution tends to shift the downward trend in extrudate cross section to higher shear rates. This is expected since the critical shear rate is increased similarly. Extrudate examinations of polyethylenes of extremely dissimilar molecular weight distributions have not been competely analyzed, hence only a qualitative statement can be made here. It is observed that as the distribution becomes extremely broad, that the cross section becomes less dependent on shear rate.

Since the die entry affects the melt fracture onset so markedly, it was anticipated that noticeable changes in extrudate cross sections would be found. With the exception of the 40° included angle die, little change in cross sections between dies was observed. The smallest included angle die demonstrated a definite decrease in extrudate cross section as the shear rate increased. The other dies show a slight increase and then decrease after melt fracture, (*Figure 14*).

Spencer and Dillon (3) postulated that melt fracture originated at the die exit. Accordingly, they proposed that the differences in orientation of the cross-section of the extrudate from the highly oriented "skin" to the much less oriented extrudate core caused unequal retraction on cooling after the die exit. Subsequent uneven cooling and retraction resulted in fracture or spiral formation.

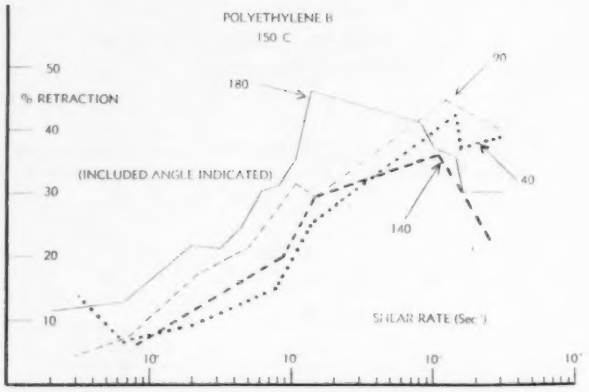


**Figure 15.** Effect of entrance angle and shear rate on retraction of extrudate after annealing.

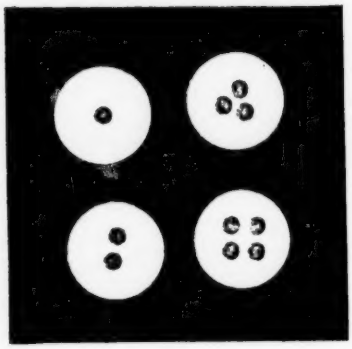

**Figure 16.** Multiple orifice used in standard melt indexer. Orifice dimensions are all equivalent to standard die, 0.315" length, .0825" diameter.

If this were true, proper annealing of extrudates should result in a marked reduction of the melt fracture. In *Figure 15* the per cent retraction of the extrudate is shown as the shear rate increases. The polyethylene used here is a high density linear with a melt index of about 1. Referring to the figure, we note that the highest retraction, i.e. greatest orientation, was found at the melt fracture point regardless of the die geometry. In the case of the 180° die, this point coincides with the sharp break in the flow curve. For the other dies, the maximum retraction does not coincide with any apparent irregularity in the flow curve. The decrease in retraction at the higher shear rates for the 140°, 90° and 40° entry angle dies appear after melt fracture occurs. From this information, it is apparent that the melt fracture point or critical shear rate coincides with the highest orientation in the extrudate. Visual examination of the annealed extrudates revealed no decrease in roughness or melt fracture, in fact, in some cases, the melt fracture was more pronounced. Changes in retraction can be made by slow cooling the extrudate or shock-quenching at the die exit. In one case, retraction was changed from *30%* to *49%* by cooling the extrudate at the die exit in a dry ice-alcohol mixture.

The practical significance of this retraction is evident when we consider the effect bath temperature, mold temperature or casting roll temperature, etc. have on the draw-down rate as well as on the shrinkage of film and molded articles.

In considering the phenomena of melt fracture further, another interesting effect has been observed when using multiple-orifice dies, as pictured in *Figure 16*. These dies were used in standard melt index equipment. While the data are fragmentary at present, it is interesting to note that the relationship between the total number of orifices per die and the flow rate per orifice is *essentially linear*. Flow interference between one orifice and another at the die entry can account for the reduction in flow rate observed as the number of orifices increases. This interesting behavior constitutes an area for further study.

## Conclusions:

1. Increased molecular weight distribution yields a polyethylene with flow properties more sensitive to pressure (shear stress) and less sensitive to temperature (lower activation energy of viscous flow).
2. Melt index is a valuable parameter in predicting flow properties under processing conditions for polyethylenes of the same series, otherwise the flow curves are essential.
3. Die entry geometry is vital in determining the critical shear rate at a given temperature. Conical (inverted) dies with included angles of about 40° reduce surface roughness or melt fracture.
4. *Optimum* die entry geometry for maximum critical shear rates may be different for different polyethylenes depending on the fundamental parameters of the polyethylene such as long-chain branching and molecular weight distribution.
5. Extrudate relaxation studies indicate that maximum recovery occurs at the critical shear rate independent of the die entry geometry.
6. Melt fracture is observed to depend on die entry, temperature, molecular weight, molecular weight distribution and long-chain branching. It apparently occurs when the elastic limit of the polyethylene or polyethylene "skin" is exceeded, (In this case, at the point of maximum shear stress, i.e. die entry). This is in accord with Tordella and Bagley and others who attribute melt fraction to die entrance effects.

## Literature References

1. To be published.
2. Westover, R. F., and Maxwell, B., *SPE Journal*, p. 27, August, 1957
3. Spencer, R. S., and Dillon, R. E., *J. Colloid Sci.*, 241, *4* (1949).
4. Tordella, J. P., *Transact of Soc. of Rheology*, p. 203, *1* (1957)
5. Schott, H., and Kaghan, W. S., *Ind. Eng. Chem.*, p. 844, *51* (7) (1959).
6. Fox, T. G., Jr., and Flory, P. J., *JACS 70* 2384(1948)
7. Bagley, E. B., *Ind. Eng. Chem.*, p. 714 *51* (5) (1959)

## Acknowledgment

The authors wish to acknowledge the assistance of other members of the Polymer Service Laboratory, U.S. Industrial Chemicals Co., and in particular, Mr. E. V. Arbuckle and Mr. P. Hoff who performed much of the experimental work.

**Marjorie C. St. Cyr**

*Adhesives and Plastics Research Section, Picatinny Arsenal, Dover, New Jersey*

# Hydroxy Alkyl Phosphate Esters as Curing Agents for Epoxy Resins

*A novel curing system yields epoxy resins compatible with explosives*

Chiefly because they can produce strong bonds with a wide variety of adherends, epoxy adhesives are used to bond many different materials. Although the room-temperature-curing epoxy systems are the easiest to use, they are incompatible with a number of explosives. As a result, many of the more common of these systems cannot be used in Ordnance end items where they would be in close proximity to explosives. This incompatibility involves either chemical or physical reactions with undesirable effects upon either the explosive or the adhesive.

Acids, acid anhydrides, and aromatic amines, which normally are not incompatible with explosives, can also be used in epoxy adhesives systems. Unfortunately, these systems generally require elevated cure temperatures, which are undesirable for items containing explosives.

It was clear that a curing agent was needed for epoxy adhesives systems which would be compatible with explosives and would also cure at room temperature. In an effort to develop such a curing agent, the hydroxy alkyl phosphate esters were investigated.

## Background of Choice of New Curing Agents

As an introduction to the discussion of hydroxy alkyl phosphate esters as curing agents for the bisphenol type epoxy resins, it is desirable to discuss briefly the reasons for developing these esters.

Among the various acids listed in the literature as curing agents for epoxy resins is phosphoric acid. It is stated that this acid reacts with the epoxy group as shown by the following equation (1).

$$\begin{array}{l} \text{O} \\ \wedge \\ 3\text{>C-C<} \end{array} \quad + \quad \text{OP(OH)}_3 \rightarrow \text{OP} \equiv (\text{O-C-C-OH})_3$$

In coating formulations, 1% — 2% of the acid is used to catalyze phenol formaldehyde/epoxy blends (2). An evaluation of the bond strength of the reaction product between a low-molecular-weight bisphenol A type epoxy resin and ortho phosphoric acid showed that the resultant product had relatively good bond strength as an adhesive but that it was exceptionally brittle. Also, the rapidity of the reaction (½ — 1 minute) limited the use of the unmodified acid as a curing agent for many adhesives applications. (3)

Since the brittleness or flexibility of a cured epoxy adhesive depends partially on the frequency of crosslinking between the molecules, the more numerous the linkages, the more brittle the material. It is likely that ortho phosphoric acid transforms epoxy resins into dense, closely packed structures incapable of uniform internal distribution of applied stresses. The softening point is likewise affected by the degree of crosslinking between

The Chart shows the adhesive shear strengths to steel at various temperatures when using an HEP-cured bisphenol epoxy resin and a DETA-cured epoxy as a control. It also shows the effect of modifiers on the shear strengths of the HEP-cured adhesive.

the molecules. As before, the more numerous the linkages, the higher the softening point. An adhesive based on a low-molecular-weight bisphenol epoxy resin cured with ortho phosphoric acid was crudely tested by manual pressure and flexing at five-minute intervals for approximately one hour between 77° and 374°F (25°-190°C). The film showed no visible signs of deterioration or softening until the temperature had reached 347°-356°F (175°-180°C). Modification of the adhesive by incorporating a cashew epoxy resin into the system considerably reduced the temperature at which a film of the adhesive began to soften.

The ability of certain polyesters to act simultaneously as plasticizers and curing agents for epoxy resins, and the fact that n-butyl and diethyl ortho phosphates are known curing agents for epoxy resins (4) led to the evaluation of monobutyl and dibutyl ortho phosphate as curing agents for epoxy adhesives (5). Although these acid esters cured the resin at room temperature to hard materials capable of exhibiting high adhesive strengths, films of these adhesives deteriorated to soft viscous masses at temperatures of 135°-140°F (57°-60°C).

Reactants used to cure epoxy resins into hard, infusible materials either become an integral part of the cured resin or initiate self-polymerization of the resin. The material that becomes an integral part of the resin must of necessity be either di- or polyfunctional and it will exert considerable influence on the properties of the cured product. Since the functionalities of monobutyl and dibutyl ortho acid phosphate are 2 and 1, respectively, crosslinking is much less frequent in the cured product than in the parent acid. It may, therefore, be seen from the above changes in functionality of both resin and hardener that frequency of crosslinking and high softening point are criteria for providing good high-temperature adhesives.

Hydroxy alkyl phosphate esters were synthesized for evaluation as room-temperature-curing agents for epoxy resins because (1) the unmodified phosphoric acid produced an adhesive with good bond strength and fairly high softening point even though it was limited in use due to brittleness and rapidity of cure of the resin, and (2) the modified butyl phosphate esters, with decreased functionalities, produced good room-temperature bond strength but low softening points. It was therefore felt that the addition of a hydroxy radical to an alkyl phosphate ester producing functionalities of 3 or more would result in adhesives with good bond strength and high softening points minus the excessive brittleness and the rapid cure.

The separation of the reactive hydroxy sites by alkyl chains should slow down reactivity and increase the flexibility of the polymer cured with this material as compared with the phosphoric-acid-cured adhesive. On the other hand, the higher functionality of the hydroxy alkyl

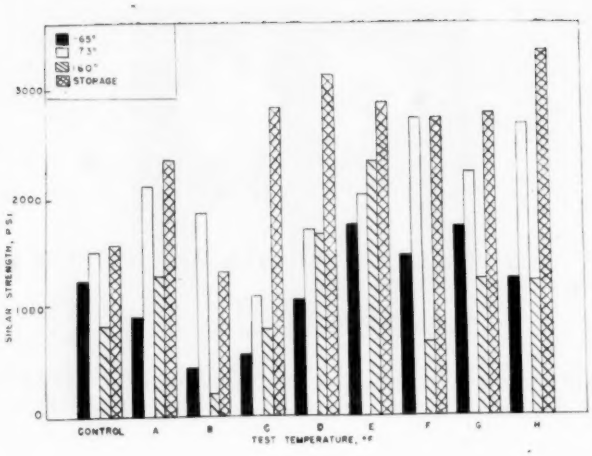


**Table 1. Adhesive Formulations**

| Formulation | Materials | Quantity, Parts by Weight |
|---|---|---|
| A | Epoxy resin | 100 |
| | β-hydroxy ethyl ortho acid phosphate | 12 |
| B | Epoxy resin | 100 |
| | β-hydroxy ethyl ortho acid phosphate | 24 |
| | Monobutyl ortho acid phosphate | 4 |
| C | Epoxy resin | 100 |
| | β-hydroxy ethyl ortho acid phosphate | 12 |
| | Tris-(β-hydroxy ethyl) ortho phosphate | 20 |
| D | Epoxy resin | 90 |
| | β-hydroxy ethyl ortho acid phosphate | 10 |
| | Silicone resin | 10 |
| E | Epoxy resin | 50 |
| | β-hydroxy ethyl ortho acid phosphate | 24 |
| | Phenolic epoxy resin | 50 |
| F | Epoxy resin | 20 |
| | β-hydroxy ethyl ortho acid phosphate | 12 |
| | Polyester plasticizer | 20 |
| G | Epoxy resin | 90 |
| | β-hydroxy ethyl ortho acid phosphate | 12 |
| | Cashew epoxy resin | 10 |
| H | Epoxy resin | 90 |
| | Cashew epoxy resin | 10 |
| | Phosphoric acid | 7.5 |
| Control | Epoxy resin | 100 |
| | DETA | 10 |

**Table 2. Shear Strength of Epoxy-Alkyl Phosphate Ester Adhesive Formulations**

Table 2 shows the shear strength of a low-molecular-weight bisphenol cured with alkyl phosphate esters and a DETA-cured bisphenol epoxy used as a control (5).

| Bisphenol Epoxy, gms. | Monobutyl ortho Acid Phosphate, gms. | Dibutyl ortho acid Phosphate, gms. | Number of Specimens | Curing Schedule | Average Shear Strength, psi |
|---|---|---|---|---|---|
| 100 | 10 | — | 2 | 25 days at 73°F | 2102 |
| 100 | 15 | — | 2 | 25 days at 73°F | 1447 |
| 100 | — | 20 | 2 | 25 days at 73°F | 1857 |
| 100 | — | 25 | 2 | 25 days at 73°F | 2014 |
| 100 (DETA-10) | — | — | 2 | 25 days at 73°F | 1446 |
| 100 | 10 | — | 1 | 9 days at 73°F<br>16 days at 160°F | 2010 |
| 100 | 15 | — | 1 | 9 days at 73°F<br>16 days at 160°F | 1362 |
| 100 | — | 20 | 1 | 9 days at 73°F<br>16 days at 160°F | 1754 |
| 100 | — | 25 | 1 | 9 days at 73°F<br>16 days at 160°F | 2182 |
| 100 (DETA-10) | — | — | 1 | 9 days at 73°<br>16 days at 160°F | 1508 |

**All failures occurred at the adhesive-metal interface.**
**All specimens tested at room temperature.**

phosphate ester should provide greater rigidity and heat resistance than is obtained with the alkyl phosphate esters.

The hydroxy alkyl phosphate esters prepared were β-hydroxy ethyl ortho acid phosphate (HEP), the acid ester, and tris-(β-hydroxy ethyl) ortho phosphate, the neutral ester. Each compound has a functionality of 3. It has been stated in the literature that the product of reacting molar quantities of phosphoric acid and an olefin oxide produces the mono hydroxy ester of phosphoric acid (6) with a structure as follows:

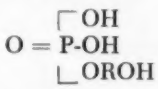

STRUCTURE 1

However, a private communication has indicated that phosphoric acid and olefin oxides react in a 3:1 or 6:1 ratio of oxide to acid, depending on the batch size of the reaction (7). Specifically, three moles of ethylene oxide will polymerize to the trimer before phosphoric acid adds to the ends of the compounds. If such be the case, the structure of the reaction product would be:

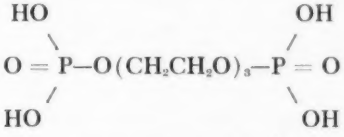

STRUCTURE 2

Since the precise structure of the reaction products has not been established and since it is beyond the scope of this investigation to enter into proof of structure, the results of this study have been formulated on the basis of β-hydroxy ethyl ortho acid phosphate, as shown in Structure I.

An attempt to isolate the purified ester was unsuccessful. Therefore, the compounds used in this study probably contain some polymerized olefin, unreacted acid, and products of competing reactions. Nevertheless, different batches of the crude reaction products produced reproducible bond strengths.

Room-temperature tests show that the shear strength of the HEP-cured epoxy adhesive is 40% greater than that of the standard diethylene triamine (DETA) used as a control. Likewise, the HEP-cured adhesive tested at 160°F (71°C) is 90% higher in shear strength than the control specimen tested at the same temperature. At −65°F (−54°C) however, the shear strength of the HEP-cured material is 25% lower than that of the control (*Figure*). The above observations indicate that there is more crosslinking between the molecules of the HEP-cured adhesive than between those of the control specimens.

In an effort to improve the shear strength of the HEP-cured adhesive at −65°F (−54°C) various modifiers were incorporated into the adhesive system. A phenolic epoxy modification improved the shear strength 45% at −65°F (−54°C) and at the same time increased the bond strength 54% at room temperature and 121% at 161°F (71°C). Other modifiers showed improvements at either 160°F (71°C) or −65°F (−54°C). However,

the improvement was not consistent at the three test temperatures. It may be noted that the monobutyl ortho acid phosphate (MBOAP) modification, which shows a 24% improvement over the DETA control epoxy at room temperature, is significantly poorer at 160°F (71°C) and at −65°F (−54°C) the shear strengths being 77% and 66% lower, respectively.

The phosphoric acid cashew epoxy resin system has significantly higher (77%) shear strengths than the conventional DETA-cured epoxy when tested at room temperature. This system also shows a higher shear strength than the HEP-cured system at room temperature. However, it loses a larger percentage of its bond strength at 160°F (71°C) than the control. Storage at 160°F (71°C) of HEP, modified HEP, and DETA control specimens for seven days improves the shear strength in all cases except the MBOAP modification which is reduced 30% and the HEP polyester modification, which remains constant.

Tris-(B-hydroxy ethyl) ortho phosphate (THEP), the neutral ester of phosphoric acid, unlike HEP, the acidic monoester of the acid, does not cure the bisphenol epoxy at room temperature but does cure it at elevated temperature 160°F (71°C). This ester was incorporated into the HEP system in an attempt to lengthen the pot life of the system. When enough THEP was used to lengthen the pot life, incomplete room temperature cures resulted. With smaller ratios of THEP to HEP, bond strength decreased in the room-temperature tests. Storage at 160°F (71°C) improved shear strength significantly, which indicates that even small amounts of THEP do not react at room temperature.

Unfortunately, the pot lives of the phosphate ester epoxy mixtures, like that of ortho phosphoric acid, were still much too short to be practical (1-3 minutes). This is probably due in part to the use of the crude reaction products. Possibly the crude reaction mixtures as reported here may be useful in some situations where automatic catalyst type spray guns can be adapted to apply adhesives in rapid assembly work. For such purposes, the catalyst and resin would be automatically mixed as the materials were sprayed, and it would not be necessary to mix large quantities of catalyst and resin in bulk.

In general, the chemical resistance of the HEP-cured adhesive system is poorer than that of the DETA-cured system, and its extremely poor alkali resistance is possibly due to the presence of ester linkages which are susceptible to hydrolysis. In oleic acid the HEP-cured epoxy adhesives gain less than 1% whereas the DETA-cured system gains over 30%. The solvent resistance of the HEP-cured system varies. The HEP-cured system showed fair resistance to chlorinated hydrocarbons; the DETA-cured system disintegrated in ethylene dichloride.

Although the pot life of the epoxy cured with the hydroxy alkyl phosphate ester was not lengthened, the apparent brittleness associated with the phosphoric-acid-cured adhesive was reduced. Also tests show that the HEP-cured epoxy is compatible with many of the explosives with which amine-cured epoxies are usually incompatible.

## Preparation of β-Hydroxyethyl Ortho Acid Phosphate (HEP)

β-Hydroxyethyl ortho acid phosphate (HEP) was synthesized by reacting molar quantities of ethylene oxide and ortho phosphoric acid at temperatures ranging from 23° − 41°F (− 5° to 5°C). (6) The resulting product was a colorless liquid, soluble in water but insoluble in benzene. The equation for the reaction is as follows:

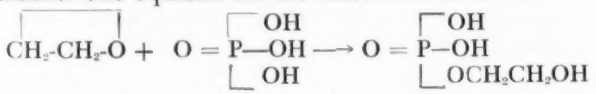

Ethylene Oxide — Ortho Phosphoric Acid — β-Hydroxyethyl ortho acid Phosphate (Structure I)

## Preparation of the Tertiary Ester of Phosphoric Acid (THEP)

Tris-(B-hydroxy ethyl) ortho phosphate (THEP) was prepared by reacting 3 moles of ethylene oxide with 1 mole of ortho phosphoric acid within the temperature range of 23° −41°F (−5° to 5°C). (8) The product formed was a hygroscopic, viscous, colorless liquid.

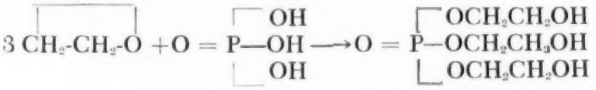

Ethylene Oxide — Ortho Phosphoric Acid — Tris-(β-Hydroxyethyl) ortho phosphate

## Calculation of Amount of Curing Agent

In calculating the amount of the hydroxy alkyl phosphate ester needed to cure a bisphenol A type epoxy resin, it was decided to use stoichiometric quantities of the curing agent, with no allowance for impurities. The stoichiometric ratio theoretically provides the exact amount of curing agent needed for the complete consumption of the reactive groups in the epoxy resin (2). Since the hydroxy alkyl phosphate esters used were not purified products, the quantities of curing agents only approximate the calculated stoichiometric amounts. An example of a typical calculation using a low-molecular-weight bisphenol epoxy and crude β-hydroxy ethyl ortho acid phosphate is as follows:

| Compound | Molecular Weight | Equivalent Weight |
|---|---|---|
| Bisphenol epoxy resin[1] | 350-400 | 197 |
| β-hydroxy ethyl ortho acid phosphate | 142 | 47.3 |

[1] Values taken from sales literature of supplier.

In this case 47.3 grams of the purified phosphate ester will provide one reactive point for each 197 grams of resin; that is, approximately 24 parts of the ester per 100 parts of resin will be required. In formulations where the use of stoichiometric quantities of the curing agent prohibited adequate mixing before gelation, the amount of curing agent was reduced to approximately 50%.

### Preparation of Shear Specimens

Lap shear specimens were prepared using cold-rolled steel panels 4 inches long, 1 inch wide, and ⅛ inch thick. The surfaces of the specimens were cleaned with an acetone-dampened cloth and then vapor degreased for ½ hour with perchloroethylene. Slightly over ½ inch of each panel was brush coated with a 2-to-4-mil film of the formulated adhesive, and the faying surfaces were immediately joined to form ½ inch lap joints. Sufficient manual pressure was applied to assure intimate contact of the faying surfaces without glue line starvation. After assembly, all the specimens except the storage specimens were allowed to cure for seven days at room temperature. The storage specimens were cured at room temperature for one day and then stored at 160°F (71°C) for seven days. The properties of each adhesive formulation are reported in terms of shear strength in pounds per square inch of bonded area. The specimens were tested in accordance with Federal Test Method Standard No. 175, Method 1033, except that the rate of load was 1200-1300 lbs/min/in$^2$ bonded area instead of the 600-700 lbs/min/in$^2$ called for in the test method.

### Table 3. Chemical Resistance of HEP-Cured Bisphenol Epoxy and Control

Table 3 provides chemical and solvent resistance data for unmodified HEP-cured bisphenol epoxy and DETA-cured bisphenol epoxy as a control. The results are reported in terms of weight gain after 7 days immersion in the various chemicals at room temperature.

**Test Temperature: 78°-80°F (24.5°-26.6°C)**
**Sample Size: 2" x 1" x 1/16"**

| Reagent | HEP-Cured Adhesive, % Weight Gain | DETA-cured Adhesive (Control), % Weight Gain |
|---|---|---|
| Sulfuric acid, 30% | 4.1 | 0.59 |
| Sodium hydroxide, 10% | 70.1 | 0.61 |
| Sodium hydroxide, 1% | 177.5 | 0.68 |
| Ethyl alcohol, 95% | 24.1 | 2.61 |
| Ethyl alcohol, 50% | 32.2 | 1.25 |
| Acetone | Disintegrated | 24.46 |
| Ethyl acetate | 20.6 | 21.08 |
| Ethylene dichloride | 40.1 | Disintegrated |
| Carbon tetrachloride | 3.7 | 3.19 |
| Toluene | 8.1 | 32.03 |
| Heptane | 2.6 | 0.09 |
| Sodium chloride, 1% | 5.6 | 1.26 |
| Distilled water | 3.5 | 0.86 |
| Nitric acid, 10% | 3.4 | 1.83 |
| Hydrochloric acid, 10% | 5.2 | 1.28 |
| Acetic acid, 5% | 12.5 | 8.80 |
| Oleic acid | 0.93 | 32.69 |
| Ammonium hydroxide, 10% | 112.6 | 1.02 |
| Sodium carbonate, 2% | —1.2 | 0.84 |
| Hydrogen peroxide, 3% | 9.0 | 0.98 |

### Test for Resistance to Chemicals (Table 3)

Test samples were cut from a sheet of HEP-cured epoxy adhesive film in the form of strips 2 inches long, 1 inch wide, and approximately 1/16 inch thick. Each sample was conditioned for 24 hours at room temperature and then weighed. The samples were then placed in separate containers and totally immersed in approximately 60 ml of reagent for seven days at room temperature. The containers were rotated manually once every 24 hours for five days. After removal from the various reagent solutions the samples were washed with running water, wiped with a dry cloth, and immediately weighed as described in ASTM Designation: D 543-56T.

### Conclusions

- The hydroxy-substituted acid phosphate esters may be useful as room-temperature-curing agents for the Bisphenol A type epoxides when very fast curing times are desirable. These materials yield cured epoxy systems which are compatible with many explosives. However, the pot lives of these adhesives will be very short. The phosphate ester with phenolic resin modifier is superior in bond strength and heat stability to the epoxies cured with diethylene triamine.

- In general, the bisphenol A type resin cured with hydroxy alkyl phosphate acid esters yields higher room-temperature shear strength bonds than those cured with aliphatic amines, as the chart on p. 48 shows.

- The softening point of the HEP-cured epoxy resin appears to exceed that of the DETA-cured epoxy resin.

- The alkali resistance of the HEP-cured epoxy adhesive is much poorer than that of the DETA-cured adhesive.

- Post curing of all the formulated adhesives at elevated temperatures improve their shear-strength properties.

### Literature References


1. Shrade, V., "Les Resins Epoxy", Dunod, Paris, 1957.
2. Lee, H. and Neville, K., "Epoxy Resins", New York City, McGraw-Hill Book Company, Inc., 1957.
3. Lee, H. T. and Swick, E. R., "Inorganic Acids as Curing Agents for Epoxy Resins", Picatinny Arsenal Laboratory Report, 59-TGl-10, 1959.
4. U. S. Patent 2,528,932, Wiles.
5. Schrader, W. H. and Bodnar, M. J., "Evaluation of Room Temperature Acid Curing Agents for Epoxy Resins", Picatinny Arsenal Laboratory Report 57-TM2-38, 1957.
6. Kosolapoff, G., "Organophosphorus Compounds", New York City, John Wiley and Sons Inc., 1950, p. 230.
7. Private communication from Toy, Dr. E. and co-workers, Victor Chemical Works, Chicago, Illinois.
8. U. S. Patent 2,372,244, Adams and Shoemaker, 1945.



### Acknowledgments

The author wishes to express appreciation to Mr. W. C. Tanner who helped to prepare the various esters synthesized, to Mrs. E. R. Swick and Mr. H. Lee who performed the evaluations on phosphoric acid, to Messrs. W. Schrader and M. J. Bodnar for their work with monobutyl and dibutyl ortho acid phosphate, and to Dr. E. Toy and co-workers of the Victor Chemical Works, who supplied information and various samples of phosphate esters.

## *Editorial*

# Research is Key to Progress in the Plastics Industry

The synthetic plastics industry has now traveled the road from phenolformaldehyde to polypropylene and polyurethane—or at least I know of no newer plastic in quantity production. The path we have traveled is clear. The future is not. There will be new plastics. There will be better plastics. Whether the plastics of the future will be new ones or better versions of the present ones no one is so rash as to predict.

The solution to obtaining progress is research. That is coming along in ever-increasing volume with a reasonable proportion devoted to plastics. But the tempo of progress has become ever faster over the recent decades and that presents another problem, communciations.

SPE TRANSACTIONS has been created as a contribution to communications. Prompter publication helps everyone in all the channels of plastics research to produce new plastics and better plastics.

The predictions that plastics were going to displace metals and glass have so far not been realized. So far, there is no indication that they will. Spandrels of the new buildings are metal or glass rather than plastic. But plastics cover the floors and literally have crawled up the walls. They have displaced quantities of rubber and oxidized linseed oil. There is reason to believe that the flat paints based on plastic emulsions may shortly be accompanied by gloss paints with analogous bases. The size of plastic moldings becomes ever larger. Literally they cover the range from hard and brittle to elastomeric products.

So, the communications function of SPE TRANSACTIONS reenters to show the results of basic research and development work and, therefore, to act as one of the guides of the industry in the progress into new uses of existing plastics and the discovery of new polymers.

Congratulations on the recognition of the need and best wishes in fulfilling it.

FOSTER DEE SNELL, Ph.D.
*President*
*Foster D. Snell, Inc.*

# A *preview* of several articles for the second quarterly issue (April) of SPE TRANSACTIONS

## Cryogenic Adhesive Properties of Bisphenol-A Epoxy Resins

by M. J. Hiza and P. L. Barrick

The effect of dropping the temperature of epoxy bonded aluminum joints from 300°K to 76°K is studied in terms of tensile-shear and impact-shear tests and the linear thermal contraction of the resin. This article tells how to formulate epoxies for good low temperature performance.

## Thermodynamic Diagrams for Polyethylene Resins

by J. M. Lupton

Here are thermodynamic diagrams applicable to both existing and new polyethylene resins. Starting with fusion and crystallographic data and a few simplifying assumptions, charts are calculated relating enthalpy and internal energy to pressure, specific volume and temperature, for amorphous and crystalline polymers.

## Electrical Resistivity of Polymers

by R. W. Warfield and M. C. Petree

Measurements of the temperature dependence of volume resistivity of a variety of polymers are used to elucidate polymer structure and the mechanism of electrical conduction. This follows this month's article on resistivity measurements during polymerization.

## A Method for Determination of Maximum Heat Resistance of Plastics

by I. F. Kanavetz and L. G. Batalov

A translation from "Plastics Magazine" (USSR) by George Lubin will show how the Russians are standardizing and improving their heat resistance tests. The new tests relate thermo-mechanical and thermal degradation properties to the fundamental properties of the polymer.

# SPE TRANSACTIONS